# A METHODOLOGY TO CAPTURE THE ACOUSTIC PROPERTIES OF SMALL UNMANNED AERIAL SYSTEM NOISE USING A NOVEL FREQUENCY WEIGHTING

A Dissertation
Presented to
The Academic Faculty

By

Ana Bella Gabrielian

In Partial Fulfillment
of the Requirements for the Degree
Masters of Science in the
Guggenheim School of Aerospace Engineering
Department of Aerospace Engineering

Georgia Institute of Technology

August 2021

**A METHODOLOGY TO CAPTURE THE ACOUSTIC PROPERTIES OF SMALL UNMANNED AERIAL SYSTEM NOISE USING A NOVEL FREQUENCY WEIGHTING**

Thesis committee:

Dr. Dimitri Mavris
Advisor Guggenheim School of Aerospace Engineering
*Georgia Institute of Technology*

Mr. Greg Busch
Acoustics Engineer
*Genesis Air Mobility*

Dr. Aharon Karon
Senior Research Engineer
*Georgia Tech Research Institute*

Date approved: August 2021

Fight for the things that you care about, but do it in a way that will lead others to join you.

*Ruth Bader Ginsburg*

For Leo Gabrielian, 1957-2020.

## ACKNOWLEDGMENTS

I would to thank Dr. Mavris for funding my Master's degree at the Aerospace Systems Design Laboratory. I am so grateful and honored to be a part of such a talented and intellectual group. I thank Mr. Gregory Busch for taking me under his wing during this thesis and being the technical advisor that I needed. Greg is a very busy man and him using some of his time in his schedule to mentor me is very special to me. I would also like to thank Dr. Aharon Karon for advising me with the technical details of signal processing and handling of the noise recordings from NASA.

I would like to thank Andrew Christian and Randolph Cabell from the NASA Langley Structural Acoustics Branch for sharing their data with me – without which this thesis would not have been possible.

I would like to thank my family, my mom Anita, my dad Leo, my sisters Lauren and Jessica for their support during this process. I would like to thank my Tillita for inspiring me to pursue a career in engineering. I would like to thank my best friends Vanessa, Monica, Aarya, Justin and Yerik for letting me lean on them when times grew tough.

Finally I would like to thank myself for taking the road less traveled although it was more difficult. I would like to thank myself for keeping my standards high and persevering to reach them.

## TABLE OF CONTENTS

## LIST OF TABLES

## LIST OF FIGURES

## SUMMARY

Urban Air Mobility (UAM) is the term used for air vehicles transporting either freight or passengers using short take off and landing (STOL) or vertical take off and landing operations (VTOL). This solution to congestion on the ground is versatile in the operations that it can accomplish: last mile package delivery, medical transportation, search and rescue evacuation, air taxi, and the list continues. However, there are obstacles to the adoption of such vehicles, noise being a main contributor to a lack of public acceptance.

Noise is a public concern as it has been shown to contribute to lack of sleep, lack of cognitive abilities in children, and decline in overall cardiac health. There is extensive noise policy in the form of land use compatibility guidelines and noise certification limits on traditional aircraft. Currently, no noise policy exists for vehicles in the category of UAM. Entities like Amazon and Joby Aviation are well into the testing phase of their vehicles. As these concepts become more mature, it is important that regulation stay equally paced in order to ensure appropriate rules are in place. When faced with new technology which pushes past existent laws, regulators turn to incautious action or immobility. The latter is usually the case, and it has the consequence of retarding the arrival of such a technology to the market. The use of the former has the outcome of regulation that is overly lenient resulting in public retaliation and complaints to lawmakers.

Entities like the National Aeronautics and Space Administration (NASA) and the Federal Aviation Administration (FAA) recently created a survey recommending that studies be conducted on the use of current noise metrics on vehicles in the UAM category. As a part of the NASA project named the Design Environment for Novel Vertical Lift Vehicles (DELIVER), engineer Andrew Christian conducted a psychoacoustic test on small Unmanned Aerial Systems (sUAS) to measure human annoyance toward these vehicles in comparison to current delivery vehicles such as box vans. The study found that at the same decibel level, test subjects found sUASs more annoying than they did delivery vehicles. The study

also found that the correlation between annoyance and decibel level using four different noise metrics was relatively low.

In a preliminary comparison of spectral content between a helicopter and one of the sUASs in the study, it can be seen that the sUAS's spectral content has more tones in the region of increased human sensitivity. To account for human sensitivity to these tones, the hypothesis is posed: A new frequency weighting, which allows Sound Exposure Level to better correlate with human annoyance caused by an sUAS noise event, will create a larger SEL contour area that is more indicative of sUAS noise.

In the first phase of the approach, this hypothesis was tested by creating a design of experiments of different frequency weightings created by modifying the A-weighting scale in order to find a new weighting yielding a larger coefficient of determination than that found in Christian's study. In the second phase, sound exposure level contours were created using the new frequency weighting and current frequency weightings in order to observe an area change.

The resulting frequency weighting (the X-weighting) increased the $R^2$ value from 0.784 to 0.853. The weighting itself has obvious peaks and valleys at specific one-third octave bands causing curiosity regarding the acoustic phenomena within these recordings that is causing annoyance to these particular frequency bands. Without in-depth acoustic analysis in the form of high fidelity CFD and anechoic chamber testing, these speculations cannot be answered; however, within the power spectras and spectrograms of these recordings, it can be seen that there are tones that stand out in the recordings themselves.

This new weighting was applied to Sound Pressure Level (SPL) values and used in NASA's Aircraft Noise Prediction Program (ANOPP2) to create SEL contours that were A-, C-, and X-weighted. Because of the different frequencies that are depressed and amplified from weighting to weighting, a large variation in contour area shape and size is seen. For all dB levels, the contour area saw an increase when comparing the A- and the X-weighting. The SEL 65 dB contour experienced a 79%, 18%, and 78% increase in width, length, and

area respectively between then X- and the A-weighting for one of the sUASs investigated.

This methodology grants stakeholders such as regulators and original equipment manufacturers a process to assess frequency weightings and their efficacy in capturing human annoyance; in doing so, this could enable all sUAS stakeholders to create a common "language" with which to discuss the noise created by these vehicles effectively.

# CHAPTER 1
# INTRODUCTION

## 1.1 Motivation

Urban areas have become increasingly congested; the space within these metropolitan areas is demanded for use by commercial businesses, housing, infrastructure, transporting goods, services, and people. An overview of urban growth statistics show staggering numbers: according to a study published by the United Nations, by 2050, 68% of people will live in urban areas compared to 55% in 2018 [1]. Because of this, services such as personal transportation are in high demand and are only forecasted to grow [2]. The ride sharing company, Uber, recorded 6.9 billion trips in 2019 [3]. In September 2018, Uber's main competitor, Lyft, logged 1 billion trips [4].

Accompanying these thriving transit companies are delivery services with larger amounts of momentum. During the Covid-19 Pandemic especially, delivery services saw a large increase in demand with UPS reporting an 11% increase in profits on a yearly basis and a 28.8% increase in the number of packages delivered on a daily basis [5]. Amazon increased its employee count to a total of 1.1 million people to account for the larger demand caused by the pandemic [6].

The main takeaway from these facts is that delivery services are booming, urban area population density is increasing, and the demand for transportation is growing as well. This raises concern regarding passenger commute times, emissions, noise pollution, and air quality hand-in-hand with public health. The aerospace industry has acknowledged this issue and identified a potential solution: utilizing civil airspace, which is not being taken advantage of, in order to alleviate the congestion on the ground. The industry coined the term "Urban Air Mobility" (UAM): utilizing air vehicles to transport freight or passengers

in short take off and landing (STOL) or vertical take off and landing operations (VTOL) [7].

Because of the versatility of these vehicles, they have been proposed for use by emergency medical services, search and rescue, taxis, last-mile package delivery, and the list continues. Companies such as Ehang (China), Joby Aviation (US), and Kitty Hawk (US) have made strides by creating prototypes, which can be seen in Figure 1.1. Although first received apprehensively, the idea of aerial mobility on this scale has gained momentum, according to Uber regarding their "Uber Elevate" Program, which has been a collaborative project with the National Aeronautics and Space Administration (NASA) and the Federal Aviation Administration (FAA) [8]. Uber has since sold their Elevate program to Joby Aviation and has invested 75 million dollars in the company as well [9].

Figure 1.1: (Left to Right) Medical Care concept by Jaunt, Air Taxi by Joby, Last Mile Package Delivery by Amazon [10] [11] [12].

### 1.1.1 Last Mile Delivery

The most mature path of UAM is the use of small Unmanned Aerial Systems (sUASs), also known as drones, for Last Mile Delivery (LMD). LMD is known to be the most expensive stage of a shipping process. This is because this stage has the most human interaction, the most uncertainty due to delivery vans and trucks having to interact with everyday traffic on urban roads, and the lowest mileage per gallon for transportation vehicles [13]. Today, companies are having to become more competitive as customers expect a "free delivery" option such as the one provided by Amazon Prime delivery. The advent of sUASs for LMD is forecasted to be within reach; the FAA has projected it to be viable at $4.20 per delivery

for an estimated 500 million deliveries per year by 2030 [14]. LMD has been looked into by many companies like FedEx, UPS, Amazon, and even Dominos for Pizza Delivery. These concepts can be seen in Figure 1.2.


Figure 1.2: FedEx Wing concept (Left) Dominos Pizza Delivery (Right) [15] [16].

Although UAM lends itself as an idea with great returns, it has many obstacles to its implementation. A study presented by MIT explains how the obstacles to UAM present themselves [17]. Firstly, the airspace that would be used for UAM vehicles is much closer to the ground than traditional aircraft as stated by the FAA [18]. The amount of air traffic controllers (ATC) employed will need to increase in order to manage such an increase in operations, especially in an airspace that is not currently managed by ATC. Secondly, the infrastructure needed for operations involving air taxis, or even last-mile package delivery using sUASs, are not fully developed. VTOL airports (also known as vertiports) and fulfillment centers for LMD, may be needed for the take off and landing portions of operations. Finally, the study mentions the impact of noise from these vehicles on community acceptance. These vehicles will be much closer to the ground and suburban infrastructure during their operations than traditional aircraft that take off from airports and are usually hundreds if not thousands of feet above ground level. Because of this, the sound levels experienced by humans will be much different than conventional aircraft. Keeping in mind that the FAA has forecasted a magnitude of 500 million annual operations, noise is obviously a barrier to take into account. In this thesis, this last obstacle to UAM is explored.

Overarching Research Objective: Contribute to the understanding of noise as a roadblock to Urban Air Mobility by investigating noise metric efficacy.

Aviation noise has been shown to affect many facets of everyday life from negatively impacting children's cognitive abilities and performance at school to being linked to quality of sleep and overall health [19]. The FAA has taken steps in the direction of noise mitigation by creating noise limit levels on different types of aircraft such as large transport airplanes, jet airplanes, helicopters, tilt-rotorcraft, and small propeller-driven airplanes. The FAA also created the Noise Complaint Initiative (NCI); this is a portal where the general public can submit a noise complaint for review by the FAA [20]. Currently, no noise policy for UAM vehicles exists for even the most mature vehicles in this category: sUASs.

Policies are created with the assistance of metrics which allow technical experts/engineers, law creators, and lay-people to "speak the same language" with regards to a certain subject. For example, when creating rules for the roads, one of the key metrics that is used is speed (with the unit being miles per hour or kilometers per hour). In this thesis, the understanding of sUAS noise is detailed by investigating the competence of current metrics to describe the annoyance that is created by such vehicles. This leads to the first Motivating Question for the literature review:

**Motivating Question #1**: What current noise metrics exist and what kinds of acoustic phenomena do they account for?

Recently, the technical paper, "Urban Air Mobility Noise: Current Practice, Gaps, and Recommendations" written by NASA, the FAA, and others was published regarding UAM noise. The paper identified gaps in current practices and recommendations for law makers and Original Equipment Manufacturers (OEMs) [21]. In this paper, a high-level goal was to assess metrics for audibility and annoyance, on a single-event basis, using predicted and measured data. The authors identified that existing metrics such as maximum A-weighted Sound Pressure Level (SPL), A-weighted Sound Exposure Level (SEL), and Effective Per-

ceived Noise Level (EPNL) could be appropriate for UAM vehicle regulation. Later, they recommended that in order to assess human response to UAM noise, more data should be simulated and acquired for subjective and community studies. To begin to answer Motivating Question #1, a closer investigation of current noise metrics and their use in regulation must be reviewed.

## 1.2 Background

In the study conducted by Rizzi et al [21], they reference multiple noise metrics that are currently used in noise policy. These metrics are all calculated differently and take different acoustic properties into account. In the following subsections, these calculations will be discussed further.

### 1.2.1 Sound Pressure Level

Sound Pressure Level (SPL) is the starting point for most acoustic measurements. The calculation of SPL uses the atmospheric pressure variation caused by a sound and relates it logarithmically with a reference pressure. This is shown in Equation 1.1

$$SPL_{dB} = 10 \log_{10} \left( \frac{P^2}{P_{ref}^2} \right) \tag{1.1}$$

where $P_{ref}$ is equal to $20\mu Pa$ for sound traveling in air and $P$ is the acoustic pressure caused by a source. Frequency weightings and scales can be applied to SPL in order to capture the sensitivity of the human auditory system to sounds at different frequencies.

### 1.2.2 Human Auditory System

An illustration of the human ear's response to different sounds is shown in Figure 1.3. It shows how, at different frequencies, sound can be lower in intensity but still have the same effect when it comes to the actual amount of pain a person experiences. The auditory

system is especially sensitive to sounds at frequencies between 2 and 5 kHz (highlighted in yellow), this is due to these frequencies resonating inside of the ear canal [22].

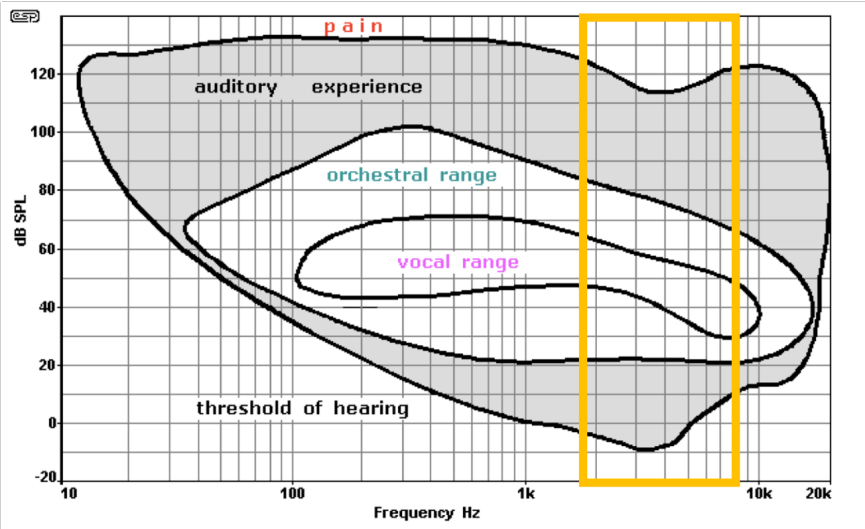


Figure 1.3: Human hearing envelope [23]

Notice how in Figure 1.3, the scale used to measure the noise level is the decibel (dB). Because of the wide range of human hearing, dB is used on a logarithmic scale, which objectively measures the strength of sound created. Although this is objective, the actual loudness of a sound is subjective and can vary from person to person. The phon unit was created in order to take an individual's perception of loudness of 1 dB at 1 kHz [24]. Decibels are most commonly used in practice and are modified to take into account the non uniformity of human response.

### 1.2.3 Frequency Weighting

Human perception to noise is dependent on the characteristics within the noise itself. This can be things such as:

1. Loudness: the magnitude a listener seems to experience when hearing a sound. Loudness is subjective. [25]

2. Sharpness: When a sound has more high frequency content than low frequency con-

tent. This is measured with the acum. [25]

3. Roughness: Sound that has fluctuations in loudness (50 to 90 fluctuations per second) [25]

4. Tonality: Sound containing a high amount of energy in one frequency relative to neighboring frequencies [26]

5. Impulsiveness: short duration noise [27]

In an attempt to take into account frequency dependent sensitivity, different scales have been created to add or subtract corrections from certain one-third octave frequency bands. One-third octave bands divide the audible frequency spectrum into 32 parts. The International Standards Organization (ISO) has standardized the center frequencies (these can be found in Appendix A) of these bands and the upper and lower limits can be calculated using Equation 1.2

$$f_c = f_{lower} 2^{1/6} = \frac{f_{upper}}{2^{1/6}} \tag{1.2}$$

where $f_c$ is the center frequency. The standardized weightings that can be applied to these bands can be seen in Figure 1.4.

1. The A-weighting scale is used to characterize the human auditory system's response to pure-tone noise at 40 phon and for sounds between 24 and 55 dB of Sound Pressure Level [28]. The A-weighting curve was created by Fletcher and Munson in 1933 by averaging the perceived loudness recorded by many subjects. This study was validated by a more contemporary study in 2003 [29]. The A-weighting is the most commonly used weighting in aviation noise metric calculations.

2. The B-weighting scale is made to de-emphasize the low frequency portion of the frequency spectrum and is also used to approximate the human ear's response to medium-level sounds (approximately 70 phon or between 55 and 85 dB) [23].

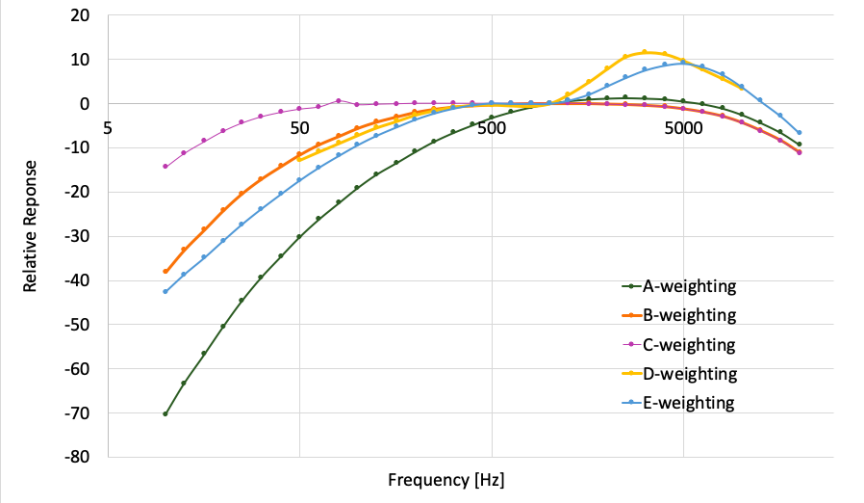


Figure 1.4: Response to A-E Noise Weightings [23]

3. The C-weighting scale is made to characterize human response to higher-level sounds (approximately 100 phon or above 85 dB). It includes low and mid-frequency energy which A-weighting understates.

4. The D-weighting scale was made to especially emphasize the high frequencies in a sound, which can be seen in Figure 1.4, and to mimic the weighting of equal loudness curves which will be discussed later.

5. The E-weighted scale was made to emphasize higher-level frequencies relative to the D-weighting scale and to characterize the human auditory response to aircraft flyovers.

These weightings are used by adding the corresponding corrections shown in Figure 1.4 to the spectral content, i.e., the pressure levels measured from microphones or predicted by a program at different frequencies. An example calculation is shown in the Appendix A using the A-weighting.

### 1.2.4 Effective Perceived Noise Level

Effective Perceived Noise Level (EPNL) is calculated in a multi-step process starting with the Perceived Noise Level (PNL). This is calculated using “Noy Bands” or equal loudness

curves, which can be seen in Figure 1.5. These curves were created and standardized in 2003 by the International Standard Organization (ISO) by using models based on the human auditory system [30]. Using the relationships between SPL and Noy bands, the associated PNL (measured in PNdB) can be calculated by the following equation:

$$\mathrm{PNdB} = 40 + 10\log_2(Noy) \tag{1.3}$$

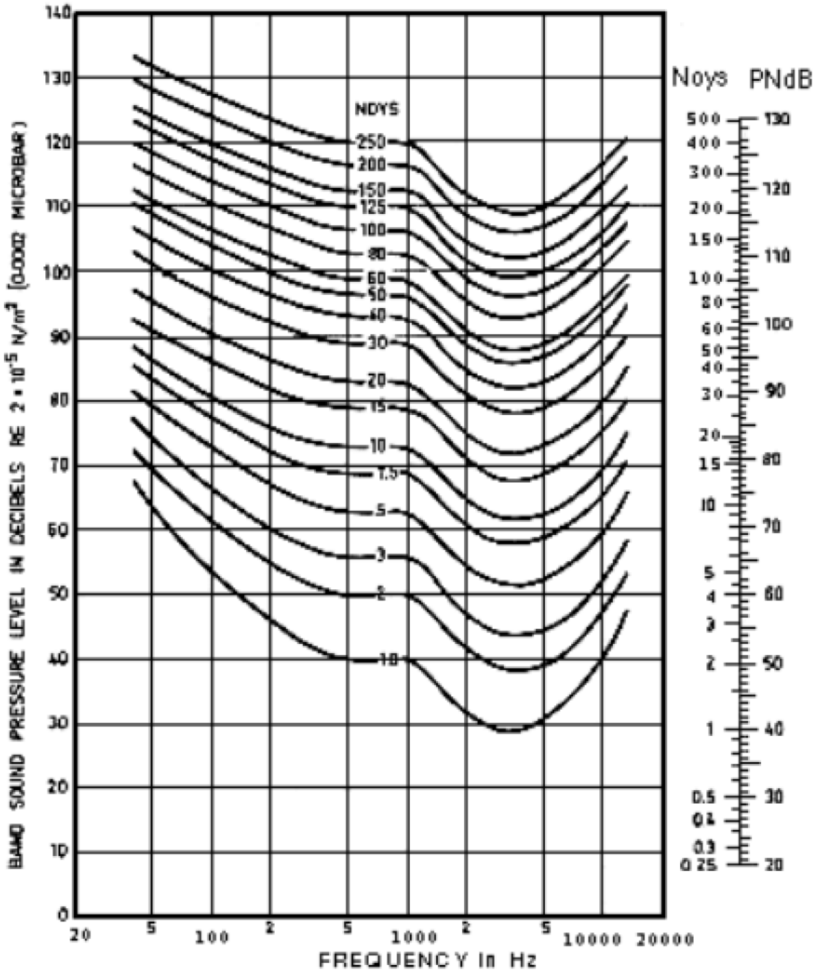


Figure 1.5: SPL to Noy Band mapping for PNL Calculation [31].

The second step toward computing EPNL is calculating the Tone Corrected Perceived Noise Level (PNLT). Pure tones have been found to be more annoying to the human ear [31]. An example of a pure tone could be the tone transmitted from a compressor

of a traditional turbofan engine [32]. A thorough explanation for the tone correcting calculation is found in the Federal Aviation Regulations Part 36 Appendix A2. In summary, the calculation identifies where there are the largest changes in slope to recognize a tone that has a larger SPL than neighboring frequencies. Depending on the one-third octave band containing the tone, a correction factor is added to the PNL decibel value resulting in a PNLTdB value shown in Equation 1.4.

$$\text{PNLTdB} = PNL + C_{max} \tag{1.4}$$

The final calculation for EPNL adds a correction for the duration of the noise event. This correction is calculated by using the time history portion that is within 10 seconds of the maximum PNLT recorded in the noise event.

$$D = 10 \log_{10} \left[ \sum_{0}^{2d} 10^{\frac{PNLT(k)}{10}} \right] - PNLT_{Max} - 13 \tag{1.5}$$

where $d$ is the time interval during which the sound level is within 10 PNLTdB of $PNLT_{Max}$. This is then added to the maximum PNL calculated to finally calculate the EPNL for that noise event.

$$EPNL = PNL_{max} + D \tag{1.6}$$

EPNL is used by the FAA for aircraft takeoff and landing certification. An example of a noise certification limit is shown in Figure 1.6. These certifications are specified for different types of aircraft as well as a function of their weight and operation. For example, Figure 1.6 shows the certification limits for a Stage 2 helicopter approach at a takeoff weight over 1000 lbs.

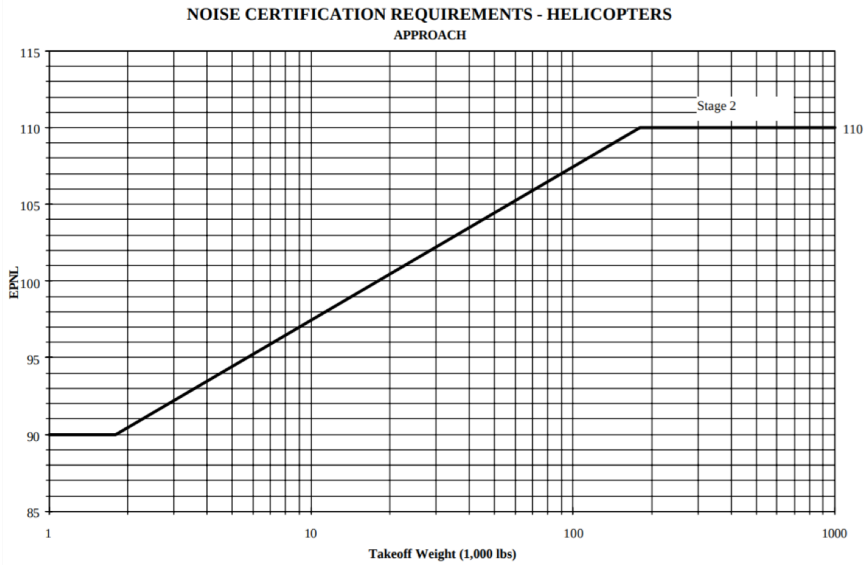


Figure 1.6: Stage 2 Helicopter EPNL Limit for Certification [33].

Aircraft stages correspond to the stringency placed on the aircraft in terms of noise regulation. Stage 1 civil jet aircraft are the loudest and Stage 5 are the quietest. For helicopters in particular, there are 3 different stages. As aircraft become older, the FAA phases them out meaning they are no longer within the fleet [34] lowering the fleet-wide noise.

### 1.2.5 $L_5$

$L_x$ is a noise metric based on statistics; the designation "x" stands for the amount of sound that is exceeded "x" percent of the time. This metric is usually used at a specific point of interest in order to monitor the noise fluctuations in that area. An example of this would be monitoring noise from road traffic [23]. As this is a metric specified to monitor noise that is exceeded 5% of the time, it yields sounds that are relatively loud. This does not take into account duration of a noise event or tonality [28].

### 1.2.6 Sound Exposure Level

Sound Exposure Level (SEL) is a metric which is used by the FAA in order to make noise recommendations to airports using Day Night Average Noise Contours. This will be dis-

cussed further below. SEL is calculated such that it is as if the noise event occurred in a single second [35]. It is made to describe the "noisiness" of a complete noise event. The formula is shown in Equation 1.7

$$SEL_{dB} = 10 \log_{10} \left[ \frac{1}{t_2 - t_1} \int_{t_1}^{t_2} \frac{P_A^2(t) dt}{P_0^2 t_0} \right] \tag{1.7}$$

where $P_A(t)$ is the A-weighted pressure as a function of time, $P_0$ is the reference sound pressure (20 $\mu Pa$), $t_0$ is one second, $t_1$ is the time at the beginning of the noise event, and $t_2$ is the time at the end of the noise event [31]. It is important to note that SEL is not required to be A-weighted; it can be weighted by the other scales shown in Figure 1.4 as well. SEL is often visualized with the use of a noise contour: a region on a map that represents equal levels of noise exposure. An example of an SEL contour of an aircraft departure is shown in Figure 1.7.

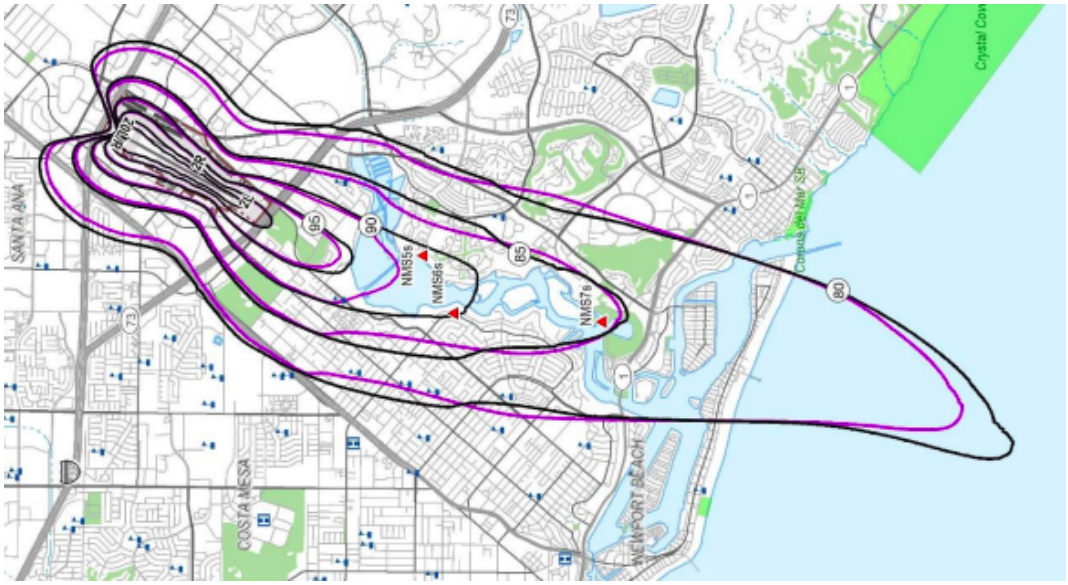


Figure 1.7: Departure SEL Contour at John Wayne Airport [36].

In this image, it can be seen that smaller areas closer to the airport are exposed to higher noise levels. As the sound travels, the intensity also spreads over a larger surface area which reduces the level. The different coloring in the lines depicts the difference in contour area

and shape given two different procedures flown by the aircraft.

### 1.2.7 Day-Night Average Sound Level

Day-Night Average Sound Level (DNL) is used by airports and the FAA in order to reflect the amount of noise exposure in a 24-hour interval. DNL takes into account the time of day of an operation as events that occur at night receive a 10 decibel noise penalty. This is done because the ambient noise in a given area at night is on average 10 decibels quieter when compared to the ambient noise in that same area during the day; this is a result of less activity in general. DNL also takes into account the number of noise events that occur in this 24 hour interval as well as their magnitude. It is calculated using Equation 1.8.

$$DNL = 10\log_{10}\left[\left(\frac{1}{86400}\right)\sum_{1}^{N} 10^{\frac{SEL_j + W_j}{10}}\right] \tag{1.8}$$

where $SEL_j$ is the SEL noise for that operation during the day, $N$ is the number of SEL noise events during the day, and $W_j$ is a weighting applied to noise events during the night time; therefore the value is 0 for day-time events and 10 for night-time events [31]. So, it can be seen that DNL is similar to an average of SELs with additional weightings to take into account human annoyance factors.

### 1.2.8 Community Noise Equivalent Level

The Community Noise Equivalent Level (CNEL) is a cumulative noise metric that was created before the DNL was adopted by the FAA. The California Airport Noise Standards state that the acceptable level of aircraft noise for persons living in the vicinity of airports is a CNEL of 65 dB [37]. It can be calculated using Equation 1.9

$$CNEL = 10\log_{10}\left[\sum_{j=1}^{N_D} 10^{\frac{SEL_j}{10}} + \sum_{j=1}^{N_E} 10^{\frac{SEL_j + W_E}{10}} + \sum_{j=1}^{N_N} 10^{\frac{SEL_j + W_N}{10}}\right] - 49.4 \tag{1.9}$$

where $N_D$ is the number of SEL noise events during the day(7AM-7PM), $N_E$ is the

number of SEL noise events during the evening (7-10PM), and $N_N$ is the number of SEL noise events during night-time (10PM-7AM). Evening and nighttime operations have corresponding weights $W_E$ and $W_N$ equal to 4.77 dB and 10 dB respectively [37]. CNEL is similar to DNL in being a quasi-average of the SELs in a 24 hour time period.

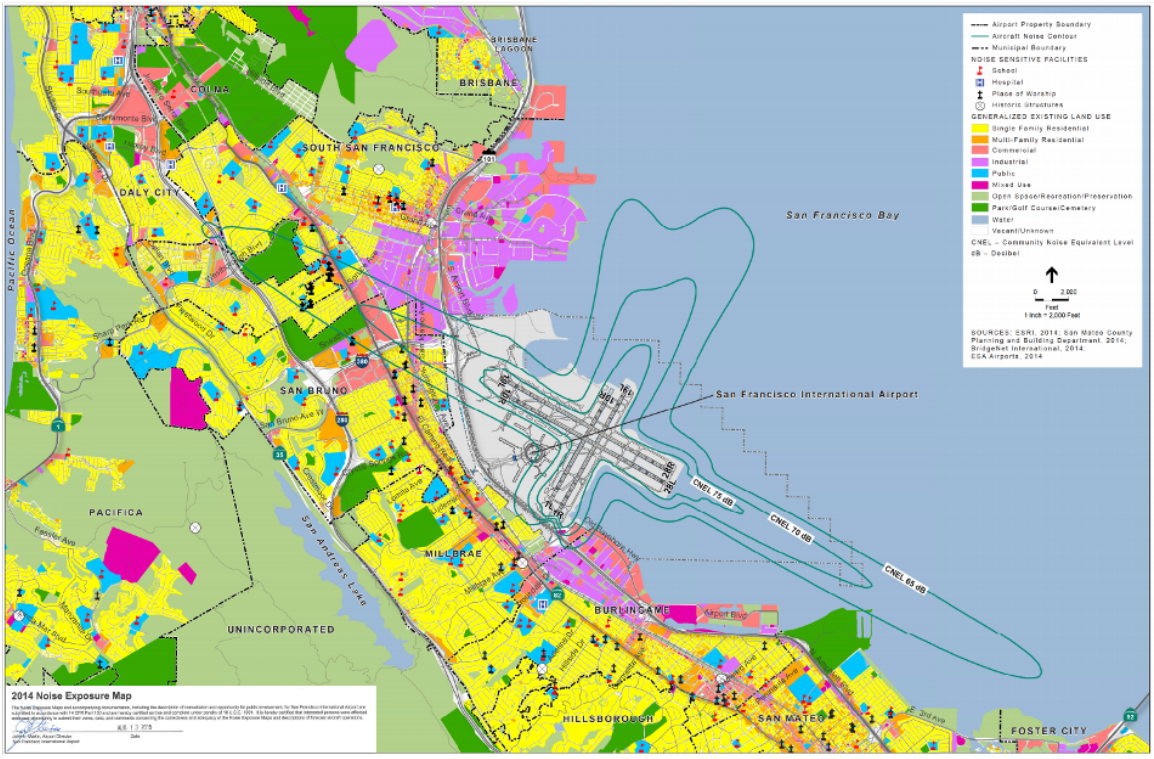


Figure 1.8: CNEL for SFO airport [38].

It can be seen that contours based on metrics like DNL and CNEL take not only time of day into account but are also dependent on flight schedules, types of aircraft, operation type, and runway location/geographic layout of the airport.

### 1.2.9 Noise Contour Generation and Usage

Contours such as those shown in Figure 1.8 are created using noise propagation methods. One method is the Ffowcs-Williams Hawkings Equations and Lighthill's Acoustic Analogy. These equations are a rearrangement of the Navier Stokes Equations into a wave equation that is a function of pressure. They are utilized in the NASA tool, the Aircraft

Noise Prediction Program (ANOPP). ANOPP has the ability to produce noise power distance curves (NPDs). NPDs allow noise levels to be obtained as a function of observer distance via spherical spreading through a standard atmosphere. Other correction factors are applied to obtain the desired sound field metrics at the location of a modeled receiver [39]. The FAA utilizes the Aviation Environmental Design Tool (AEDT), which houses Noise Power Distance curves (NPDs), in order to calculate noise radiated from an aircraft. Both of these software are constantly being validated and refined by entities like the VOLPE center, Aviation Sustainability Centers (ASCENT), and NASA.

Using these different metrics, the FAA creates guidelines regarding the handling of community noise; this is done with the assistance of noise contours. For metrics like DNL or CNEL, residential areas have been integrated into community noise initiatives where airports retrofit houses with double-paned windows and doors in order to mitigate the noise residents experience indoors should their home be within the 65 dB contour lines [40]. Not only are noise contours used for residential retrofitting initiatives, they are also used for land use guidelines. Places like hospitals, schools, mobile home parks, places of worship, and concert halls are not to be within contours upwards of 65 dB. An example of guidelines from the FAA are shown in Figure 1.9. Here, designations with Y signifies that land use is compatible with such structures, N signifies land is not compatible and should be prohibited. The subsequent designations vary with compatibility determined and enforced by local municipalities.

| Land Use | Yearly DNL Sound Level (decibels) | | | | | |
|---|---|---|---|---|---|---|
| | <65 | 65-70 | 70-75 | 75-80 | 80-85 | >80 |
| **Residential** | | | | | | |
| Residential, other than mobile homes and transient lodgings | Y | N (1) | N (1) | N | N | N |
| Mobile home parks | Y | N | N | N | N | N |
| Transient lodgings | Y | N (1) | N (1) | N (1) | N | N |
| **Public Use** | | | | | | |
| Schools | Y | N (1) | N (1) | N | N | N |
| Hospitals and nursing homes | Y | 25 | 30 | N | N | N |
| Churches, auditoriums, and concert halls | Y | 25 | 30 | N | N | N |
| Governmental services | Y | Y | 25 | 30 | N | N |
| Transportation | Y | Y | Y (2) | Y (3) | Y (4) | Y (4) |
| Parking | Y | Y | Y (2) | Y (3) | Y (4) | N |

Figure 1.9: Land Compatibility Guidelines by the FAA [41]

It is common for the validity of noise metrics to be challenged. Recently, government representatives have brought attention to the applicability of the DNL. In 2018, the FAA Reauthorization Act was published which states "the Administrator of the Federal Aviation Administration shall complete the ongoing evaluation of alternative metrics to the current Day Night Level (DNL) 65 standard" [42]. On September 23, 2020, 27 members of the House of Representatives sent a letter to the administrator of the FAA stating that the report the FAA created in response to this mandate was "wholly inadequate" and "unacceptable". These representatives have also asked for a new report to be written in response to the Reauthorization Act [43]. In addition to this, the FAA has newly released a report discussing that people are more annoyed with aircraft noise compared to previous years [44]. This causes further scrutiny to be applied on metrics for new noise policy.

The existence of these many noise metrics leads one to think that there are many available ways to regulate the noise made by sUASs thereby raising the following Motivating Question:

Motivating Question 2: Can noise metrics that are currently used for traditional aircraft operations be used to capture the annoyance caused by vehicles like sUASs?

### 1.2.10 Past sUAS Acoustic Studies

Major companies like Amazon, the USPS, UPS, and Fedex are creating prototypes for LMD by drone causing organizations like NASA to dedicate projects to UAM vehicles in order to understand their physical characteristics in parallel to their design development. The findings of these projects have the ability to contribute to the answer of Motivating Question #2.

NASA has outlined a project titled the Design Environment for Novel Vertical Lift Vehicles (DELIVER) [45]. The project aims to use current conceptual design tools that are used for rotorcraft and apply them to unconventional vehicles that use VTOL operations for missions like air taxis or package delivery. The main tool used for these simulations is the NASA Design and Analysis for Rotorcraft (NDARC). Multiple data sets for full analysis must be supplied to NDARC and those originate from Aeromechanics tools (CAMRAD2, Propeller Analysis System - PAS), Aerodynamics tools(OVERFLOW, RotCFD, FUN3D, and XFoil), Acoustics Tools (PSU-WOPWOP, and Broadband Acoustic Rotor Codes - BARC), and Propulsion Tools (NPSS).

In addition to the computational analysis and simulation work being conducted, there is also a significant amount of experimental data being generated and collected for validation purposes. This is one part of the recommendations posed by the UAM noise study by Rizzi et al discussed earlier [21]. In the acoustics portion of DELIVER, experimental work is in the form of actual sUAS noise recordings using microphones as well as psychoacoustic testing: asking human test subjects about their auditory response to noise recordings in terms of their annoyance.

A psychoacoustic study performed by NASA Langley engineer Andrew Christian sought

to evaluate human annoyance to sUASs and compare that annoyance to delivery vehicles such as box trucks and vans [28]. Delivery vehicles and sUASs were used for comparison because, if these sUASs are used in the future for delivery purposes, then these vehicles would hopefully generate the same amount or less annoyance given the same level of noise created. This study would assist one in making the observation regarding the ease of adoption of sUASs into a delivery service, replacing or supplementing the vehicles that are already present.

The recordings played for the test subjects consisted of different vehicles in the ground vehicle category and the sUAS category. The ground vehicles consisted of a box truck, a utility van, a step van, and a Subaru Impreza. These are shown in Figure 1.10.

Figure 1.10: Ground Vehicles studied in Psychoacoustic Test. [28]

For the sUASs, the recordings were from the Drone America DaX $8^4$ fix-pitched octocopter, the Stingray $500^5$ (VPV) variable-pitched quadcopter, the DJI Phantom $2^6$ fixed-pitch quadcopter, and the Endurance Drone from Straight Up Imaging (SUI). Images of the vehicles are shown in Figure 1.11 and vehicles specifications shown in Table 1.1.

(a) SUI Endurance

(b) Stingray 500 (VPV)

(c) Phantom

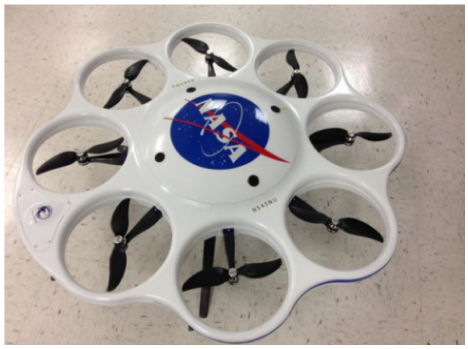

(d) DaX $8^4$

Figure 1.11: sUASs used in psychoacoustic test [28].

Table 1.1: sUAS Vehicle Specifications [28].

| Vehicle | Pitch Type | # Blades | Weight [kg] |
|---|---|---|---|
| DaX $8^4$ | Fixed | 8 | 8.0 |
| Stingray $500^5$ (VPV) | Variable | 4 | 4.0 |
| DJI Phantom | Fixed | 4 | 1.6 |
| SUI Endurance | Fixed | 4 | 3.2 |

There were 38 test subjects that participated in the study from the community around NASA Langley. The requirements for participation in the study were that the candidates had no more than 30 dB of hearing loss between 250 Hz and 4 kHz, the subjects were within 18 and 50 years of age, and the proportion of subjects were between one-third and two thirds female. The test was conducted in the NASA Langley Exterior Effects Room (EER)

in 4, 15-minute intervals. During these intervals the recordings were played in random orders for each subject so as to remove biases from the subjects' annoyance responses. The recordings played went through post-processing in the form of filtering, upsampling, windowing, and applying gains. The subjects were asked to rate the recording they heard on a scale from "Not at all annoying" to "Extremely Annoying" as seen in Figure 1.12.

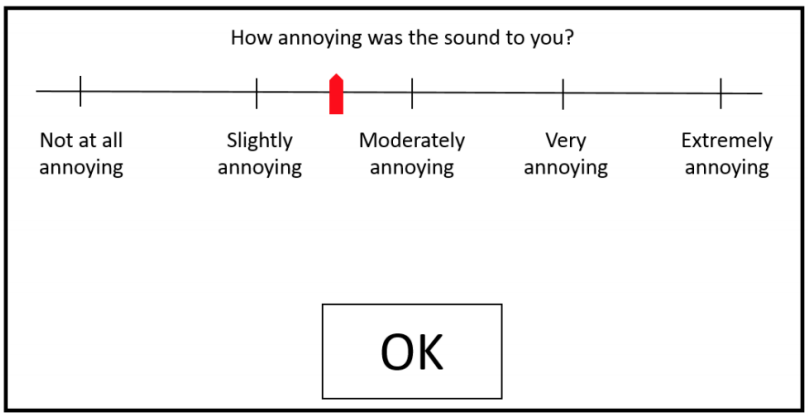


Figure 1.12: Test Subjects Response Input. [28]

Using the recordings, each sound was measured using four noise metrics: $SEL_A$, $SEL_C$, $EPNL$, and $L_5$. $SEL_A$ and $SEL_C$ is the SEL calculated using the A-weighted and C-weighted pressure of frequency content. In the study, Christian related the noise levels and the annoyance levels using a pooled linear regression method, Equation 1.10, to fit a line. In this equation,

$$\hat{Y} = \beta_0 + X\beta_1 \tag{1.10}$$

$\beta_0$ and $\beta_1$ are regression coefficients, $\hat{Y}$ is a column vector of model predicted mean responses to the sample sounds and $X$ is a column vector of noise metric values. Using this method, a coefficient of determination, $R^2$, was calculated between the dB level calculated for each metric and the annoyance level recorded by the participants. This coefficient shows the percentage of variation described by the line created from linear regression compared to the entire variation in the sample. The values of this coefficient can range between 0 and

1, with values closer to 1 representing a linear model which explains most of the variation in the response variable (annoyance) around its mean [46]. In Fields [47], it was shown that logging data in the form of this psychoacoustic study should be related in the form of specifically a linear regression rather than a quadratic or another type of regression.

The results of this regression method can be seen in Figure 1.13. The values in each point represent an average of the annoyance from all 38 participants of a single recording. Two initial observations are taken away from the results of this study:

1. Subjects found sUASs more annoying than ground vehicles. This is illustrated in Figure 1.13 because most of the markers used for ground vehicles lie below the line of linear regression and most of the markers for the sUASs lie above this line at the same or similar decibel level.

2. There is a relatively low correlation between annoyance and dB level for multiple metrics.

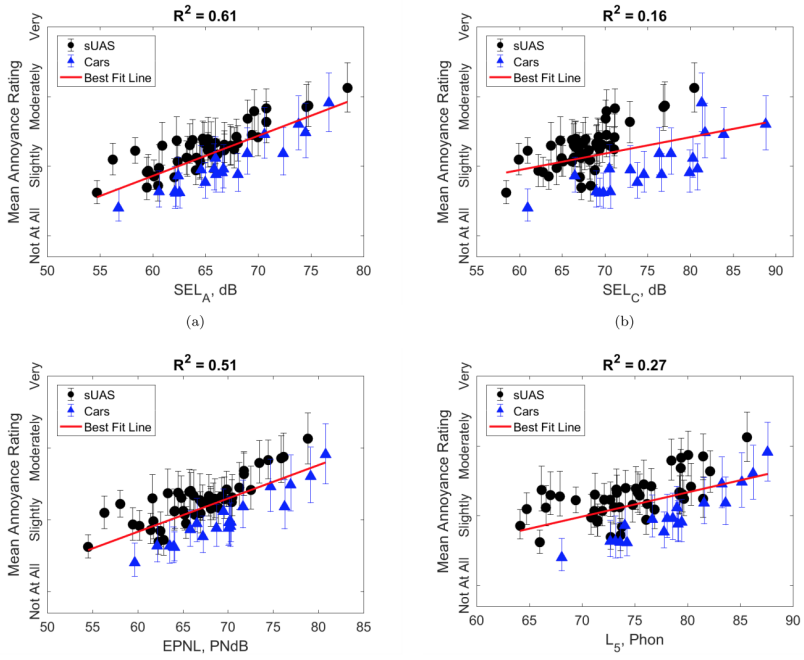


Figure 1.13: Subject Annoyance vs sUAS and Ground vehicle noise. [28]

These results have not been used to definitively comment on the usefulness of the noise

metrics because of an overlapping in confidence intervals when looking at the $R^2$ values from metric to metric; however, this does not exclude the usefulness of this data to investigate human annoyance correlation with these metrics. Christian describes different areas of future work that could come from this Psychoacoustic study:

1. Analysis of Variance (ANOVA) on samples repeated to test subjects with repeated recordings and conditions (altitude/speed combinations) to investigate the relationships between altitude, speed and annoyance

2. An exploratory work of noise metrics which include correction factors for loitering and tonality.

It is at this point in the literature review where a gap is identified. This study was conducted in 2017 and since then, this second vein of future work has not been explored

> Literature Gap: No work has been done to potentially make a new noise metric to quantify the annoyance caused by sUASs

This literature gap is the founding point for the problem formulation of this thesis. Research questions, hypotheses, and experiments will be created to fill this gap in the knowledge regarding sUAS noise.

# CHAPTER 2
# PROBLEM FORMULATION

## 2.1 RQ 1 and Hypothesis 1 Development

From the previous discussion, it can be seen that there are a multitude of noise metrics available for aircraft certification. However, their existence is not helpful for sUAS noise description if they do not capture human annoyance well. The literature gap identified in Chapter 1 leads to the first Research Question in this thesis:

> Research Question #1: How could a noise metric be created in order to better capture the relationship between sound exposure level and human annoyance to sUASs?

Before further discussion on this research question, there is a third observation that should be noted from Christian's study:

The same noise metric with the different frequency weightings was not able to correlate well with annoyance in either case. The results show that with the A-weighting only 61% of the annoyance in the noise can be explained by $SEL_A$.

An additional piece of information that assists with answering RQ1 is the spectral content of the noise from these vehicles. If one investigates the power spectra from a sUAS and a traditional rotorcraft, it can be seen that there are obvious differences between the two. Figure 2.1 shows two noise spectra which show the power in each frequency that each vehicle creates while flying overhead.

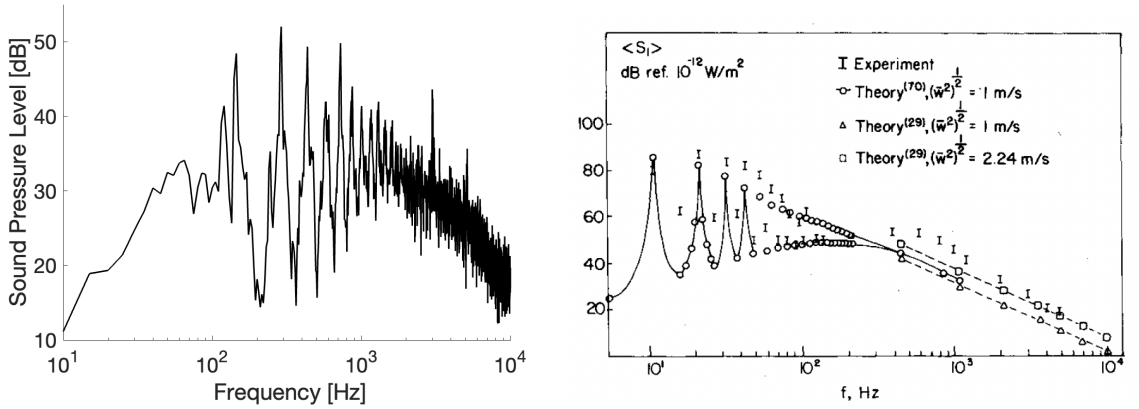


Figure 2.1: sUAS (Left) and Helicopter (Right) noise spectra comparison [48].

When observing these spectra it can be seen that the sUAS has tones in the region that are of higher annoyance toward humans as shown in Figure 1.3 such as the tone at 3 kHz. This has created the focus of this thesis to be on the weightings that are placed on frequencies in different SEL calculations and therefore on DNL and CNEL. The noise spectra for the sUAS also shows a large tonal presence; the origin of these tones cannot be known without an in depth acoustic analysis.

The spectral content and the third observation from Christian's study bring more clarity to the area that should be under investigation in the creation of noise metrics: the frequency weightings. This leads to a clarification in the wording of Research Question #1 :

> Research Question #1: How could a *frequency weighting* be created in order to better capture the relationship between sound exposure level and human annoyance to sUASs?

To answer RQ1, a new weighting, the A-weighting, and the C-weighting must be tested against the annoyance data used in Christian's study. This leads to the first Hypothesis to be tested:

> Hypothesis 1: A new frequency weighting, which allows SEL to better correlate with human annoyance caused by an sUAS noise event, will create a SEL contour area that is more indicative of sUAS noise.

## 2.2 RQ 2 and Hypothesis 2 Development

Changing the frequency weighting that is applied to noise will undoubtedly change the noise level that is calculated for any event. This can be shown in Equation 1.7 where the pressure can be weighted. This will therefore change the SEL contour area leading to the next Research Question:

> Research Question #2: How would a new frequency weighting that better correlates SEL with annoyance affect the SEL contour area?

Given observation #1 from Christian's study: that subjects found sUASs more annoying than ground vehicles, this thesis's second Hypothesis is formulated:

> Hypothesis 2: A new weighting, which allows Sound Exposure Level to better correlate with human annoyance caused by an sUAS noise event, will create a larger contour area when compared to an A-weighted SEL contour area.

In order for the weighting to better correlate annoyance with SEL, the points on the plots in Figure 1.13 will have to shift to the right, yielding a higher SEL level and therefore a larger contour area.

## 2.3 Data Acquisition

There are two major milestones that must be achieved in order to test these hypotheses:

1. Create a new, more representative noise weighting.
2. SEL noise contours using the new and current frequency weightings must be modeled.

The approach to complete these milestones is shown in a two phase methodology shown in Figure 2.2. Before the technical approach is executed, the researcher logistically organized the process of data sharing between Andrew Christian at NASA Langley and Georgia

Tech. The researchers at Langley have made this data publicly available in the form of multiple types of files:

1. The noise recordings were shared in the form of .wav files. Wav files are typically higher resolution than mp3 files as they are a "lossless" method to store recording data [49].

2. Visual trajectory files are also included within this data with information including the position of the aircraft in front of the microphone, and above the microphone. (Altitude above ground level. The position data for these files correspond to the location of the sUAS at a given time, not with respect to when a subject received the sound.

3. The human subject response data is given in the form of a 103 x 38 matrix where the 103 columns indicate the 103 sounds that were played during Christian's study and the 38 rows indicate each subject. The response data is given in values between 1 and 11 which correspond to labels on the psychophysical scale shown in Figure 1.12.

## 2.4 High-Level Technical Approach

An overview of the Technical Approach is shown in Figure 2.2. It begins in Phase 1 with creating a Design of Experiments which will allow the determination of the best weighting. This will be passed into Phase 2 where SEL contours will be created with this new weighting and the A-weighting for comparison. This technical approach is explained in detail throughout in Chapter 3.

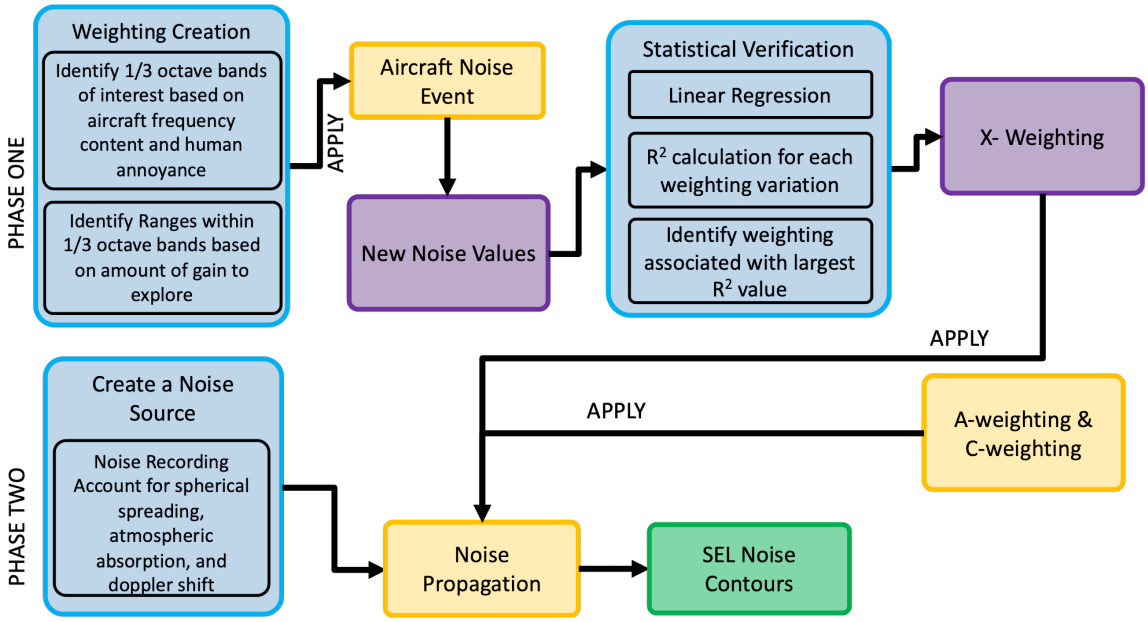


Figure 2.2: Technical Approach. [28]

# CHAPTER 3
# PHASE 1: APPROACH AND RESULTS

## 3.1 Phase 1 Technical Approach

The first step in the technical approach is to create a sequence of frequency weightings and apply them to the content of each noise recording using the process explained in Appendix A. This leads to the first Experimental Implementation Question:

> Experimental Implementation Question #1: How is a new weighting created within a reasonable weighting range?

There are multiple ways the different weightings can be made. A blind test of multiple ranges could be performed, where a large range of correction factors are tested. This approach, while comprehensive, will allow for an unnecessary amount of combinations many of which may be unhelpful. In this case, a focused Design of Experiments (DoE) was used where the ranges that are tested and the factors that are varied are specified. A full factorial design consists of all possible factor combinations in a test varying the factors simultaneously rather than one factor at a time [50]. A DoE usually has a starting place or a baseline to bring the researcher to a location closer to what should be the "optimal" solution. In this case, the baseline used will be the A-weighting; this is an appropriate baseline because it was the highest in correlation with the subjects' annoyance responses in Christian's study [28] and because it is the most widely used in current aviation noise regulations. This allows Experimental Implementation Question #1 to be answered.

In this DoE, the factors are each of the one-third octave bands from 50 Hz to 10,000 Hz. The reasoning for changing the values in one-third octave bands and not narrow band frequency is because of the method in which traditional frequency weightings (like the A- and C-weighting) are created. These are the frequency bands that are most commonly used

in aviation applications. A full factorial DoE created for all 24 frequency bands at 3 levels (high, low and baseline) would yield over 282 billion combinations. The calculation for each $SEL_X$, the SEL with each case applied as the weighting ("X" standing for experimental), lasts approximately 0.23 seconds. This leads a computation time of over 2000 years. This emphasizes the need to focus on certain bands of interest and the second Experimental Implementation question:

> Experimental Implementation Question #2: Which one-third octave bands should be varied and by how much?

The content of the noise in these flyover recordings can assist with the specification of frequency bands. In Figure 3.1, it can be seen that the point corresponding to a Phantom II flyover had a higher annoyance level but a lower SEL level. This also causes it to lie further away from the line of linear regression. In this plot, only the sUAS data are shown. This is to focus on a weighting that will characterize the noise to the sUASs rather than both the aerial and ground vehicles. This will help to satisfy the objective of creating a common "language" to describe sUAS noise, not sUAS noise and delivery van noise. The reasons for this data point to have a higher annoyance value can be speculated based on the noise spectra and spectrogram.

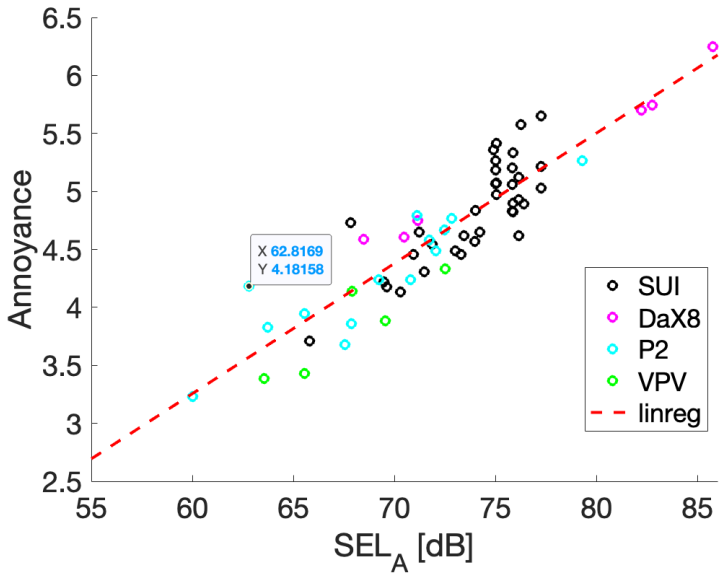


Figure 3.1: Linear Regression Location of Flyover Data

Another qualitative takeaway from Christian's psychoacoustic study is, that in a discussion between the researchers and the participants, the participants stated that "sounds which appeared to linger were judged more annoying than those which did not" [28]. This characteristic can be seen in the spectrogram in Figure 3.2. Spectrograms allow users to see the power in the frequency content throughout the flyover. In this spectrogram, frequencies at 475 Hz and 730 Hz extend the length of the flyover time, which could be attributed to the subjects complaints of lingering noises.

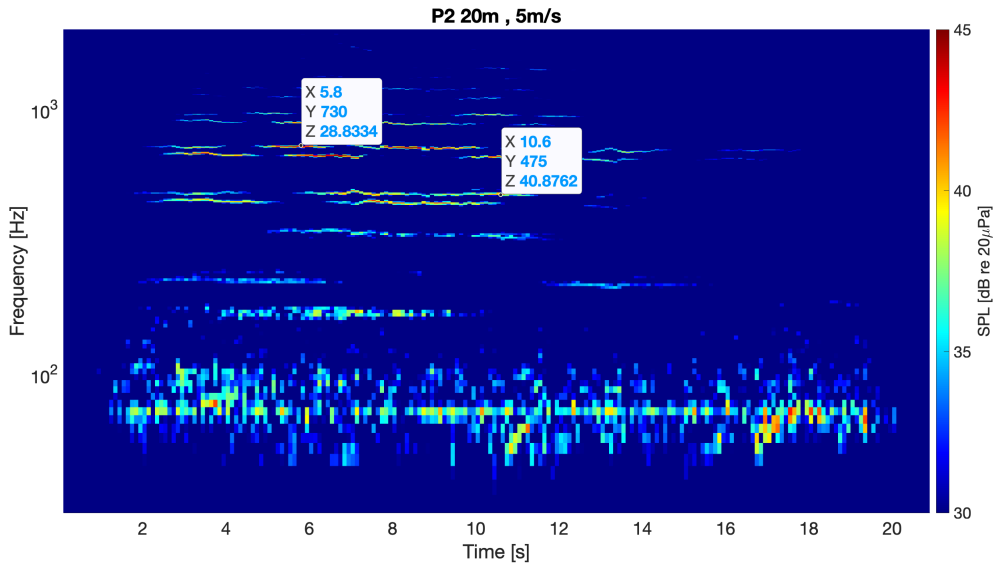


Figure 3.2: Full Flyover Spectrogram of Phantom II

Another characteristic of this noise is the large variation in frequency content in low ranges seen in Figure 3.3. This could be attributed to the presence of large tonal content variation, harmonics from the blade passage frequency and rotor airframe interaction in flight. As it was mentioned previously, this cannot be definitively stated without an in-depth acoustic analysis.

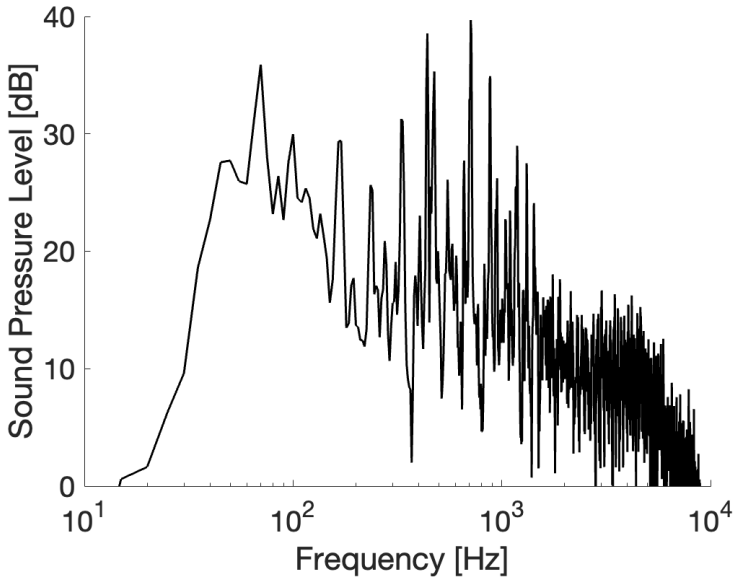


Figure 3.3: Direct Flyover Noise Spectra of Phantom II.

An investigation of the points similar to the one found in Figure 3.1 were identified, allowing for certain bands to be focused on and therefore answering Experimental Implementation Question #2. This finalized the frequency bands of 315 Hz to 5000 Hz to be varied in the DoE. The combinations used in the DoE can be seen in Figure 3.4. In this DoE, the frequency bands 315 Hz to 800 Hz were given a high and low variation of 10 decibels in correction and the frequency bands 1000 Hz to 5000 Hz were given a high and low variation of 5 decibels in correction – all relative to the baseline A-weighting curve . These ranges and frequencies were chosen to comprehensively cover bands, which have lingering frequencies throughout the flight as well as any tonality that could be present in the higher frequency domain. It was also created to capture the variation from current frequency weightings. For example, the C-, D- and E-, weightings all attenuate low frequency less than the A-weighting. This is captured in the larger +/- 10 dB for the lower frequency bands. The D- and E- weightings both mimic equal loudness curves in their correction factors. This is captured in the +/- 5 dB in the higher frequency bands in the DoE. This DoE yielded 1,594,323 combinations with a computation time of approximately 4.25 days.

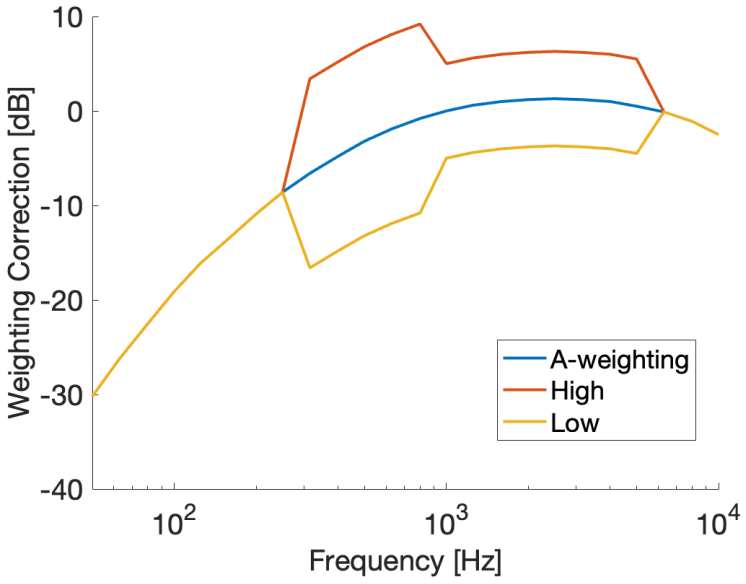


Figure 3.4: Design of Experiments Ranges and Frequency Specification.

In order to combat any biases that could have been made in the weighting, an equal

amount of each sUAS recording was used. Figure 3.5 shows that a large majority of the data is from the SUI Endurance sUAS. To remove any biases, 5 recordings from each vehicle were taken from a variety of locations on Figure 3.1 so as to gain a variety of subject responses and SEL (A-weighted) levels. Five recordings were taken from each vehicle as the VPV had the limiting amount of recordings.

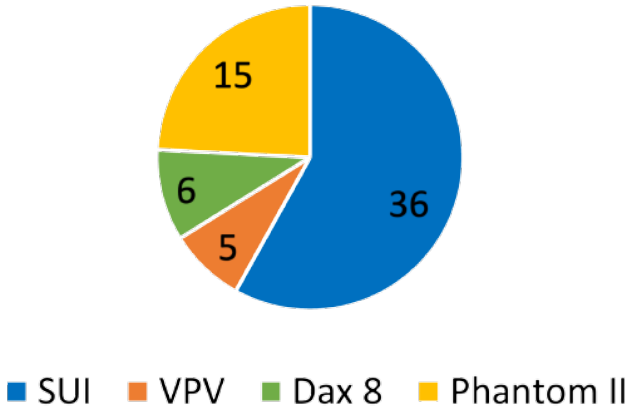


Figure 3.5: Amount of data from each Vehicle in recording set.

The recordings used were strategically picked to capture a wide array of the annoyance and SEL levels calculated. In the following figures, the A-weighted SEL values and annoyance values are shown for each of the recordings that were used.

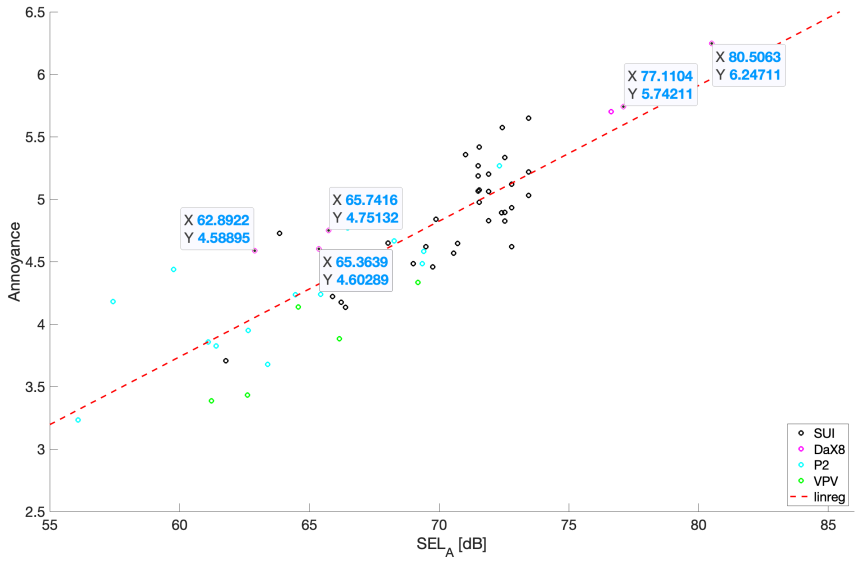


Figure 3.6: DaX8 recordings used in DoE.

The points chosen from the data available on the DaX8 was simple. There were only 6 data points from which to choose 5, shown in Figure 3.6. Making sure to keep the choice of recordings diverse, only one of the two data points close to (77.1, 5.7) was chosen. The rest were chosen by default.

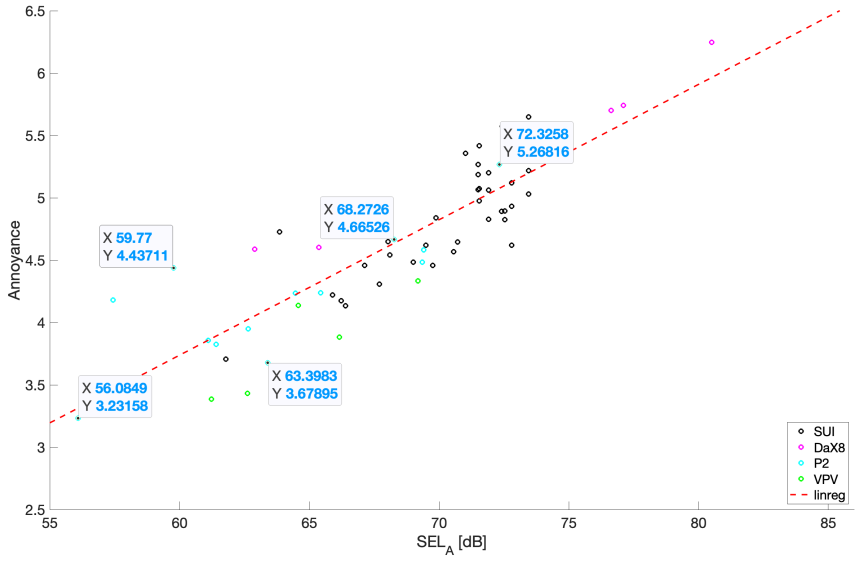


Figure 3.7: Phantom II recordings used in DoE.

The points chosen from the data available on the Phantom II, like all other vehicles, has the theme of diversity of choice. Of the points chosen, the highest and lowest in SEL were chosen, as well as one close to the line of linear regression, one further away and one that was further away from all the points previously chosen. These points are shown in shown in Figure 3.7.

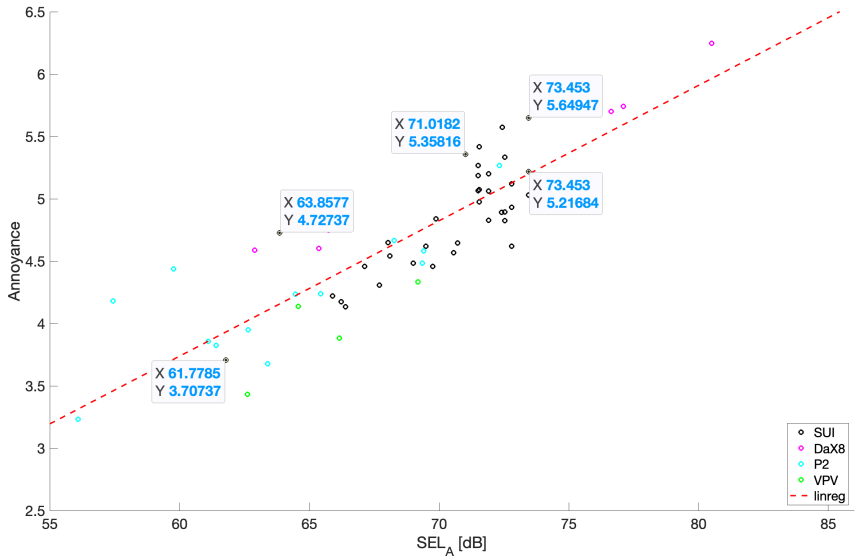


Figure 3.8: SUI Endurance recordings used in DoE.

The points chosen from the data available on the SUI Endurance was more complicated being that there were 6 times the amount of choices as the DaX8. Again to ensure diversity of $SEL_A$ value and annoyance rating, the points were chosen to be on the perimeter with 2 closer to the center. The highest and lowest data points in annoyance were chosen but also a data point directly on the line of linear regression as well as a point furthest away from this line: (63.8, 4.7). The points chosen are shown in Figure 3.8.

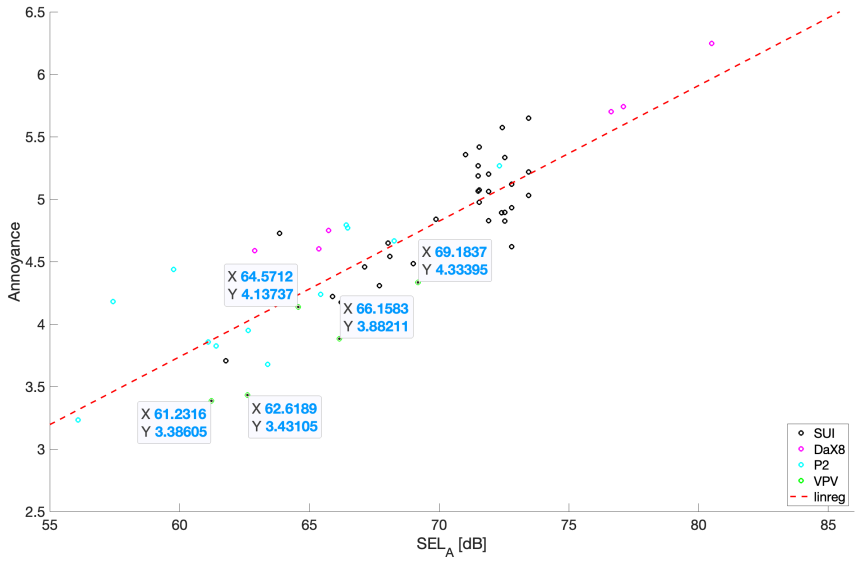


Figure 3.9: VPV recordings used in DoE.

The cases chosen for the VPV were simple as there were only 5 recordings to choose from and therefore all had to be used for the DoE. This is shown in Figure 3.9.

For each of the cases in the DoE, the coefficient of determination, $R^2$, was calculated using a linear regression to be comparable with the original data in Christian's study. The case in the DoE with the largest $R^2$ value was chosen as the weighting to be used in Phase 2.

## 3.2 Phase 1: Results

The final weighting with the highest coefficient of determination is shown in Figure 3.11. This is the weighting that is used in Phase 2 of the approach. A noticeable trend in all of the weightings with the highest coefficients of determination was for the weighting correction to be from the low variation in the DoE (the yellow line in Figure 3.4) in the 630 Hz frequency band. It is not clear exactly what has caused this; the physical reason could be found through an in-depth acoustic analysis. Investigating the spectrograms and the noise spectra of the recordings used (all of which can be found in Appendix C), shows large

variation in the lower frequencies. There is no clear reason through spectrograms and noise spectras alone.

The areas of larger "peaks" in the weightings have been highlighted in select figures in Appendix C. The transparent shading colored green, pink, and white atop the figures represents the lower and upper bounds of the 500 Hz, 800 Hz, and 1600 Hz one-third octave frequency bands respectively. This shading allows one to more easily observe any strong tonal content that could be lasting for the duration of the recording. In Table 3.1, it can be seen which recordings have tonal content which lingers during the recording for each one-third octave band highlighted.

Table 3.1: One-Third Octave Bands With Lingering Tones.

| Figure # | 500 Hz | 800 Hz | 1600 Hz |
|---|---|---|---|
| Figure C.7 | | ✓ | |
| Figure C.11 | ✓ | ✓ | ✓ |
| Figure C.13 | ✓ | ✓ | |
| Figure C.15 | ✓ | | |
| Figure C.17 | ✓ | ✓ | ✓ |
| Figure C.23 | ✓ | | |
| Figure C.27 | ✓ | ✓ | |
| Figure C.31 | ✓ | ✓ | ✓ |

The same figure as the one shown in Figure C.17 and Figure C.31 are shown in Figure 3.10.

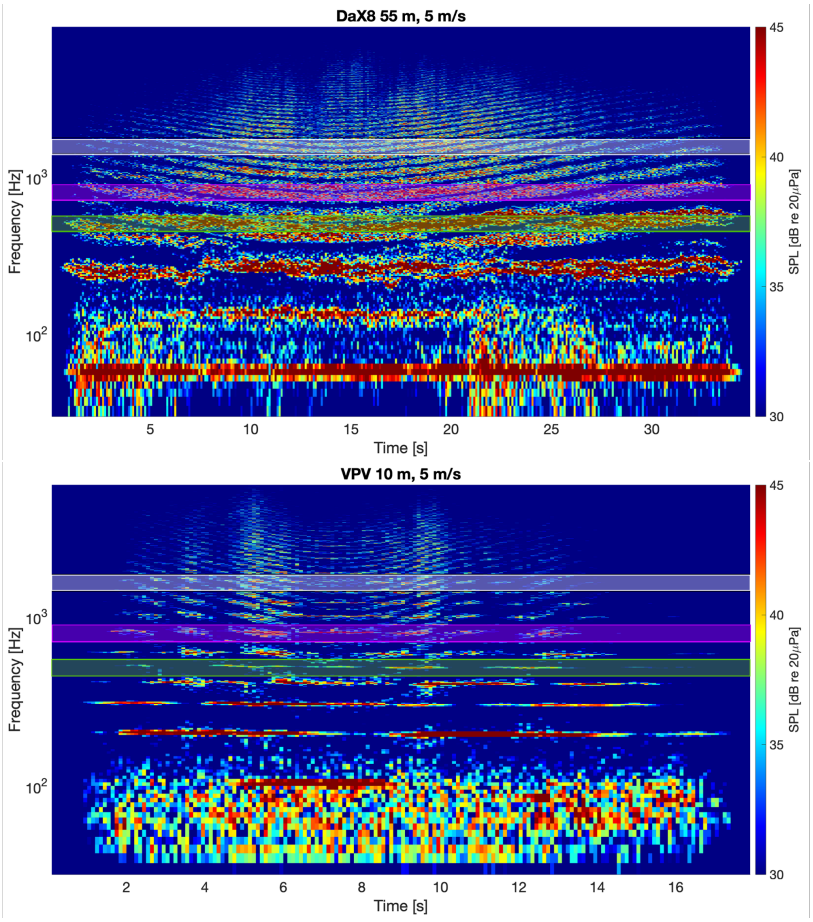


Figure 3.10: Spectrograms with High and Lingering Tonality.

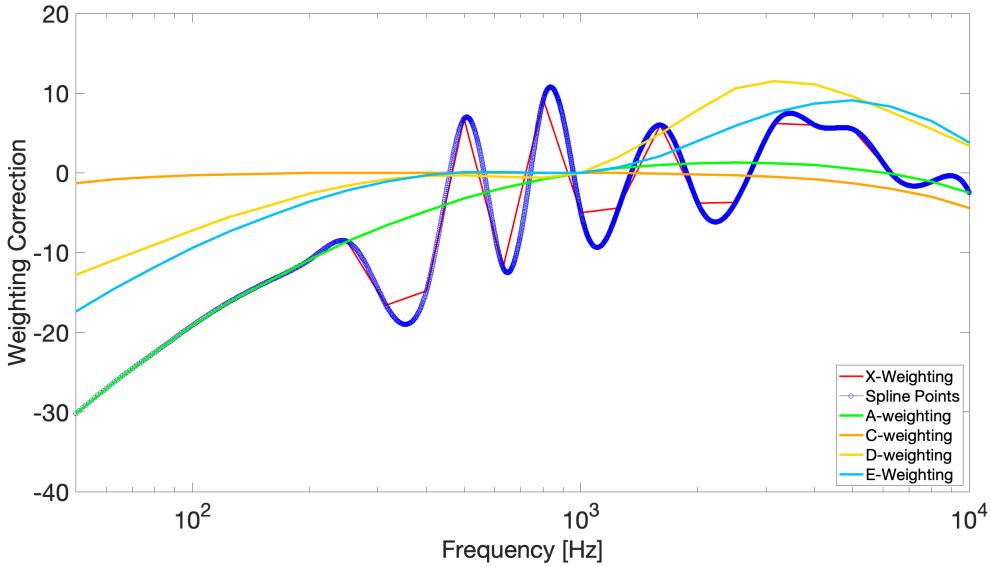


Figure 3.11: Final weighting found from DoE.

Figure 3.12 shows how the original points have shifted in SEL value by using the X-weighting instead of the A-weighting. This is a rightward shift, which is the first indication that the SEL contour area will be larger for the X-weighted SEL when compared to the A-weighted contour.

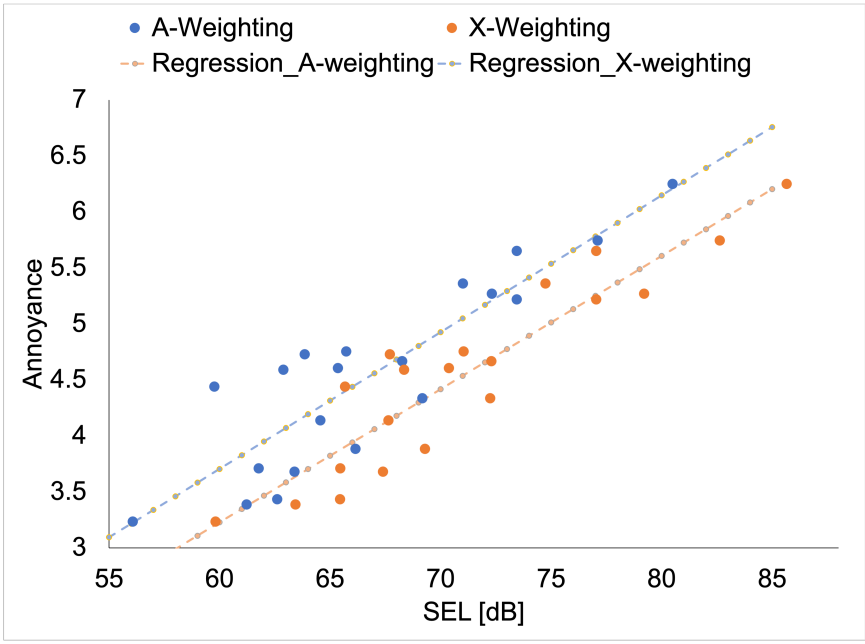


Figure 3.12: Linear Regressions of A-weighting and X-weighting.

It is important to note that the coefficient of determination values have been skewed from the original values of 0.16 and 0.61 in the results from Christian's study for $SEL_C$ and $SEL_A$ respectively . The values of $R^2$ using these 20 recordings and the corresponding annoyance values is found in Table 3.2. These values are much higher than the ones in the study. One reason for this being the absence of the ground vehicles when they were calculated and another being the 20 recordings chosen for investigation.

Table 3.2: Coefficient of Determination for different weightings.

| Weighting | $R^2$ |
|---|---|
| A-weighting | 0.784 |
| C-weighting | 0.549 |
| D-weighting | 0.734 |
| E-weighting | 0.730 |
| X-weighting | 0.853 |

## 3.3 Chapter Summary

In this chapter, Research Question #1 is answered by taking advantage of the method of design of experiments in a full factorial approach. This allowed a new weighting with a coefficient of determination higher than what was produced by the A-weighted SEL. In this weighting, certain one-third octavevbands were highlighted as contributing to annoyance more than others. The answer regarding why this is the case is difficult to precisely answer without an in depth acoustical study. With the finding of a new weighting, Phase 2 can be started where it, and the A- and C- weighting, can be applied to SELs to understand how they will change the contour area.

# CHAPTER 4

# PHASE 2: APPROACH AND RESULTS

## 4.1 Technical Approach

### 4.1.1 Choosing a Noise Propagation Method

Phase 2 of this thesis has the objective of directly answering RQ #2 and testing Hypothesis #2. In order to complete these milestones, a method for creating SEL contours is necessary.

Noise propagation is a highly researched topic especially for military purposes in minimizing detectability and maximizing stealth. For civilian purposes it is researched to minimize community disturbance. There are multiple software packages that have been developed at universities and by governmental entities like the FAA and NASA that predict and model noise, many of which also have the capability to generate SEL contours. These vehicles are of a much smaller aircraft regime compared to what is usually modeled. NASA's Aircraft Noise Prediction Program (ANOPP) is a widely used software with the capability to predict the propagated noise levels from high fidelity computational fluid dynamics (CFD) analyses of aircraft. ANOPP is in the development stages of predicting sUAS noise in its submodule the Propeller Analysis System (PAS) within ANOPP's second version, ANOPP2. PAS uses a series of its own submodules: the Improved Blade Shape Module, the Integrated Blade Aerodynamic Module, the Subsonic Propeller Noise Module (SPN) to name a few, that allow the system as a whole to predict noise from a propeller. In Figure 4.1, ANOPP-PAS's prediction is compared against the Broadband Acoustic Rotor Codes (BARC) and experimental measurements in NASA Langley's anechoic chamber at this particular sUAS's blade passage frequency. It can be seen that PAS has adequate predictive capabilities for sUAS noise.

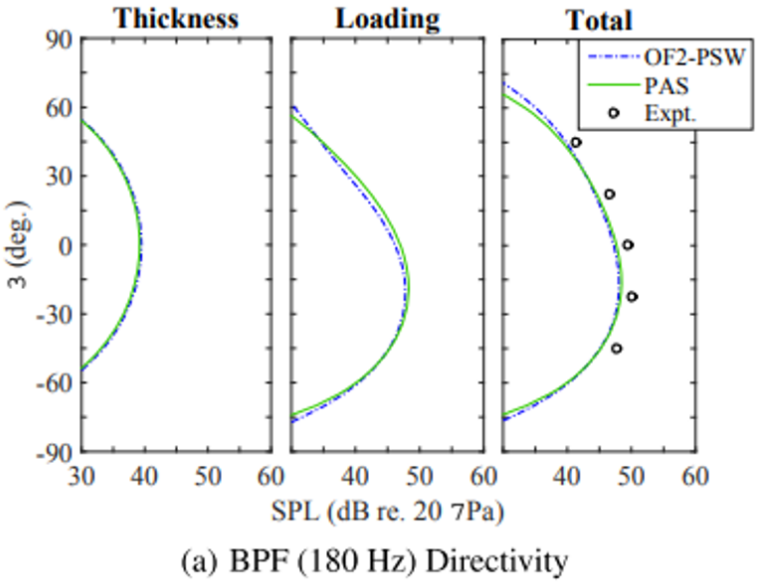


Figure 4.1: PAS Performance Compared to Experimental and Higher Fidelity Modeling Approaches [51].

Predictive capabilities are not necessary for this phase of the approach given that the noise sources are already available in the form of the noise recordings given from Christian's study [28]. This necessitates a down selection of different noise *propagation* codes. In Table 4.1 ANOPP, BARC, Pennsylvania State University's WOPWOP (PSU-WOPWOP), and the FAA's Aviation Environmental Design Tool (AEDT) are compared given their capabilities and the requirements needed for this work. The propagation method must be able to use a sUAS recording as a noise source and propagate this source to modeled receivers. It must also be computationally moderate. BARC is a noise prediction software for blade wake interaction and rotor self noise rather than a noise propagation capability. AEDT uses Noise-Power-Distance (NPDs) curves which can be made by ANOPP in order to model noise propagation and is not computationally intense in its noise propagation. ANOPP uses Acoustic Data Files (ACD) as input files which contain information about SPL values at a combination of power settings and Mach numbers for each polar/azimuthal angle. This is information that can be gathered from the noise recordings and trajectory files. PSU-WOPWOP also has similar capabilities to ANOPP. ANOPP and PSU-WOPWOP can be

computationally intense if given noise sources in the form of high fidelity CFD results. Since this is not the case, they are not as computationally intense. A distinguishing factor between ANOPP and PSU-WOPWOP is that the researcher is more familiar with ANOPP and therefore makes it the selected program for use. However, it is recognized that NPDs could be made in ANOPP for a sUAS allowing this information to be given to AEDT. This makes AEDT a third feasible alternative. In order to explore as many contours as possible, ANOPP was utilized to minimize the time required setting up the computational tools.

Table 4.1: Noise Propagation Programs

| | ANOPP | BARC | PSU-WOPWOP | AEDT |
|---|---|---|---|---|
| Use Noise Recordings as Sources | Y | N | Y | N |
| Propagate Noise to a Receiver | Y | N | Y | Y |
| Computationally Intense | N | Y | N | N |

### 4.1.2 Noise Recording to ANOPP input

As mentioned previously, ANOPP receives input ACD files with noise information at a given receiver location, Mach number, and power setting. This information can be taken from the noise recordings that are within the NASA data package received. There are a total of 62 recordings available in the package from 4 different vehicles at a variety of altitudes and speeds. After one of these has been selected the .wav file and trajectory file needs to be analyzed for the necessary information. In the ANOPP ACD files, the SPLs for polar angles ranging between 20 degrees and 160 degrees are needed in increments that are chosen by the user. In this case, the increments were 10 degrees; this was so that the recordings did not overlap more than 50% from increment to increment. This can be calculated from the recordings because of the accompanying trajectory files which recorded the spatial information about the vehicle at a frequency of 50 Hz. Because this is the information taken by a microphone during a flying forward operation, Doppler effects,

atmospheric effects, and spherical spreading will be present. In order to use ANOPP, these effects should be removed so as to make sure they are not redundantly accounted for when ANOPP propagates the sound. Figure 4.2 shows a diagram of how the polar angles can be calculated at different points in the flight. The azimuthal angle will always be zero because the sUASs were all flying directly over one microphone. Because of this, all of the contours will be symmetric about the Y axis.

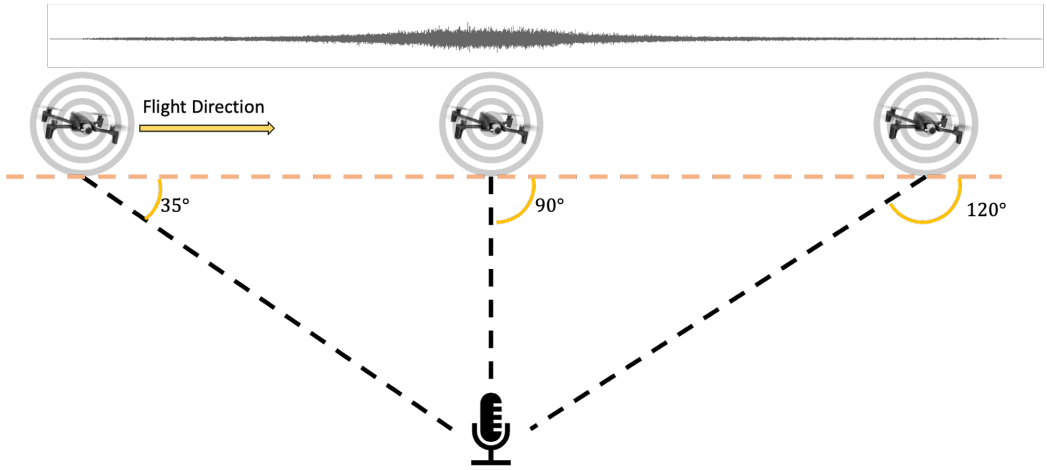


Figure 4.2: Example of Different Points in Trajectory to Extract SPL Information.

### 4.1.3 Accounting for Spherical Spreading, Atmoshperic Effects and Doppler Shift

The ACD file models the SPL values that are given to it as if the noise source is a 1 ft diameter sphere flying through the air with the noise characteristics that were extracted from the recordings. To account for spherical spreading, the SPL values must have a correction factor added to it using this equation:

$$SPL_{corr} = SPL + 20log_{10}\left[\frac{R_1}{R_2}\right] \tag{4.1}$$

where $R_1$ is equal to the distance between the sUAS and the microphone minus 1 foot and $R_2$ is equal to 1 foot. $SPL$ is the value of the SPL at the microphone and $SPLcorr$ is the value of the SPL at the one foot sphere.

Calculating the Doppler shift given a 5 m/s flyover yields a 1.5% change in the narrow-

band frequency values. This was deemed to be negligible enough that it can be ignored. When investigating the effects of the atmosphere on noise propagation, a major contributor is the humidity and wind on the day of the flights. The noise propagated over a *large* distance has the opportunity to change the spectral content considerably. However, in this recording, the vehicles are a maximum of 233 feet away from the microphone. The instances in which atmospheric absorption would be a main concern is 1000s of feet between the source and the receiver for an aircraft flyover. Atmospheric effects could make differences to frequencies above 10 kHz, however that is outside of the frequencies of interest for this calculation. Therefore, the atmospheric effects were deemed negligible.

## 4.2 Phase 2 Results

The process for creating the SEL contours is shown in Figure 4.3 where the different software and file types inputted and outputted are also shown.

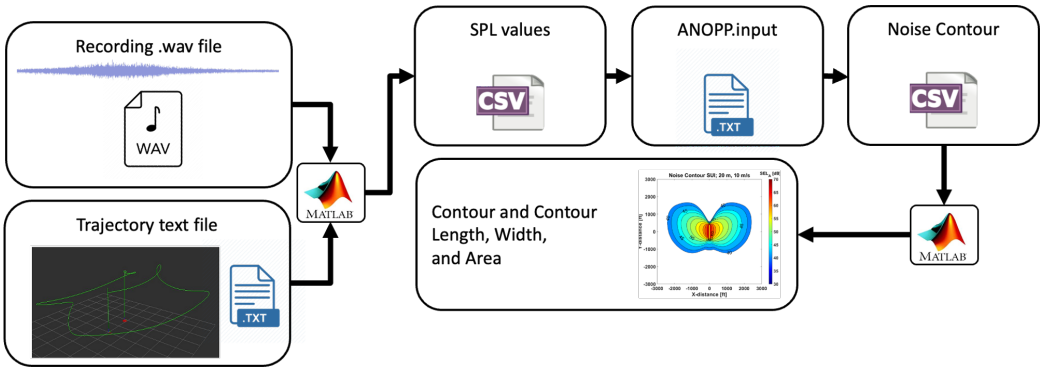


Figure 4.3: MATLAB, ANOPP2 and Available Recording and Trajectory Data Used to Create SEL Contours.

The flyovers analyzed were the SUI Endurance (SUI) at 20 m above ground level (AGL) and flying at 10 m/s, the Phantom 2 (P2) at 20 m AGL and flying at 10 m/s, the SUI at 30 m AGL and flying at 5 m/s, and the SUI at 20 m AGL and flying at 10 m/s. The specifications of the SUI and P2 can be seen in Table 1.1. These four flyovers were chosen because 1) they were not used in the creation of the weighting and 2) because they demonstrate how a variation in altitude, speed and vehicle will affect the noise contours simulated.

The simulations for all contours were created on a 3000 ft by 3000 ft grid with simulated receptor points every 50 feet. This proved to be high enough resolution while staying within ANOPP2's simulation limits.

### 4.2.1 Phantom 2: Altitude= 20 m, Speed= 10 m/s

The contours generated for all flyovers include the A-, C- and X-weighted SELs. The A- and C- weightings were chosen as they are the weightings that were used in Christian's study [28]. The contours are shown in Figure 4.4. The $SEL_A$ contour shows the flight direction and the flight path the vehicle took in the ANOPP2 simulation. This is constant for the rest of the contours that will be shown.

The reasoning for the contour differences in shape or area size cannot be definitively commented on without an in-depth acoustic analysis through the use of high-fidelity CFD and anechoic chamber testing; however, reasons for the shapes can be speculated upon.

A cursory glance of these three contours highlight how the A- and X- weightings direct the frequencies that are prominent in their weightings much differently than the C-weighting. Recall that the C-weighting barely attenuates any frequency; this can be seen in Figure 1.4. The A- and X-weightings both attenuate low frequencies, i.e those below 200 Hz, which can also be seen in Figure 1.4. This leads to the possible conclusion that there could be strong low-frequency content emanating in front of the vehicle and behind it during the flyover.

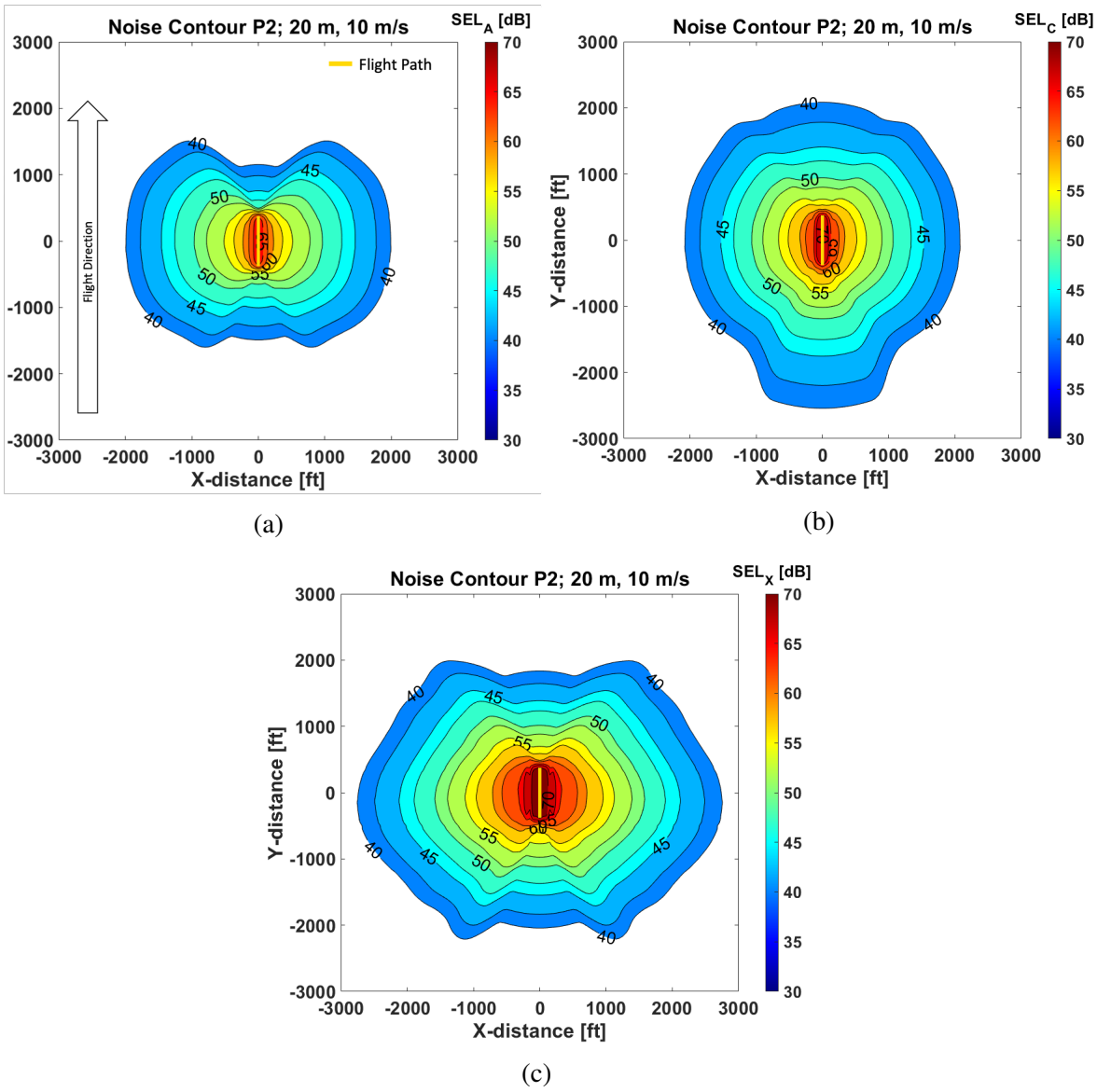


Figure 4.4: A-,C-, and X-weighted contours Phantom 2.

A characteristic of the A- and C- weighted contours that is not as apparent as the length of the C-weighted contour is the rounded shape of these contours. Laterally, it can be seen that the A- and C-weightings cause a round contour in the positive and negative x-directions. This is accentuated more in the X-weightings. The reason the A- and C-weighting contours look similarly (laterally) can be attributed to the similarities in these curves in the mid- and high- frequency region of their weightings, which can be seen in Figure 1.4. The way in which the A- and C-weightings are weighting the high and mid

level frequencies could cause their lateral shapes to be similar. The variation in weighting in the X-weighting to these same one-third octave bands cause the lateral shape to differ.

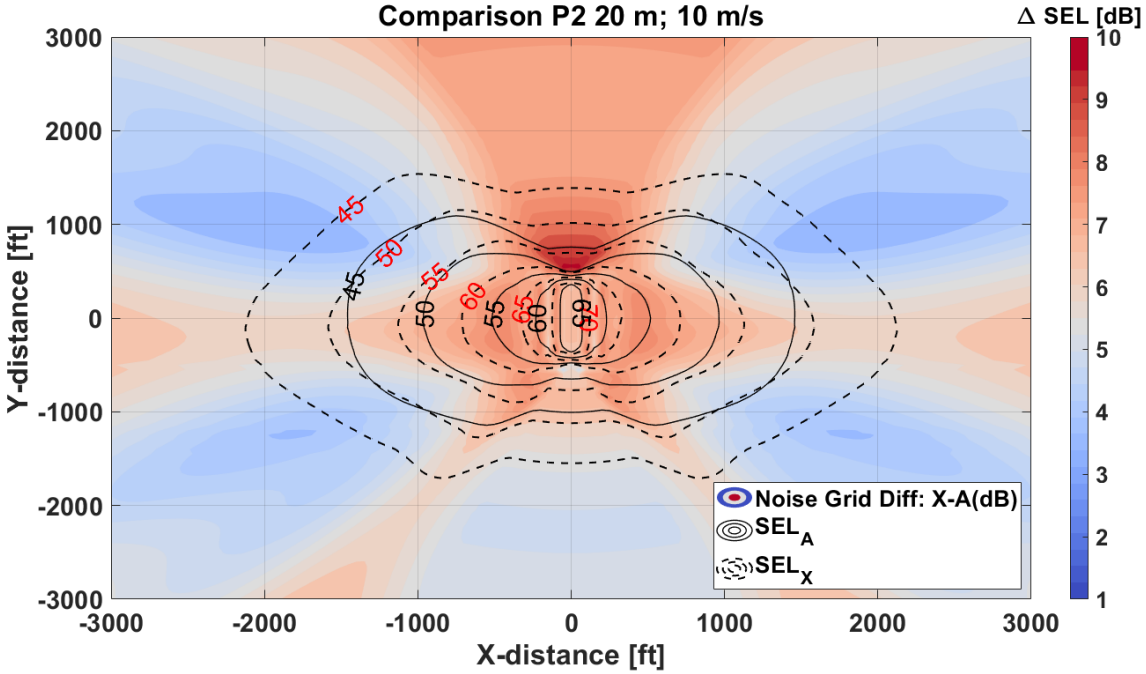


Figure 4.5: Difference between the X and A weighting Contours

Figure 4.5 shows the difference in the A- and the X- weighted SEL contours by plotting the dB difference at each receptor point and using a diverging color map to distinguish larger differences from smaller ones. The location with the largest difference is in front of the vehicle with some deltas being as high as 10 dB. This figure also makes it easy to see the how large the change in area is for each contour. For example, the 55 dB dotted line (the $SEL_X$) is approximately the same size as the 50 dB solid line (the $SEL_A$).

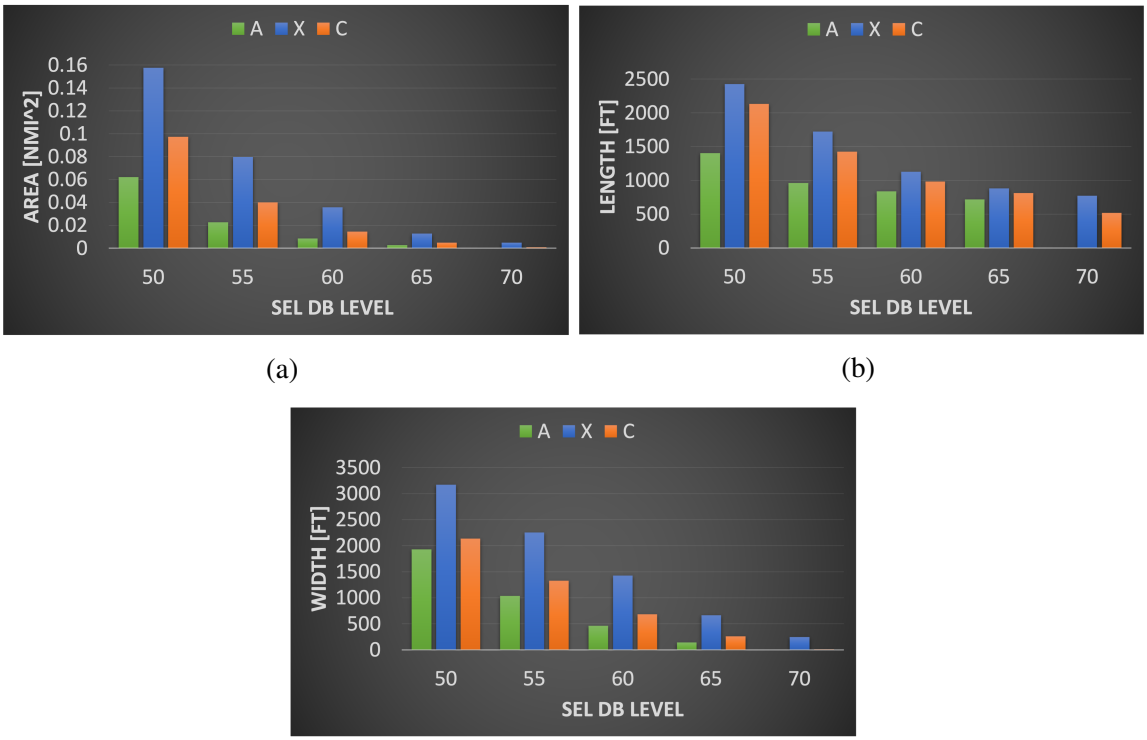


(a) (b)

(c)

Figure 4.6: Length, Width and Area of Contours for the Phantom 2.

Figure 4.6 shows the values for the area, length and width of the 50 dB, 55 dB, 60 dB, 65 dB, and 70 dB contours. Across all contour measurements for length, width and area, the X-weighting is larger. In fact, the A-weighting does not have a 70 dB contour in general. Because of this, in Figure 4.16, the data for the P2 and the SUI at 20 m AGL and 10 m/s is excluded.

### 4.2.2 SUI Altitude= 20 m, Speed= 10 m/s

Figure 4.7 shows how the directivity for the SUI at the same flyover conditions is much different than the P2. The same behavior in the C-weighted contour is seen with a larger bulge toward the bottom of the contour (behind the aircraft during its flight) and a smaller bulge in front of the aircraft as well. All three contours have a similar rounded lateral contour shape. A commonality between the X- and the C-weighting is a small pocket of higher noise level right in front of the aircraft at the end of its trajectory. This is highlighted

by the difference plot, Figure 4.8, as the brighter red region just ahead of the flight path with a 7 dB delta.

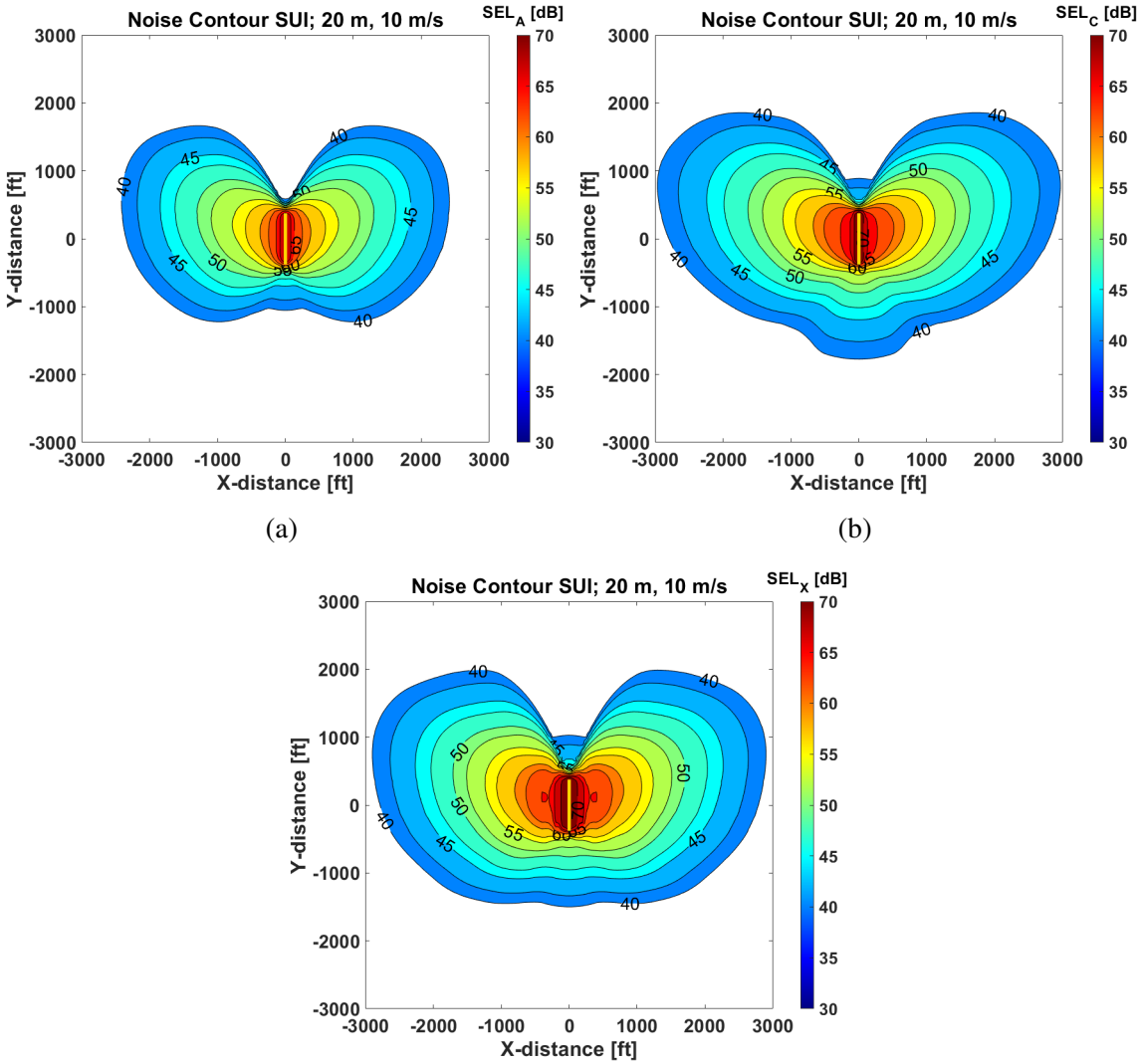


Figure 4.7: A-,C-, and X-weighted contours for the SUI Endurance.

An interesting characteristic about Figure 4.8 is the halo of lower noise difference around the 60 dB contour for the A-weighting. This is shown as a ring of lighter blue with pink inside and outside of it. This shows that the amount of noise difference does not monotonically increase or decrease in this region closer to the flight.

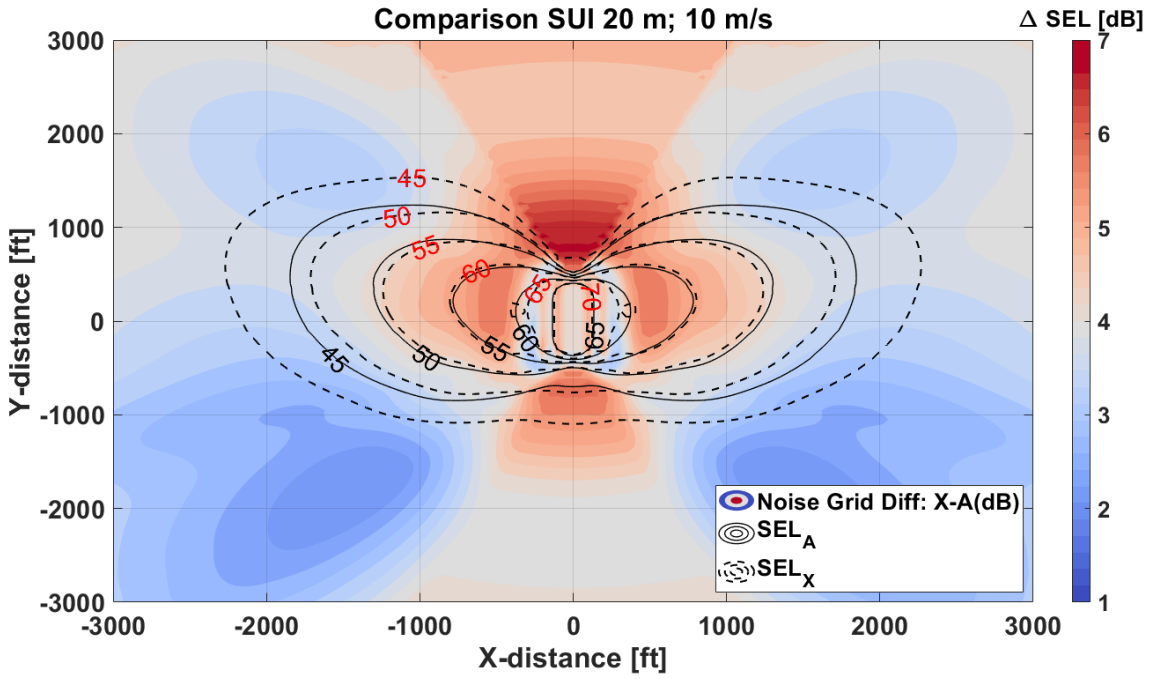


Figure 4.8: Difference between the X and A weighting Contours

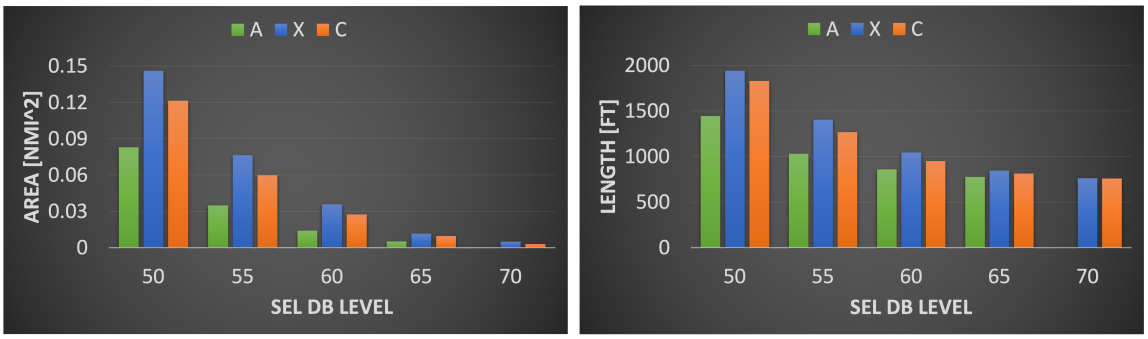


(a)




(b)

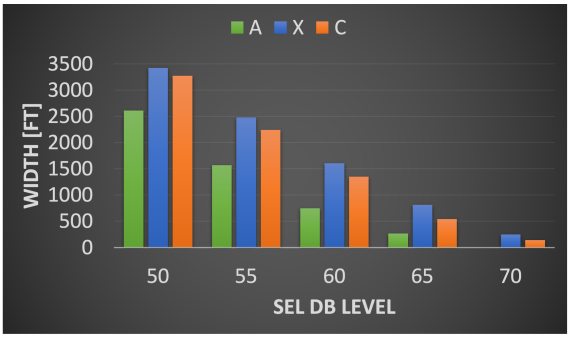


(c)

Figure 4.9: Length, Width and Area of Contours for the SUI.

Finally, in looking at the length, width, and area of the contours it can be seen that the differences in these characteristics are not as large as they were for the P2. This can also be seen in Figure 4.16. The grey bars (symbolizing the P2) is much larger than the green bars (symbolizing the SUI at the same flight conditions).

### 4.2.3 SUI Altitude= 20 m, Speed= 5 m/s

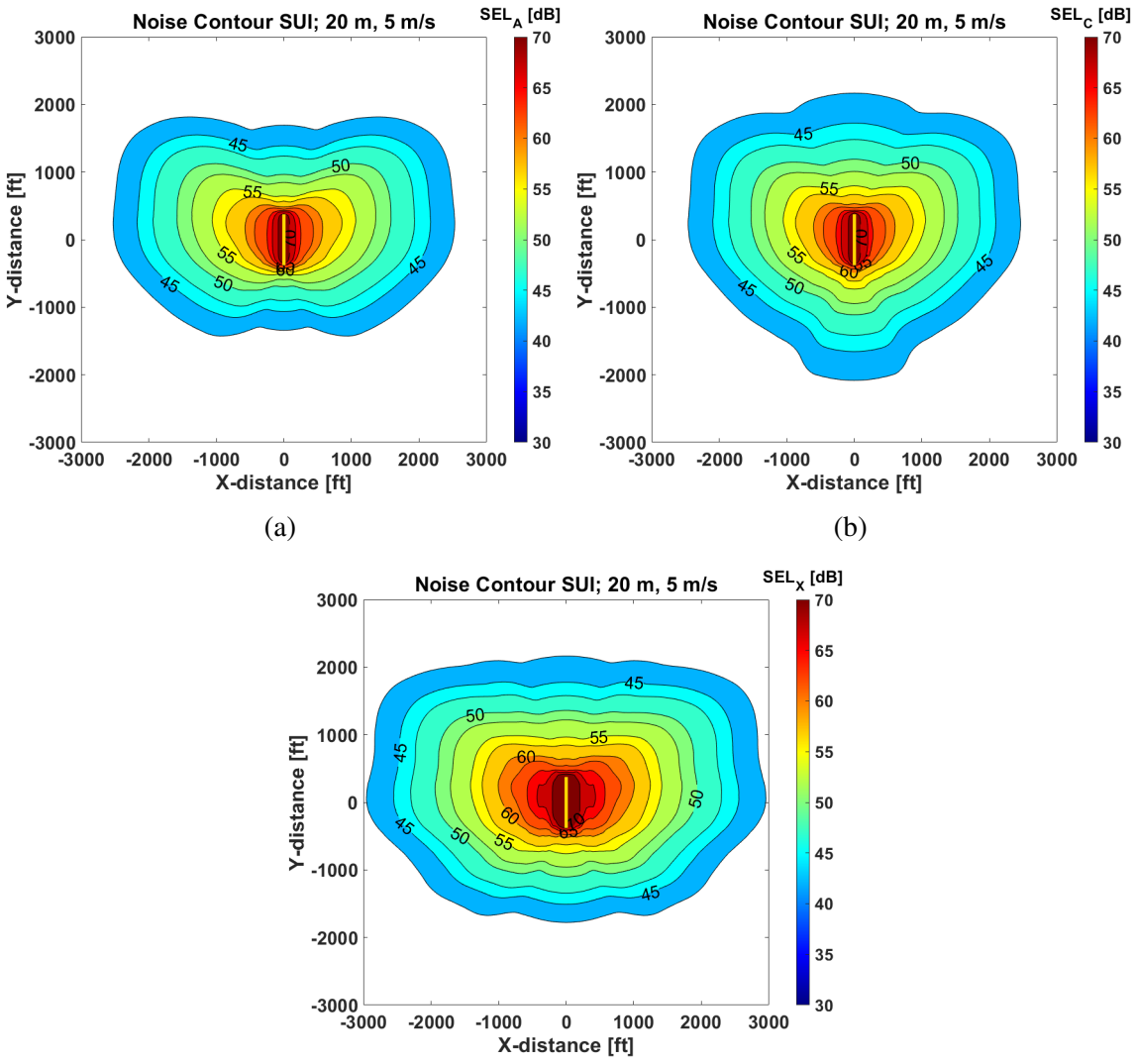


Figure 4.10: A-,C-, and X-weighted contours for the SUI Endurance 20 m and 5 m/s.

The noise contours for the SUI at 20 m and 5 m/s have similarities to both the P2 and the SUI at 20 m and 10 m/s. In the C-weighted contour, the elongation of the contours from the P2 figures (Figure 4.4) is seen similarly. Additionally the "butterfly" effect of the SUI contours is seen in the A-weighted contour but is more rounded similarly to Figure 4.7. In Figure 4.11, the amount of area that is pink or red colored is the least out of all of the flyovers.

The contour area, length and width is again larger for the X-weighting when compared to the A- and C- weightings for all dB levels. The contour lengths have the smallest percentage differences from the A-weighting (as shown in Figure 4.16) however the width differences are significant.

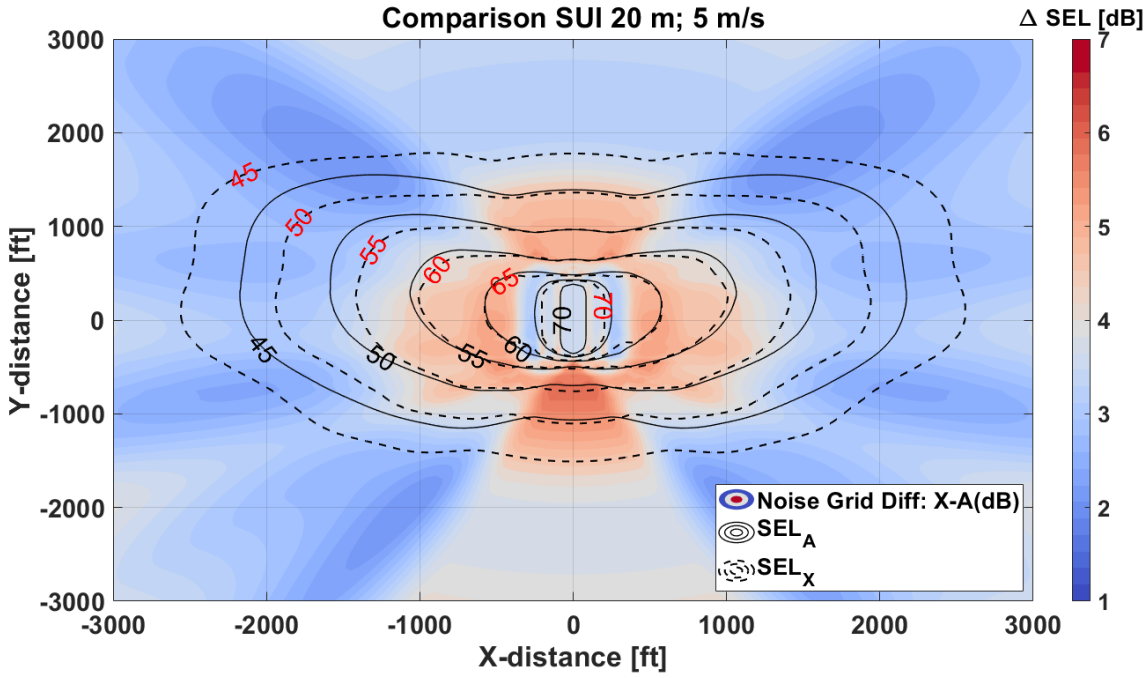


Figure 4.11: Difference between the X and A weighting Contours for the SUI Endurance 20 m and 5 m/s

The length, width and area of this flyover is larger than the SUI flying at 10 m/s. This is due to the trade-off between a higher amount of noise being generated in a smaller amount of time with a faster flyover. Because SEL is an integrated quantity (see Equation 1.7), a flyover that lasts a longer amount of time has the ability to be louder because of the duration

of the flight.

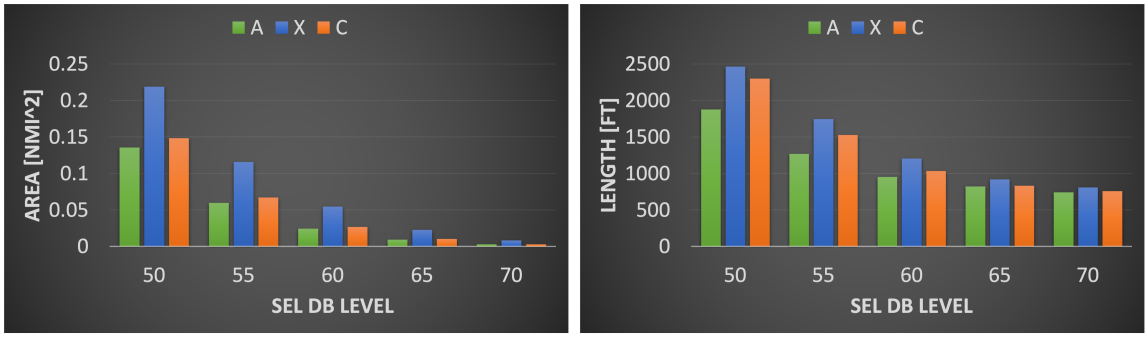


(a) (b)

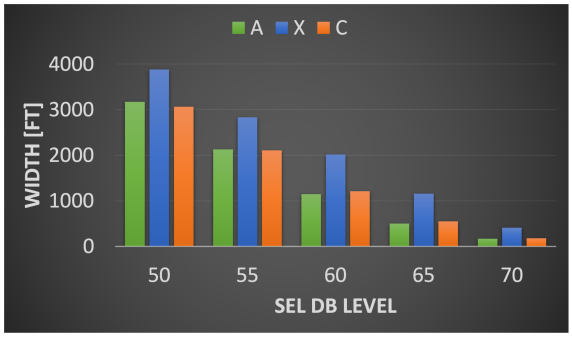


(c)

Figure 4.12: Length, Width and Area of Contours for the SUI (altitude = 20m , speed = 5 m/s).

### 4.2.4 SUI Altitude= 30 m, Speed= 5 m/s

The contour from a SUI flyover at a higher altitude and slower speed is shown in Figure 4.13.

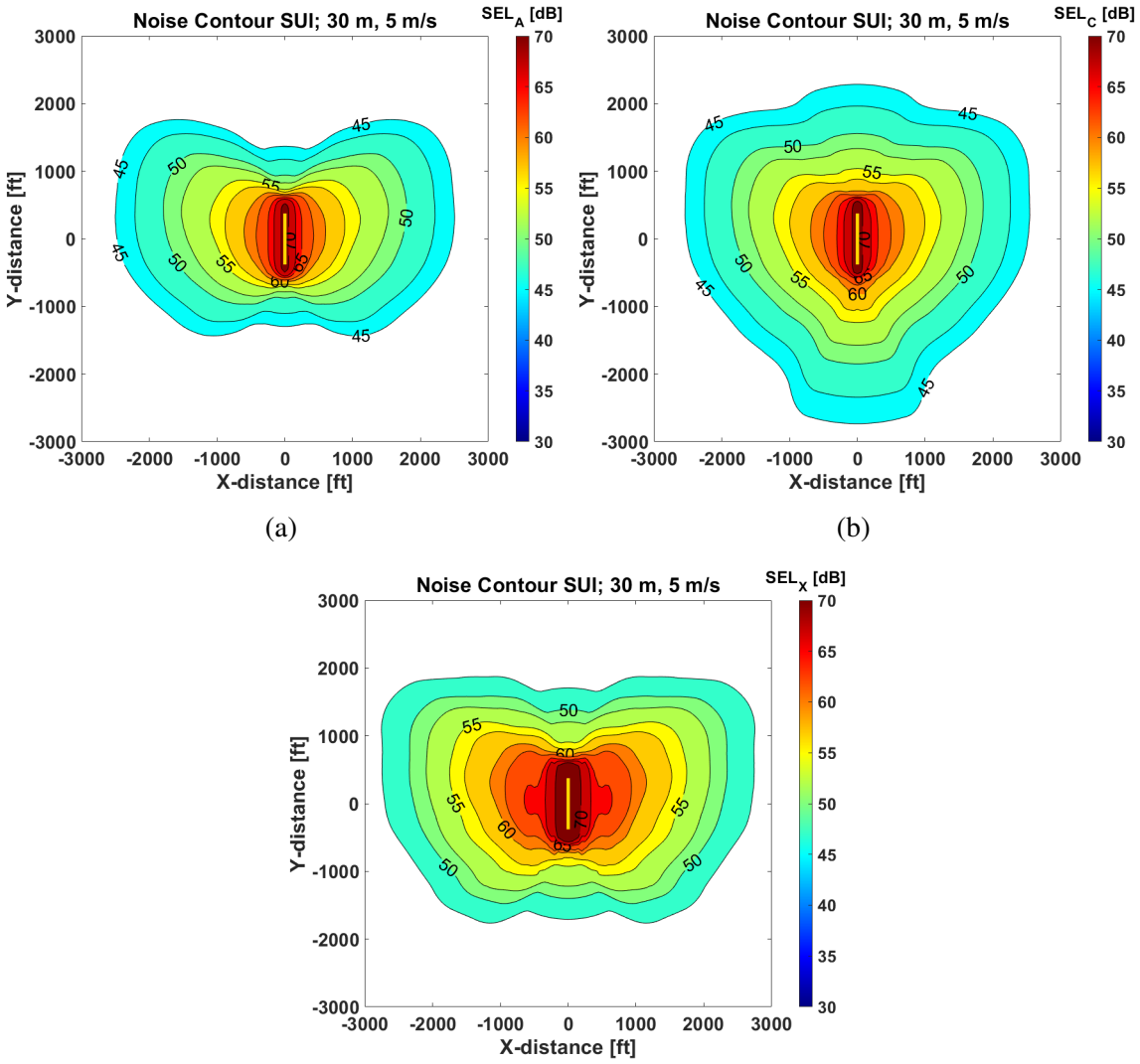


Figure 4.13: A-,C-, and X-weighted contours for the SUI Endurance 30 m and 5 m/s.

The areas which have a higher delta in Figure 4.14 are similar to the areas that have higher deltas in Figure 4.11 for the SUI flying at the same speed. However, the amount of area with the larger deltas is larger for the flight at 30 m altitude AGL than 20 m altitude AGL. This can be seen by the amount of area that is pink/red on Figure 4.11 and

Figure 4.14.

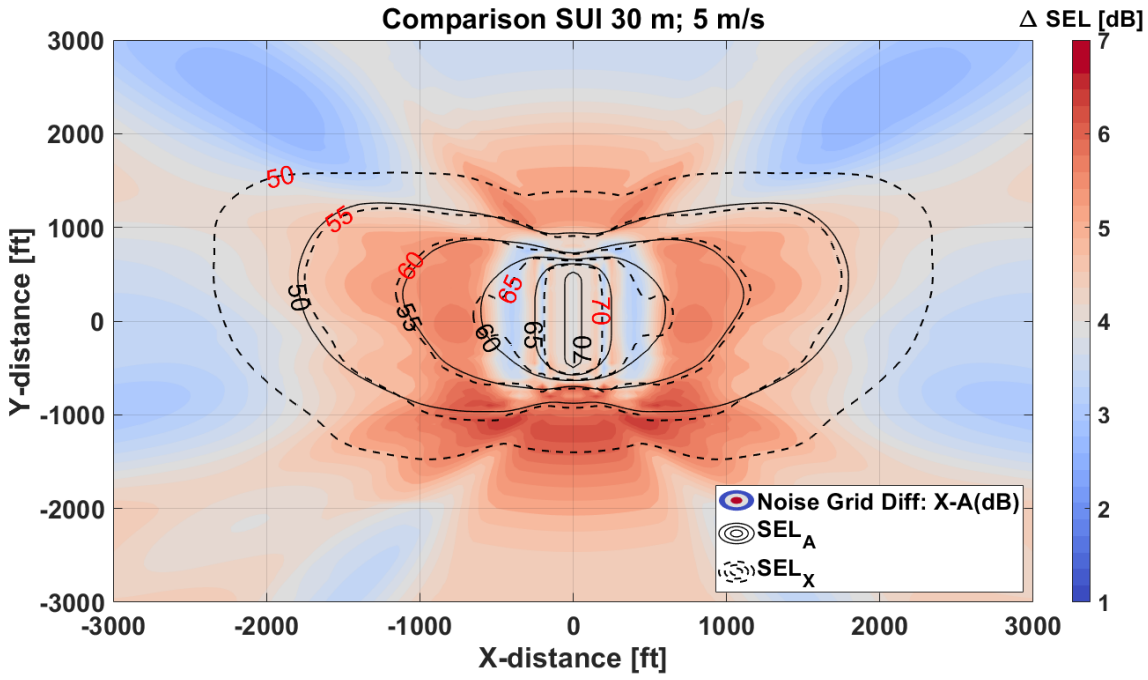


Figure 4.14: Difference between the X and A weighting Contours for the SUI Endurance 30 m and 5 m/s

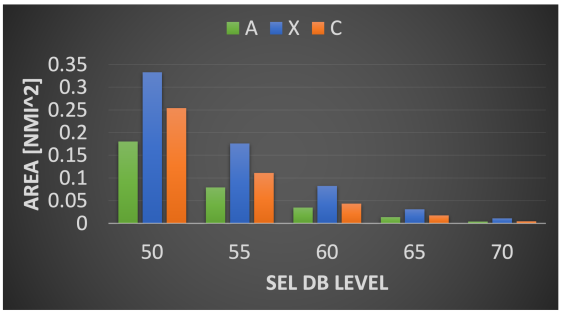


(a)

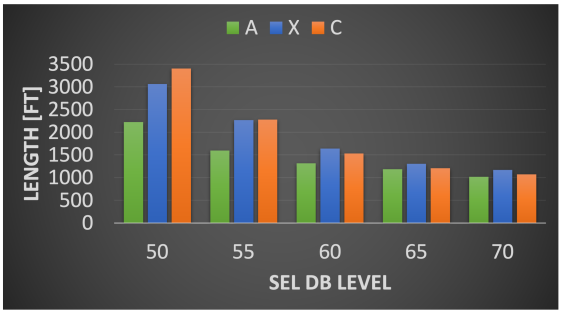


(b)

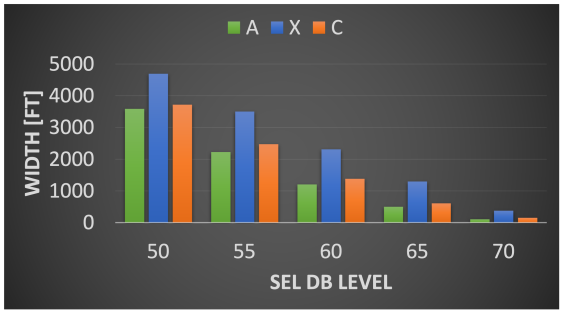


(c)

Figure 4.15: Length, Width and Area of Contours for the SUI (altitude = 30m ,speed = 5 m/s).

In these contours, the length of the C-weighting actually surpasses the X- and the A-weighting for the 50 and 55 dB noise level. For the 60, 65 and 70 dB level the X-weighting is larger in terms of length. In terms of width and area, the X-weighting is the largest at all dB levels.

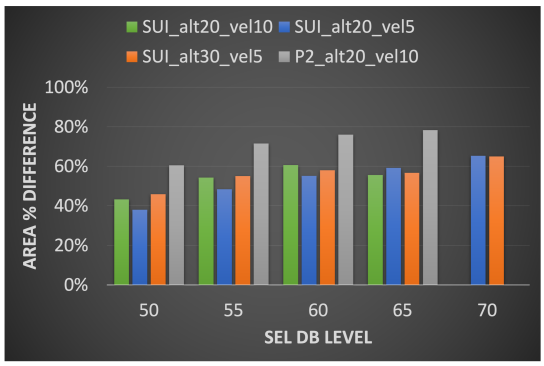


(a)

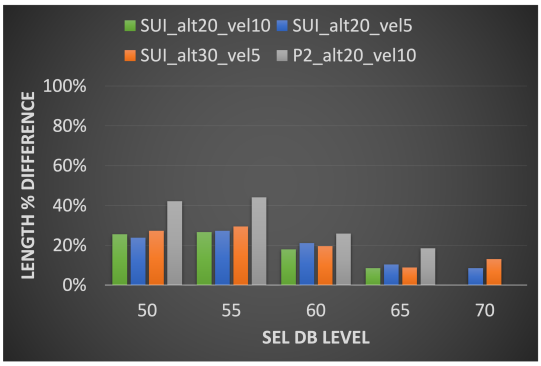


(b)

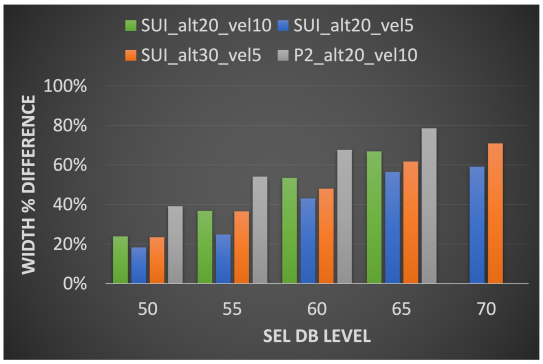


(c)

Figure 4.16: Length, Width and Area Percentage difference between X- and A-Weightings for all sUASs.

The differences in area and width between the A- and the X-weighted contours increase as the dB level of the contour increases. The largest differences are in area and width; however, the differences of all three measurements are significant.

# CHAPTER 5
# EXPECTED BENEFITS

The use of sUASs in everyday life is a very contemporary situation. News articles like this one by Fox News [52] are being published often about different companies that will be using them in the near future; this article was published June 19, 2021. This article describes how El Pollo Loco is in a test flight stage with their partner Flytrex to assess the feasibility of their restaurant inspired airline "Air Loco". Not only are new companies approaching this technology but new laws are also surfacing from the FAA regarding sUASs. On April 21, 2021, the FAA released a press briefing regarding drone operations over people, operations at night, and remote identification [53] or identifying drones in flight and the location of their control stations.

## 5.1 Response to Research Question #2 and Hypothesis #2

These new pieces of information spell out the stakeholders involved with these vehicles and their operations: regulators, companies like El Pollo Loco looking to take advantage for business opportunities, manufacturers like Flytrex, and everyday people who will be interacting with these vehicles on a daily basis. In the FAA's statement, they state that "the Department [of Transportation] looks forward to working with stakeholders to ensure that our UAS policies keep pace with innovation, ensure the safety and security of our communities, and foster the economic competitiveness of our country". This is critical for the future of these vehicles. As the amount of operations increases however, noise can become a serious concern.

As discussed throughout the noise contour analysis, the X-weighting is larger at all dB levels above 60 in length, width and area. This answers Research Question #2 and verifies Hypothesis #2. The ramifications of verifying Hypothesis #2 is of importance to the

stakeholders involved. From a regulator's perspective, the affects of a new weighting which better correlates with human annoyance can allow them to take more particular action when creating the noise policy for these vehicles. Because the X-weighting has a much larger contour area than the A-weighting at each decibel level, this brings attention especially to areas in the future that could experience higher than normal sUAS noise. Without a correct weighting, higher than normal noise complaints could be recorded by a governing body like the FAA or ICAO for creating policy that is considered relatively lenient.

The work in this thesis allows for a method where a language, or a metric, can be made in order for all stakeholders to understand one another and, while doing so, characterizing/quantifying sUAS noise in an appropriate and meaningful way. Carrying out the approach explained in Chapter 3 and in Figure 2.2 will provide commentary on the usefulness of current metrics on noise from vehicles like sUASs. This will contribute to the conversation started by NASA, the FAA and other entities regarding an investigation into current noise metrics. This thesis will show the possible repercussions of non-representative frequency weightings in the form of SEL contours and providing answers to both Research Questions posed. This commentary will provide useful information to two groups: regulators and operators. For regulators, this will provide insight to metrics used for different noise policies being made for this new vehicle type. For operators, this will be helpful for planning purposes, especially for choosing locations to start using sUASs in their day-to-day operations.

The main takeaway from this work is the methodology behind assessing a weighting and the capability of it to describe the human annoyance that is caused by the noise generated from sUASs. There are many different avenues in which this methodology can be used. These are explained in the following section.

## 5.2 Future Work

The methodology shown in Figure 2.2 is made out of building blocks. Each box is a method which can be changed depending on what area of acoustics, verification, and noise propagation one would like to explore. For example, in creating the weighting – there are multiple avenues that can be researched. A Design of Experiments has many different options in creating the combinations one would like to test. Other methods, apart from full factorial, allow combinations of the weighting correction factors in the one-third octave bands to be varied with fewer cases. Although some combinations would be left out, this could allow a larger resolution in the variations to be used (rather than 3 levels – high, low and baseline).

An additional way different weightings could be made is by taking a more electrical engineering approach and treating them as actual filters. In this way, the researcher would need to specify different combinations of poles and zeros in a transfer function. This would still proceed in the same way of applying this transfer function to the pressure values in each recording rather than the SPL values in one-third octave bands. This could allow the researcher to calculate SEL values on a narrow band basis rather than a one-third octave band basis as well.

The weighting found in this thesis was calculated given data from 20 flight recordings and 38 subject responses. To make this a higher fidelity study, more data in general would be useful. Larger surveys of human response are being made where people can perform the same psychoacoustic test from the comfort of their own homes and can submit surveys. In this way larger amounts of data can be used by scientists. Additionally, to make the propagation of the noise higher-fidelity the same flyovers could be recorded by multiple monitors so that azimuthal directivity could also be taken into account.

Like it was mentioned before, the noise propagation method had many different possibilities: PSU-WOPWOP, AEDT and ANOPP2. These can also be thought of as “blocks”

that fit into the Noise Propagation block of Figure 2.2.

Finally, Christian's mention of future work in his study can also be referenced [28]. He mentions how looking into a duration correction or lingering correction factor could be used given the complaints from the subjects. Therefore, instead of using SEL or weightings, EPNL can be tested with an added correction factor. Although making EPNL contours is not a common practice, the values can still be correlated and compared with a regular EPNL value.

# Appendices

# APPENDIX A

## EXAMPLE A WEIGHTED CALCULATION USING OCTAVE BANDS

Table A.1: Example Noise Calculation Using Weightings [54]

| Frequency [kHz] | 0.0315 | 0.063 | 0.125 | 0.25 | 0.5 | 1 | 2 | 4 | 8 | 16 |
|---|---|---|---|---|---|---|---|---|---|---|
| Level [dB] | 70.9 | 78.4 | 83.3 | 87.6 | 87.3 | 93.5 | 93.8 | 97 | 99.9 | 98.2 |
| A-weighting Correction [dB] | -39.4 | -26.2 | -16.1 | -8.6 | -3.2 | 0 | 1.2 | 1 | -1.1 | -6.6 |
| Resultant Level [dB] | 31.5 | 52.2 | 67.2 | 79 | 84.1 | 93.5 | 95 | 98 | 98.8 | 91.6 |

In this example, the A-weighted Sound Pressure Level is calculated from octave bands rather than one third octave bands. This same procedure was used for one third octave bands at the corresponding center frequencies that are shown in Table B.1 and Table B.2. First, the SPL is measured for each center octave band frequency: an example is given in the first row of Table A.1. Next, correction factors are added from the A-weighting scale shown in the second row of the table. The resultant SPLs for each frequency band are shown in the third row. These are then used to calculate the total noise level using Equation A.1

$$\mathrm{dB}(A) = \left[ \sum_{i=0}^{n} 10^{\frac{L(i)}{10}} \right] \tag{A.1}$$

where $i$ is the index corresponding to each of the 10 frequency bands. This calculation yields a value of 103.2 db(A).

# APPENDIX B

# DESIGN OF EXPERIMENTS

Table B.1: Noise Weighting Ranges Design of Experiments [54]

| Frequency [kHz] | 0.05 | 0.063 | 0.080 | 0.10 | 0.125 | 0.16 | 0.20 | 0.25 | 0.315 | 0.4 | 0.5 | 0.63 |
|---|---|---|---|---|---|---|---|---|---|---|---|---|
| Baseline [dB] | -30.2 | -26.2 | -22.5 | -19.1 | -16.1 | -13.4 | -10.9 | -8.6 | -6.6 | -4.8 | -3.2 | -1.9 |
| DoE Low Range | 0 | 0 | 0 | 0 | 0 | 0 | 0 | 0 | -10 | -10 | -10 | -10 |
| DoE High Range | 0 | 0 | 0 | 0 | 0 | 0 | 0 | 0 | +10 | +10 | +10 | +10 |

Table B.2: Continued Noise Weighting Ranges Design of Experiments [54]

| Frequency [kHz] | 0.8 | 1 | 1.25 | 1.6 | 2 | 2.5 | 3.15 | 4 | 5 | 6.3 | 8 | 10 |
|---|---|---|---|---|---|---|---|---|---|---|---|---|
| Baseline [dB] | -0.8 | 0 | +0.6 | +1 | +1.2 | +1.3 | +1.2 | +1 | +0.5 | -0.1 | -1.1 | -2.5 |
| DoE Low Range | -10 | -5 | -5 | -5 | -5 | -5 | -5 | -5 | -5 | 0 | 0 | 0 |
| DoE High Range | +10 | +5 | +5 | +5 | +5 | +5 | +5 | +5 | +5 | 0 | 0 | 0 |

# APPENDIX C

## SPECTROGRAMS AND NOISE SPECTRAS FOR FLY OVERS USED IN DOE

The following are spectrograms and spectras of the recordings that were used in the design of experiments for the creation of the X-weighting. The spectrograms show the entirety of the recording and the spectras were created from half a second of the recording before and after the aircraft is directly over the microphone. These figures can provide insight into spectral and frequency content that caused annoyance to the subjects.

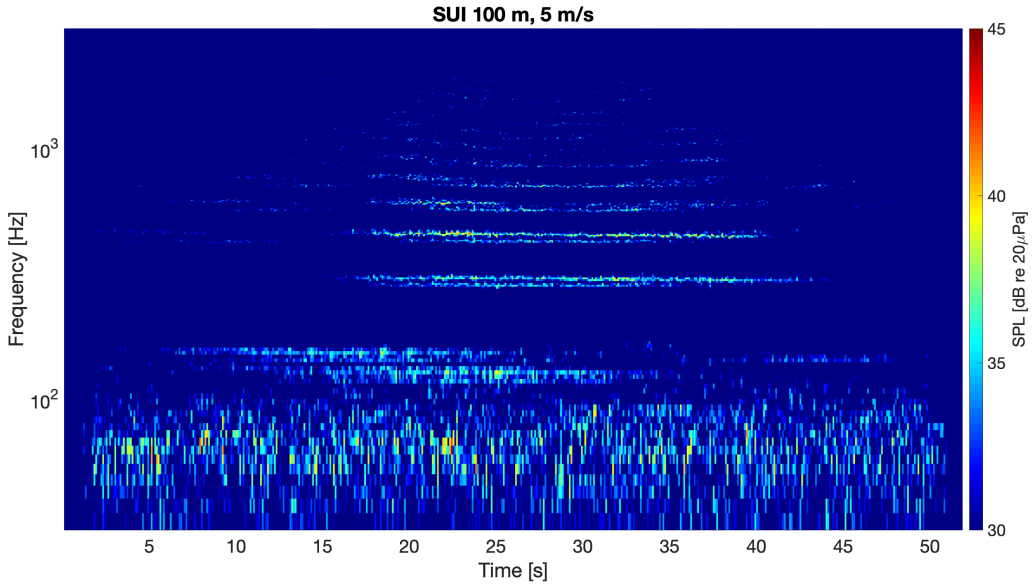


Figure C.1: Full Flyover Spectrogram of SUI Endurance sUAS: altitude = 100 m; speed = 5 m/s.

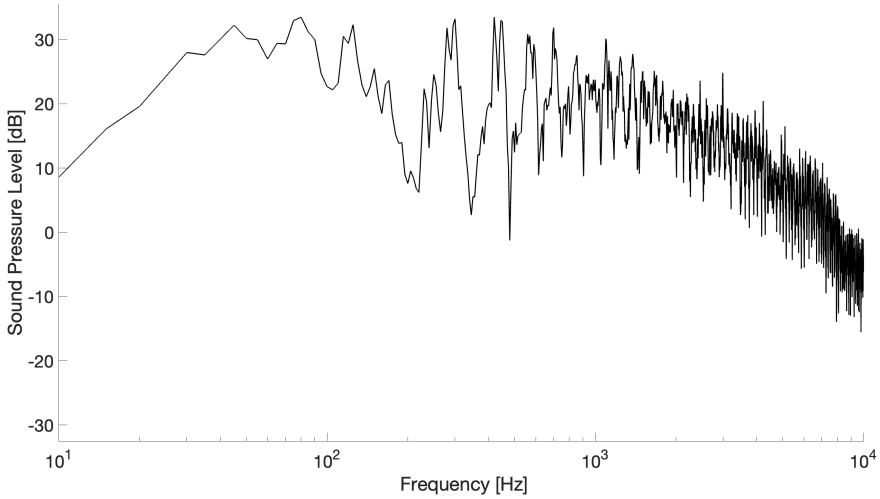


Figure C.2: Noise Spectra SUI Endurance sUAS: altitude = 100 m; speed = 5 m/s 0.5s before and after microphone flyover.

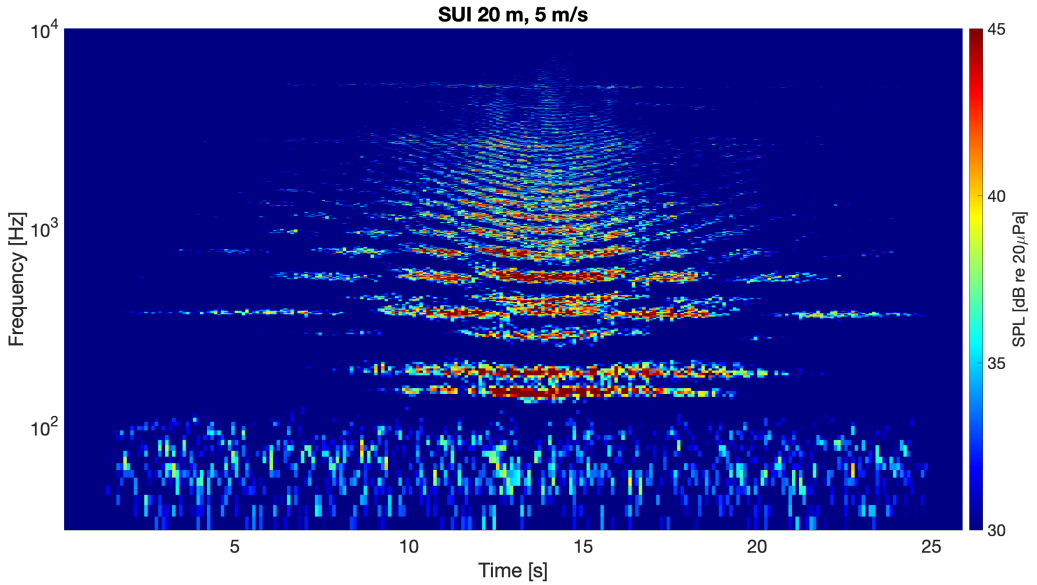


Figure C.3: Full Flyover Spectrogram of SUI Endurance sUAS: altitude = 20 m; speed = 5 m/s.

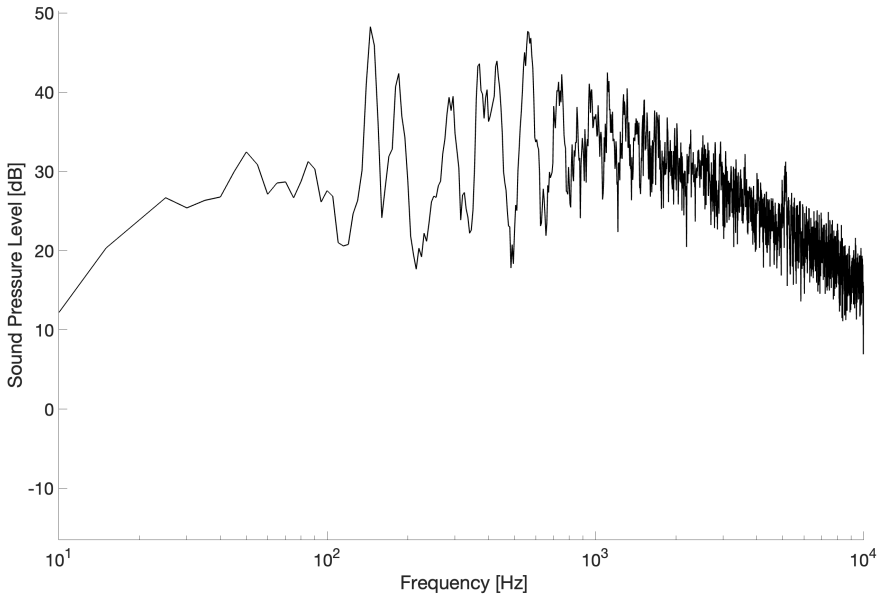


Figure C.4: Noise Spectra SUI Endurance sUAS: altitude = 20 m; speed = 5 m/s 0.5s before and after microphone flyover.

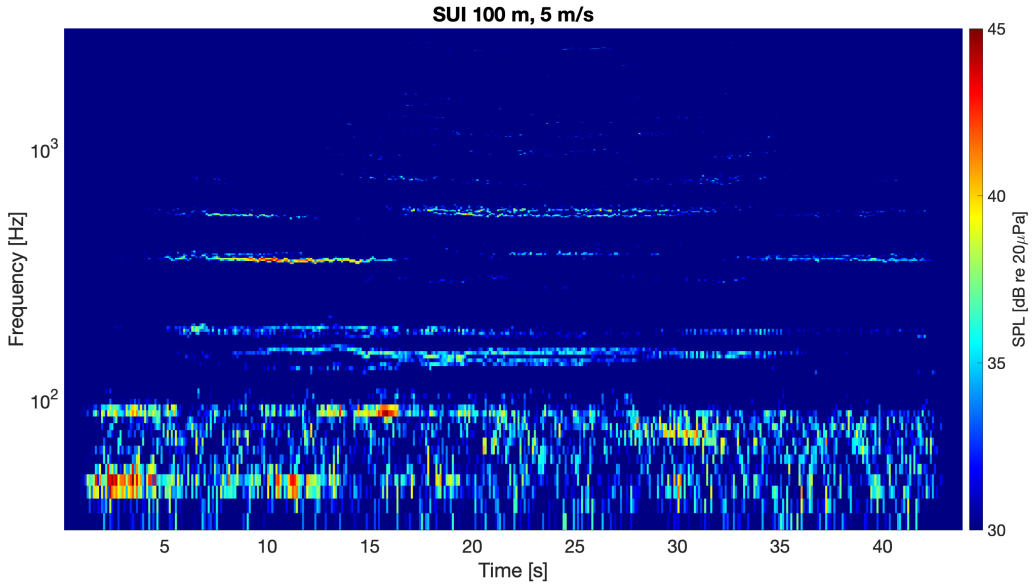


Figure C.5: Full Flyover Spectrogram of SUI Endurance sUAS: altitude = 100 m; speed = 5 m/s.

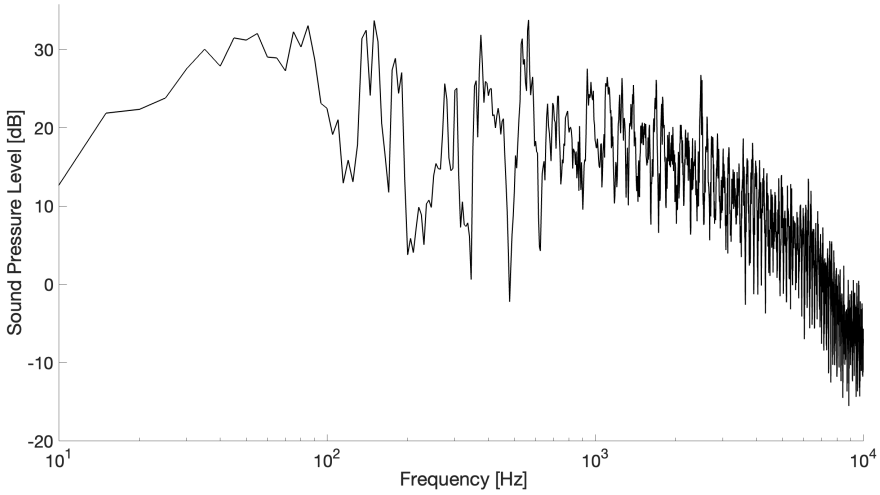


Figure C.6: Noise Spectra SUI Endurance sUAS: altitude = 100 m; speed = 5 m/s 0.5s before and after microphone flyover.

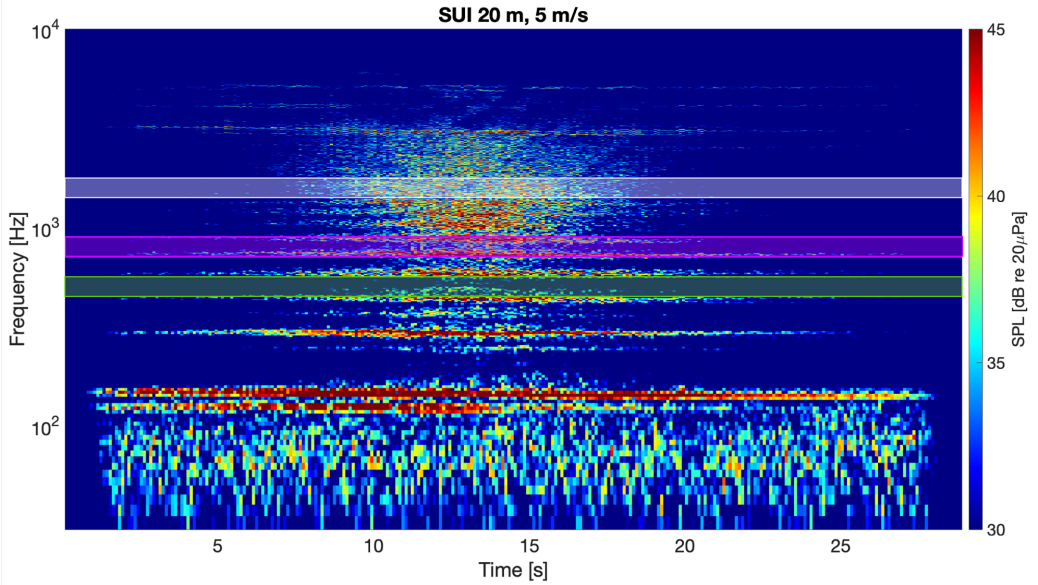


Figure C.7: Full Flyover Spectrogram of SUI Endurance sUAS: altitude = 20 m; speed = 5 m/s.

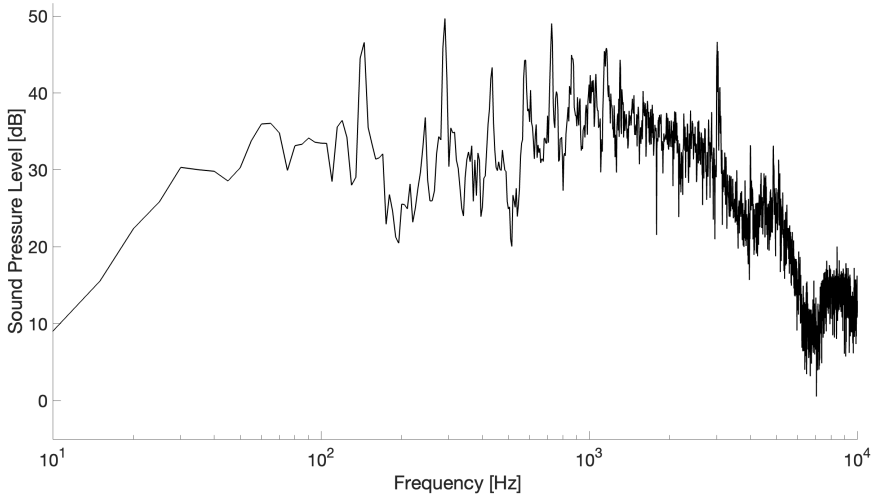


Figure C.8: Noise Spectra SUI Endurance sUAS: altitude = 20 m; speed = 5 m/s 0.5s before and after microphone flyover.

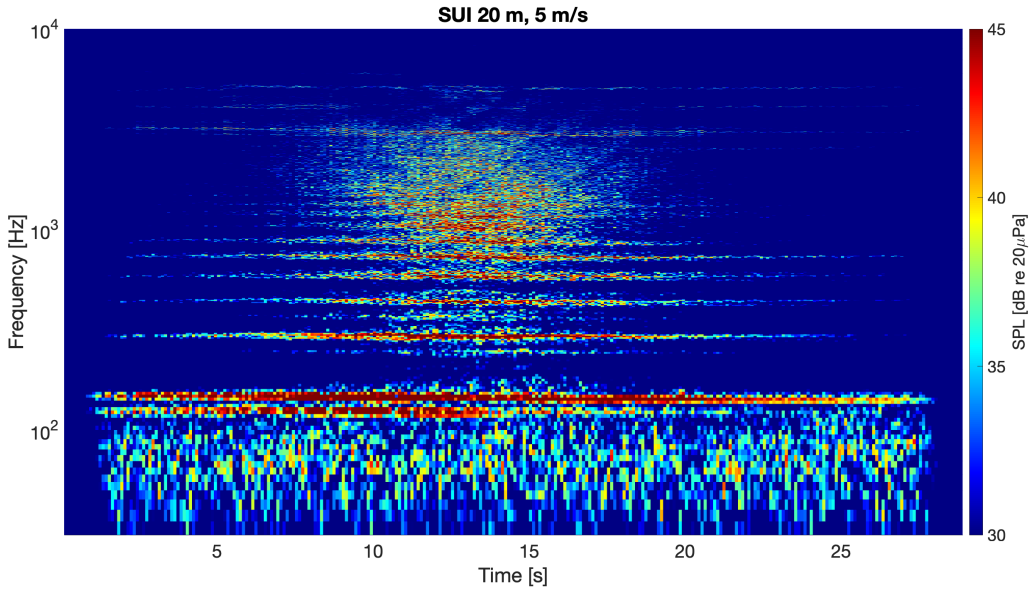


Figure C.9: Full Flyover Spectrogram of SUI Endurance sUAS: altitude = 20 m; speed = 5 m/s.

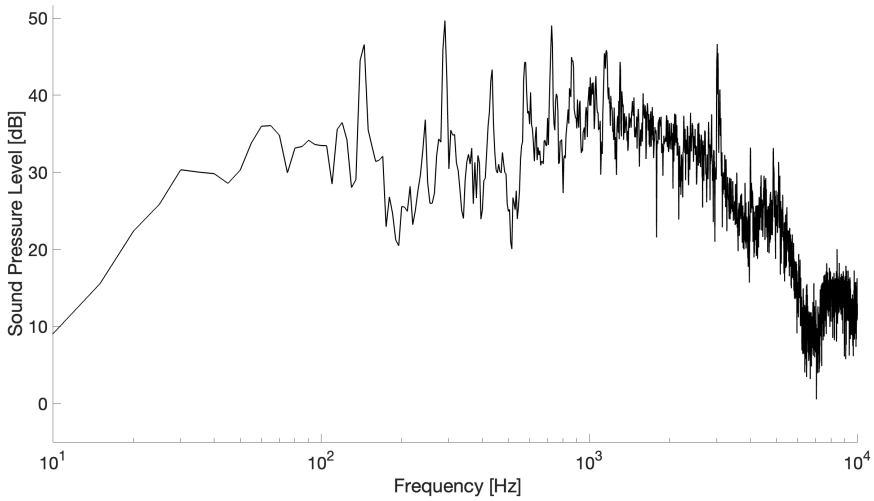


Figure C.10: Noise Spectra SUI Endurance sUAS: altitude = 20 m; speed = 5 m/s 0.5s before and after microphone flyover.

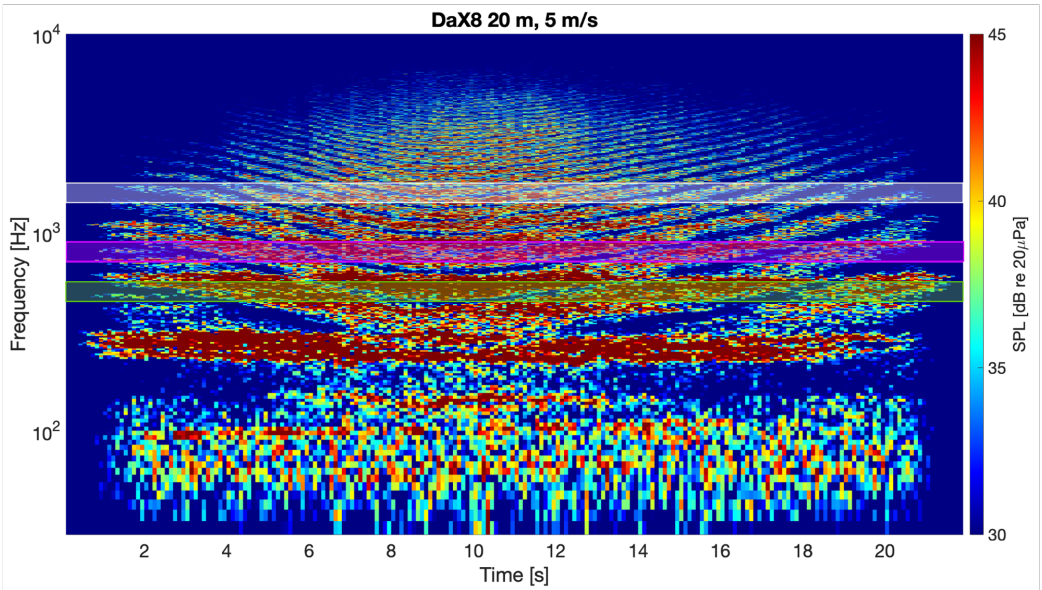


Figure C.11: Full Flyover Spectrogram of DaX8 sUAS: altitude = 20 m; speed = 5 m/s.

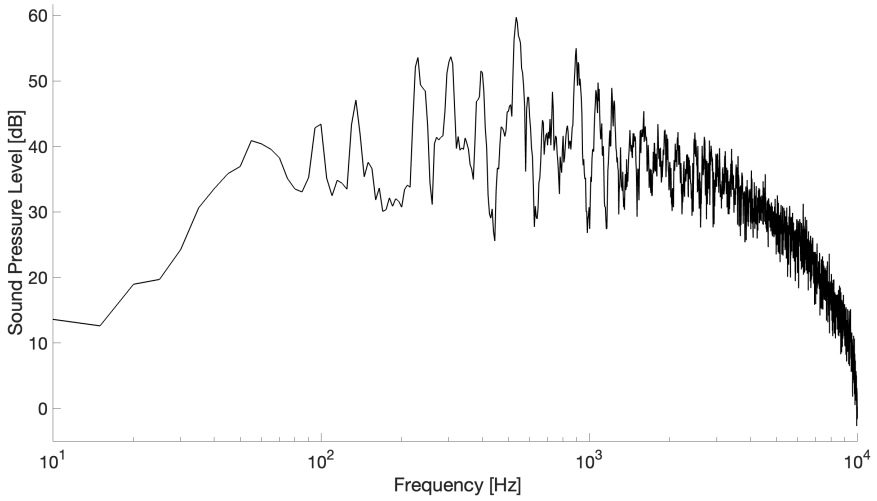


Figure C.12: Noise Spectra DaX8 sUAS: altitude = 20 m; speed = 5 m/s 0.5s before and after microphone flyover.

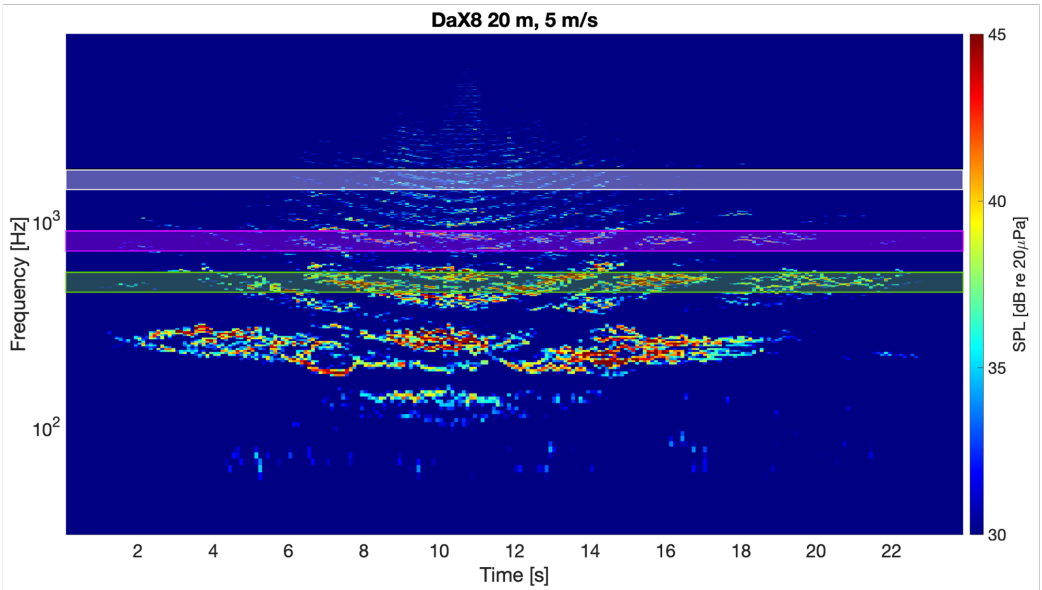


Figure C.13: Full Flyover Spectrogram of DaX8 sUAS: altitude = 20 m; speed = 5 m/s.

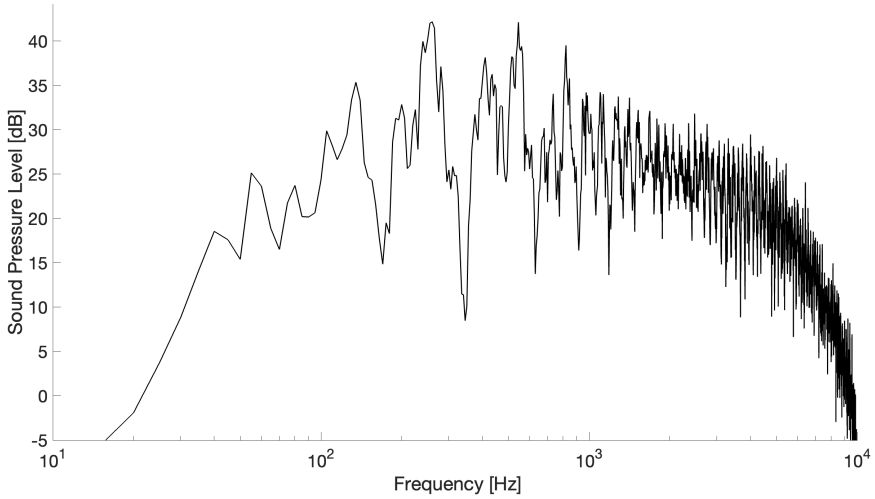


Figure C.14: Noise Spectra DaX8 sUAS: altitude = 20 m; speed = 5 m/s 0.5s before and after microphone flyover.

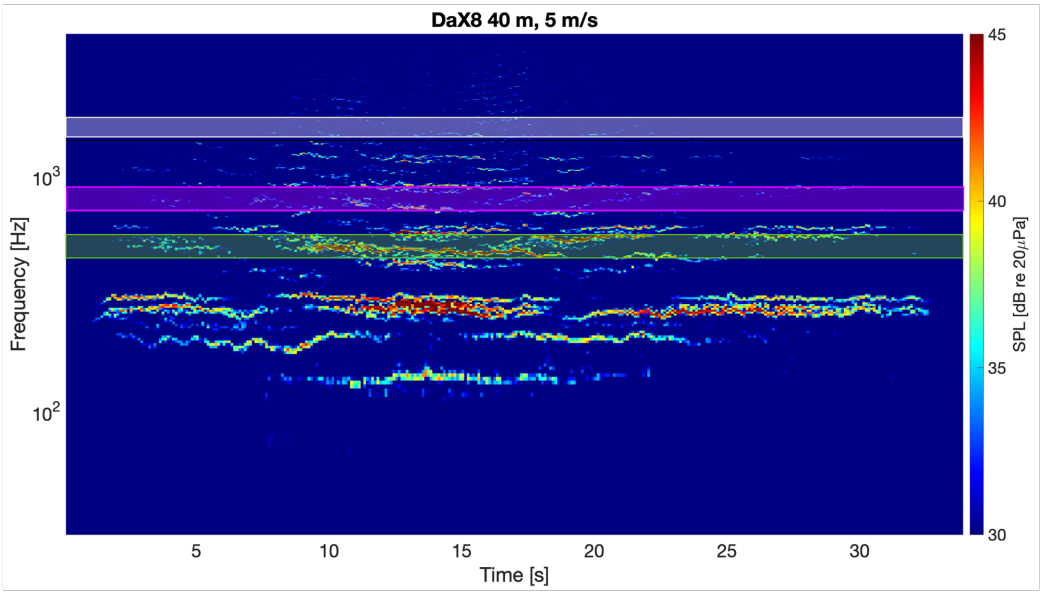


Figure C.15: Full Flyover Spectrogram of DaX8 sUAS: altitude = 40 m; speed = 5 m/s.

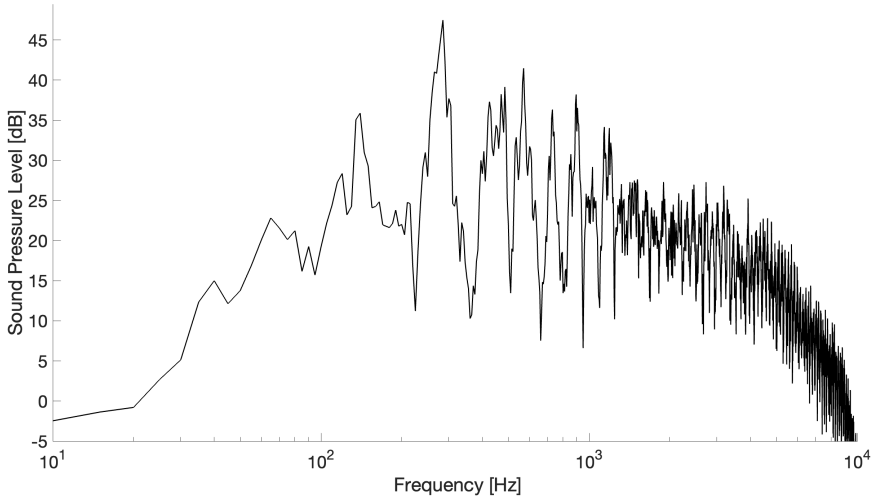


Figure C.16: Noise Spectra DaX8 sUAS: altitude = 40 m; speed = 5 m/s 0.5s before and after microphone flyover.

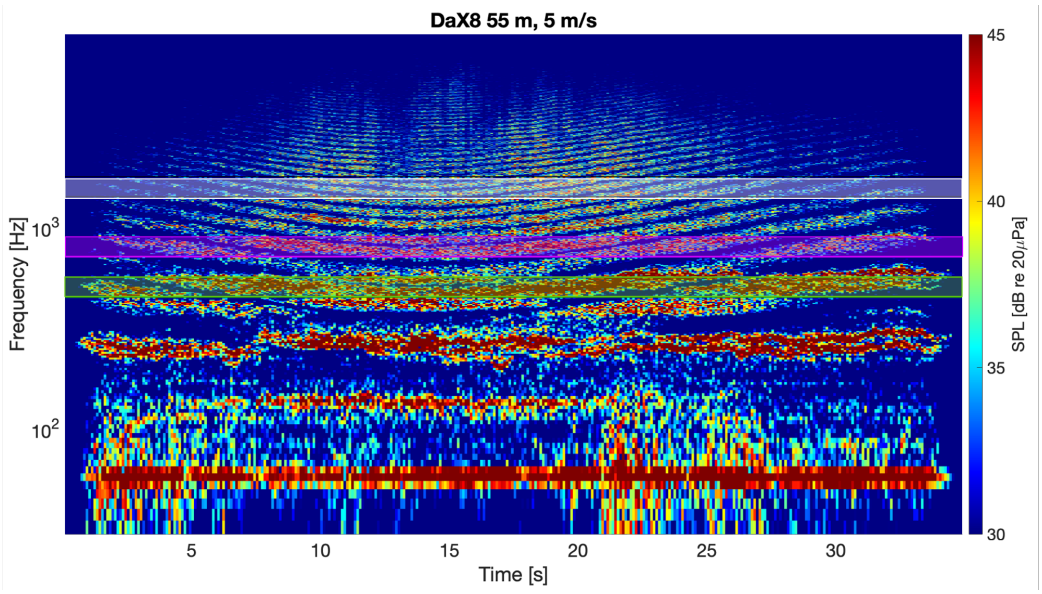


Figure C.17: Full Flyover Spectrogram of DaX8 sUAS: altitude = 55 m; speed = 5 m/s.

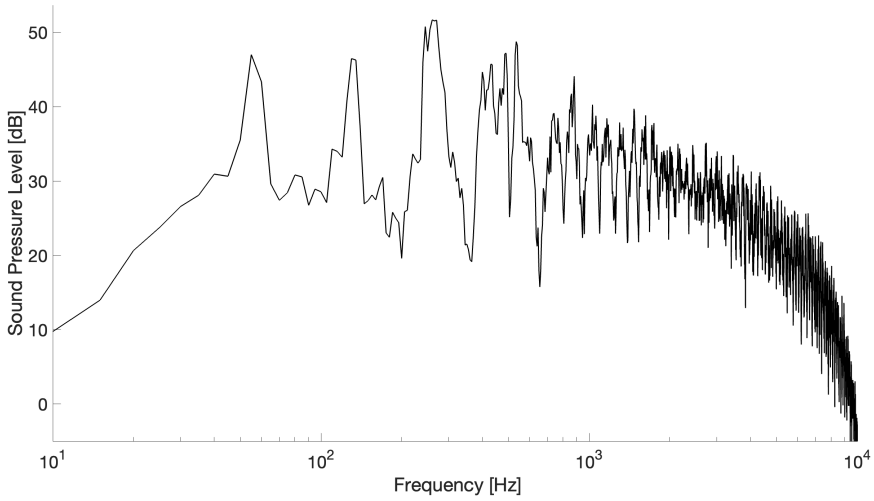


Figure C.18: Noise Spectra DaX8 sUAS: altitude = 55 m; speed = 5 m/s 0.5s before and after microphone flyover.

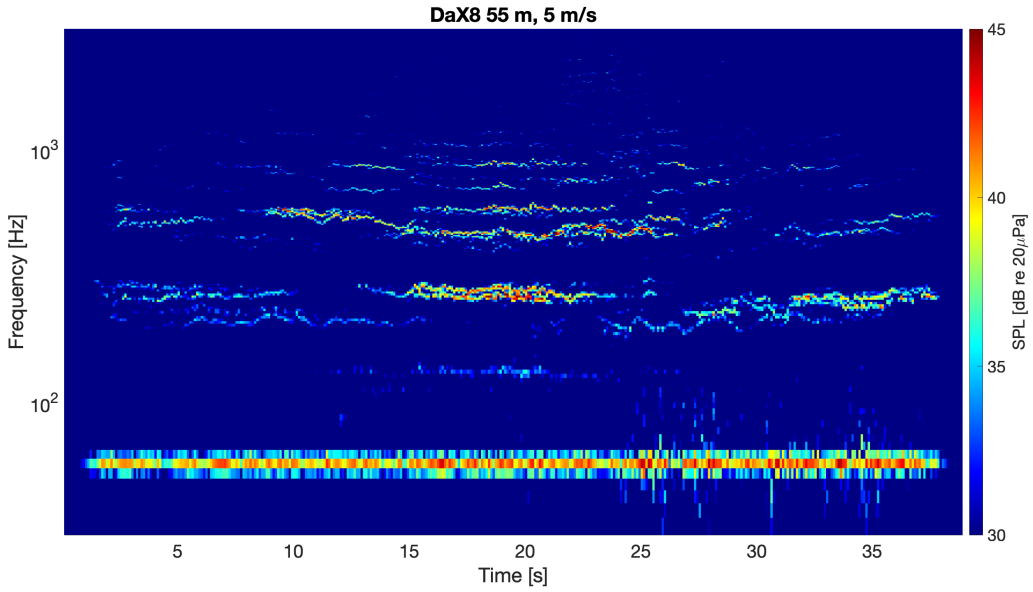


Figure C.19: Full Flyover Spectrogram of DaX8 sUAS: altitude = 55 m; speed = 5 m/s.

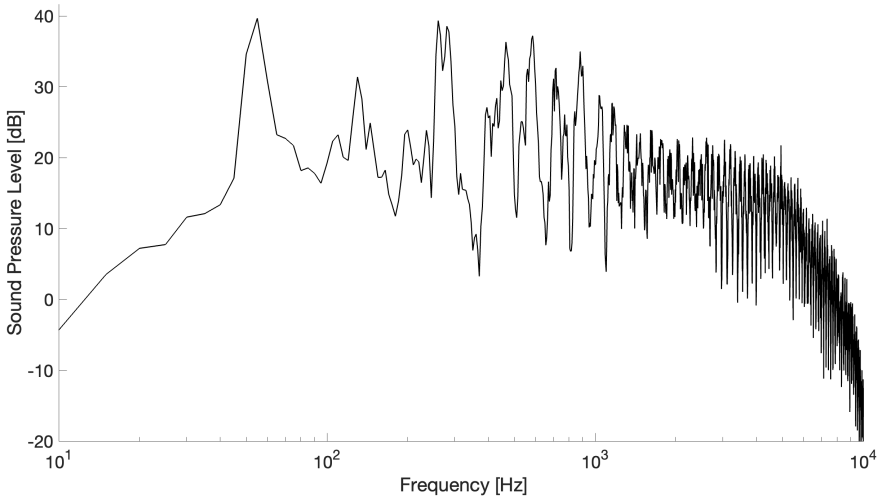


Figure C.20: Noise Spectra DaX8 sUAS: altitude = 55 m; speed = 5 m/s 0.5s before and after microphone flyover.

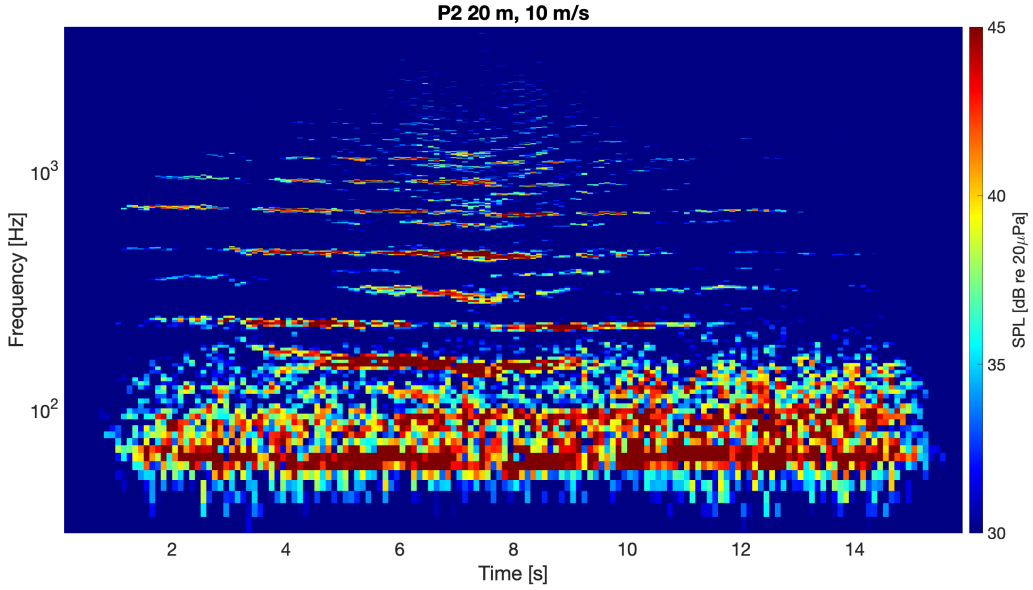


Figure C.21: Full Flyover Spectrogram of Phantom II sUAS using Blades from Advanced Precision Composites (APC): altitude = 20 m; speed = 10 m/s.

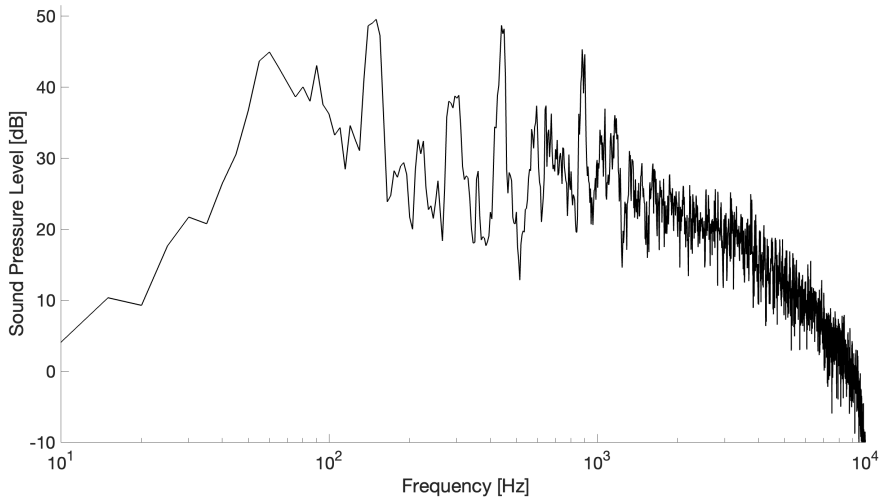


Figure C.22: Noise Spectra Phantom II sUAS using Blades from (APC): altitude = 20 m; speed = 10 m/s 0.5s before and after microphone flyover.

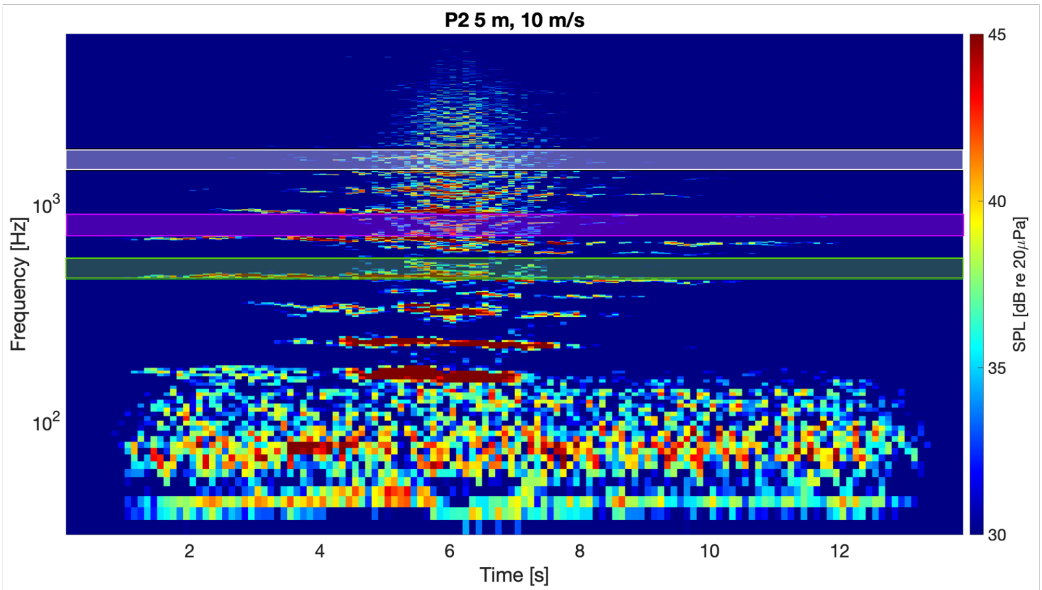


Figure C.23: Full Flyover Spectrogram of Phantom II sUAS using Blades from (APC): altitude = 5 m; speed = 10 m/s.

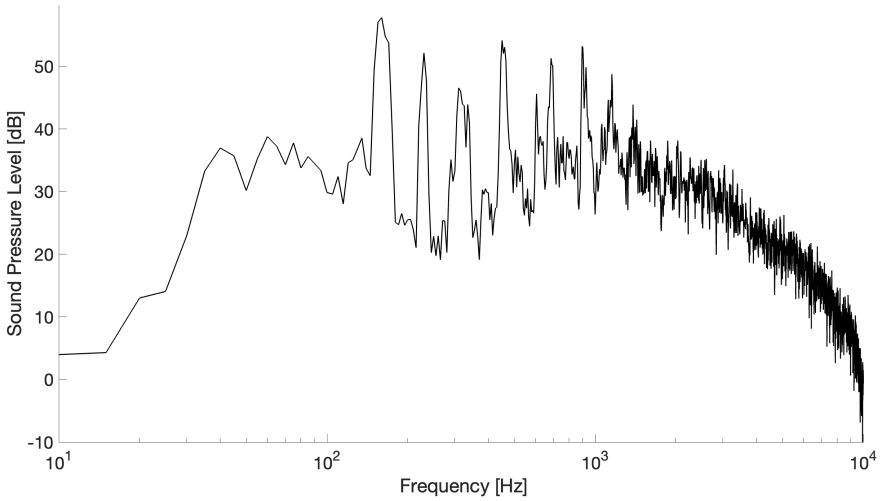


Figure C.24: Noise Spectra Phantom II sUASusing Blades from (APC): altitude = 5 m; speed = 10 m/s 0.5s before and after microphone flyover.

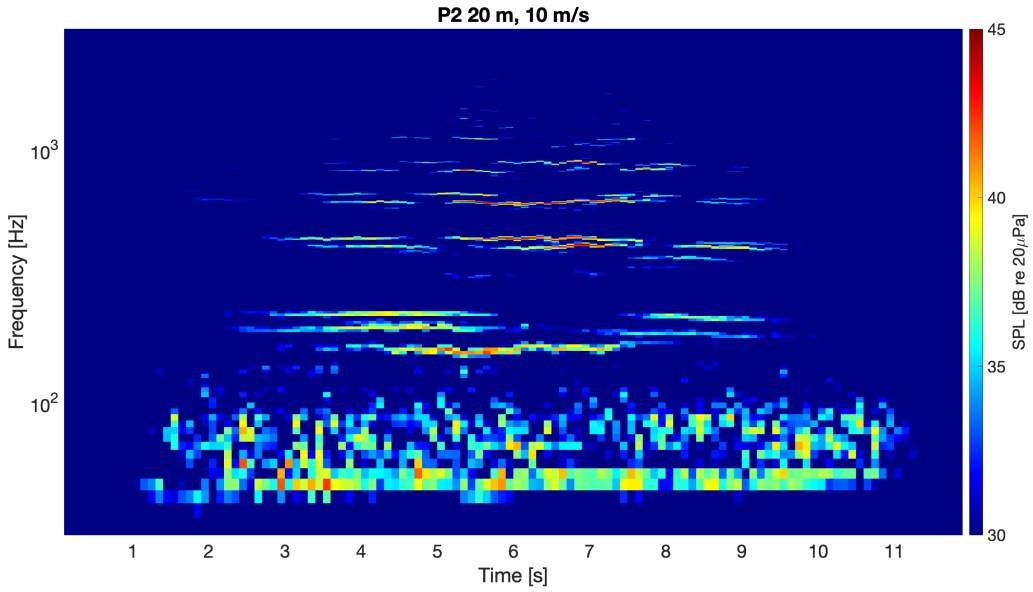


Figure C.25: Full Flyover Spectrogram of Phantom II sUAS using Blades from (APC): altitude = 20 m; speed = 10 m/s.

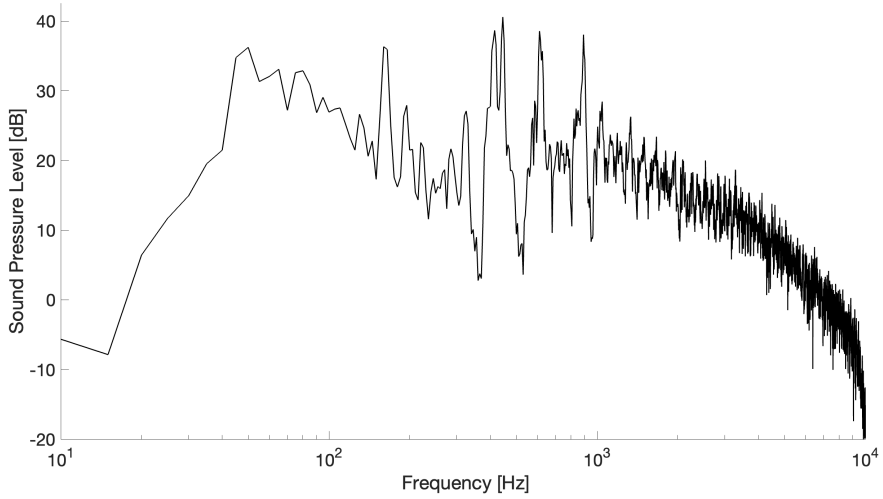


Figure C.26: Noise Spectra Phantom II sUAS using Blades from (APC): altitude = 20 m; speed = 10 m/s 0.5s before and after microphone flyover.

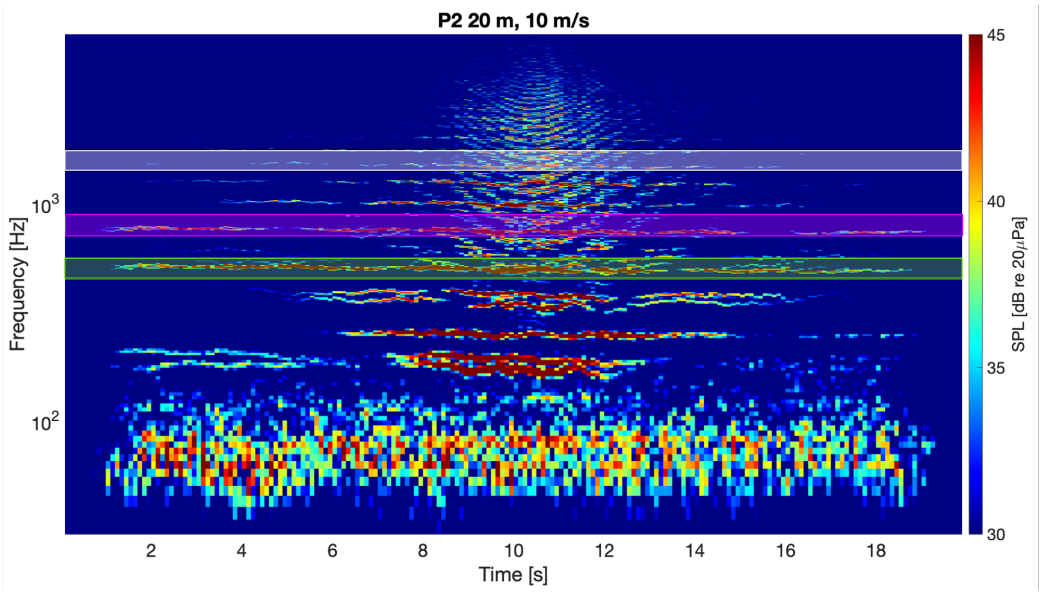


Figure C.27: Full Flyover Spectrogram of Phantom II sUAS using Carbon Fiber Blades: altitude = 10 m; speed = 10 m/s.

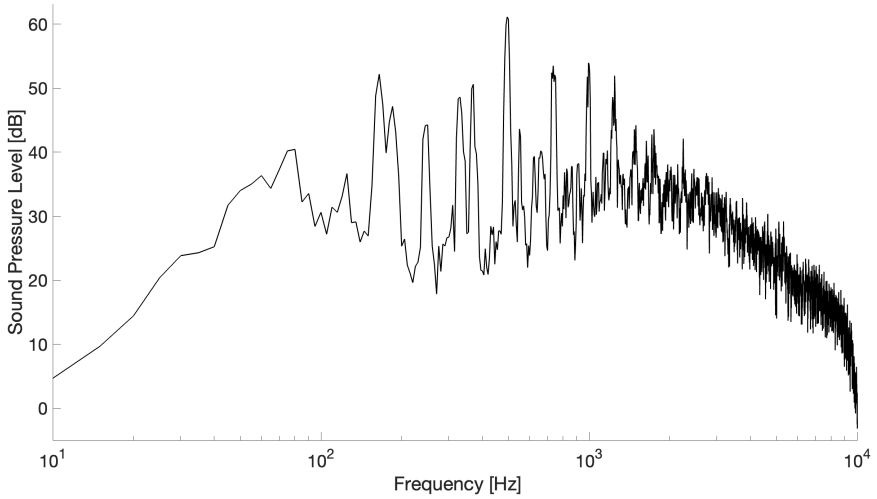


Figure C.28: Noise Spectra Phantom II sUAS using Carbon Fiber Blades: altitude = 10 m; speed = 10 m/s 0.5s before and after microphone flyover.

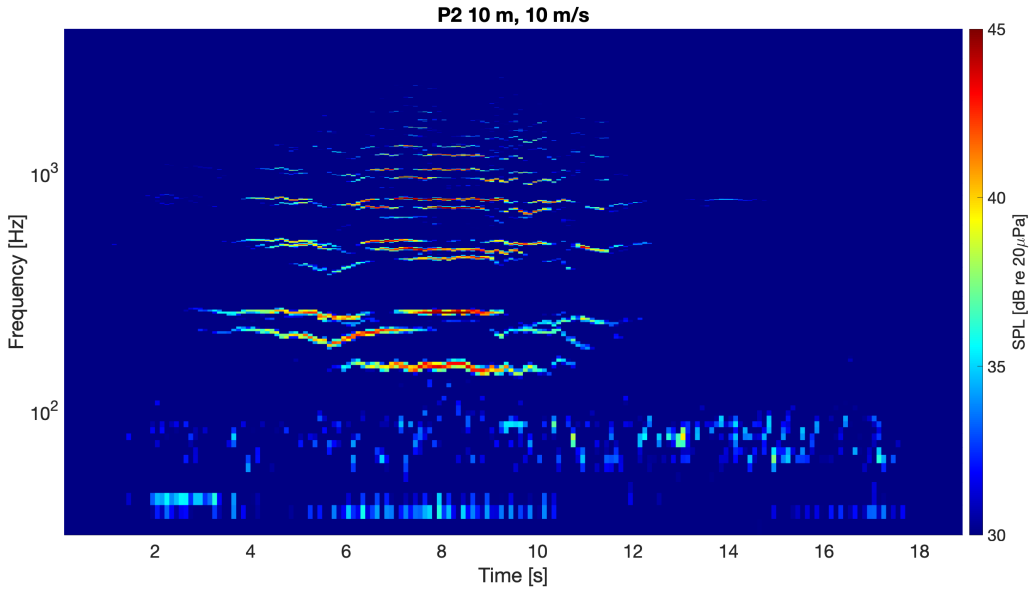


Figure C.29: Full Flyover Spectrogram of Phantom II sUAS using Carbon Fiber Blades: altitude = 20 m; speed = 10 m/s.

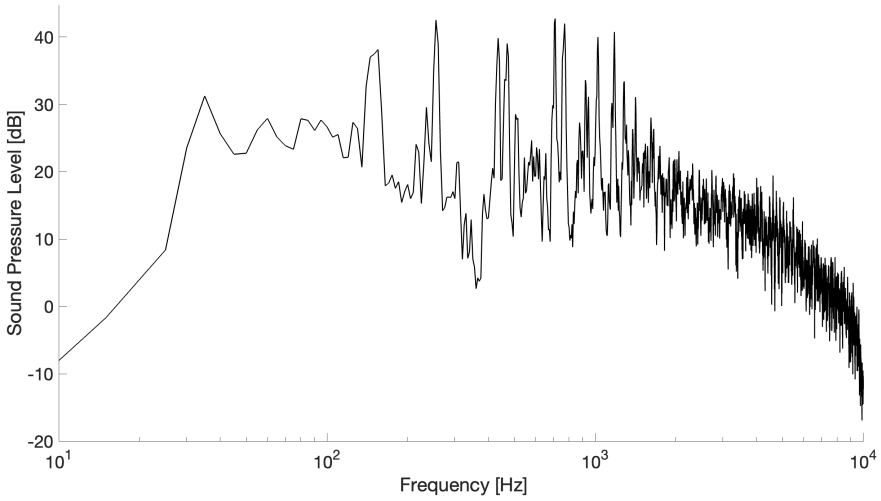


Figure C.30: Noise Spectra Phantom II sUAS using Carbon Fiber Blades: altitude = 20 m; speed = 10 m/s 0.5s before and after microphone flyover.

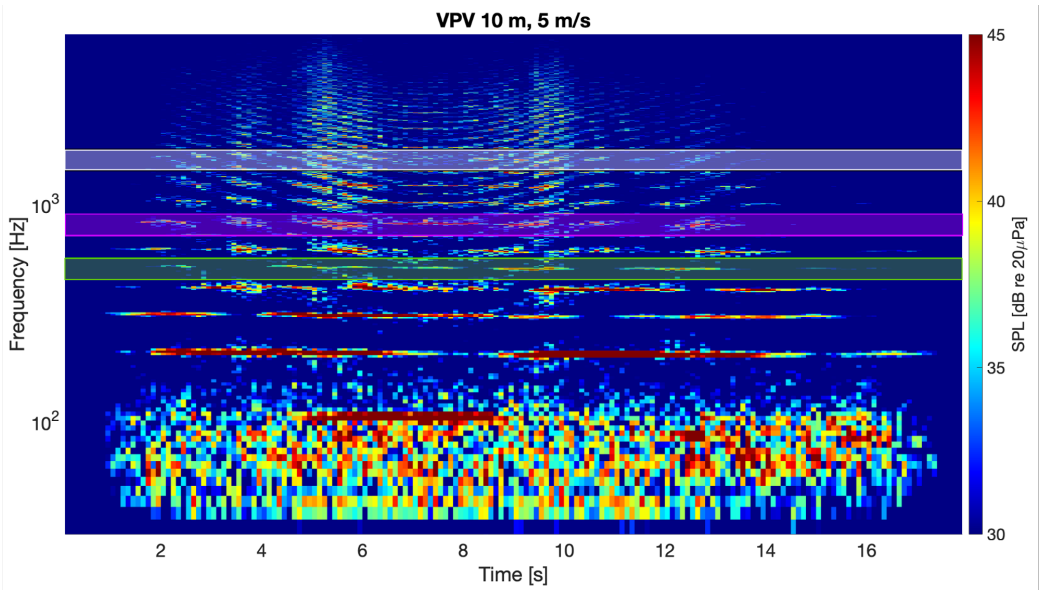


Figure C.31: Full Flyover Spectrogram of VPV sUAS: altitude = 10 m; speed = 5 m/s.

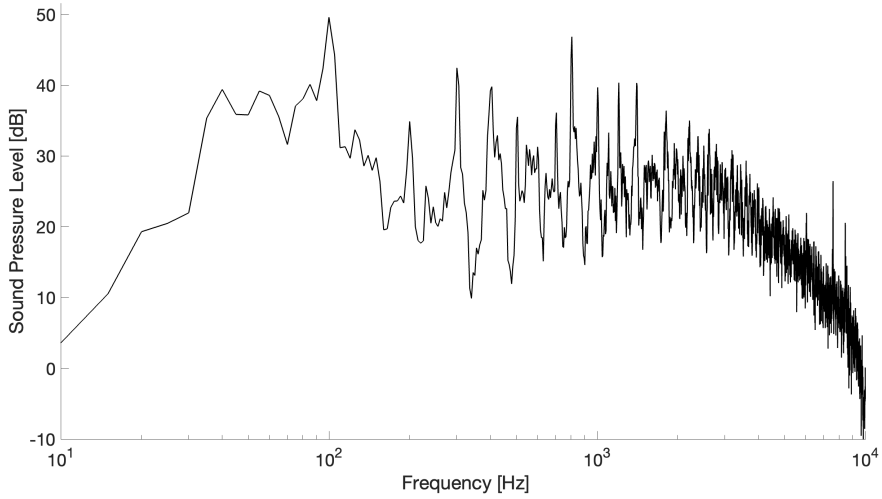


Figure C.32: Noise Spectra VPV sUAS: altitude = 10 m; speed = 5 m/s 0.5s before and after microphone flyover.

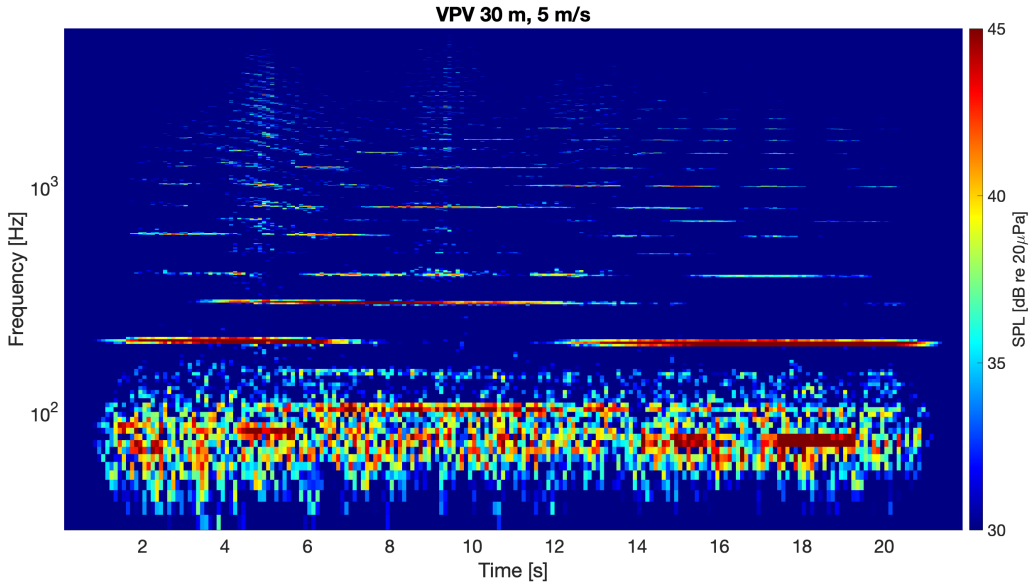


Figure C.33: Full Flyover Spectrogram of VPV sUAS: altitude = 30 m; speed = 5 m/s.

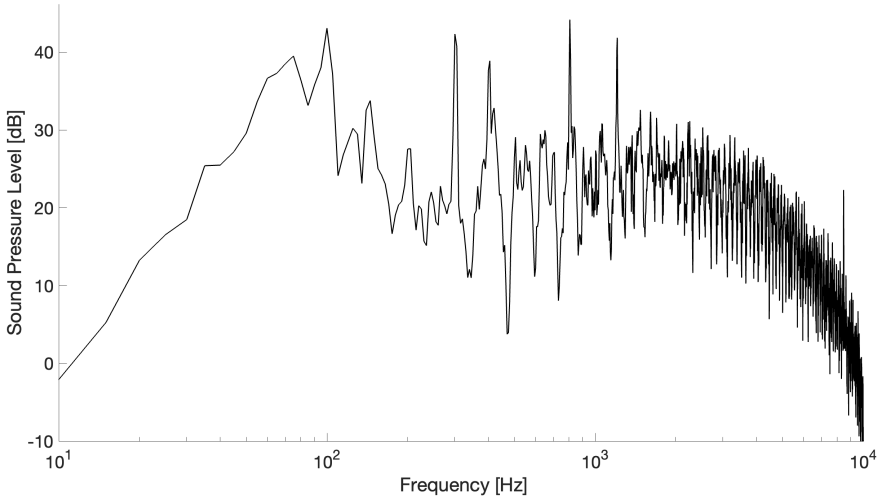


Figure C.34: Noise Spectra VPV sUAS: altitude = 30 m; speed = 5 m/s 0.5s before and after microphone flyover.

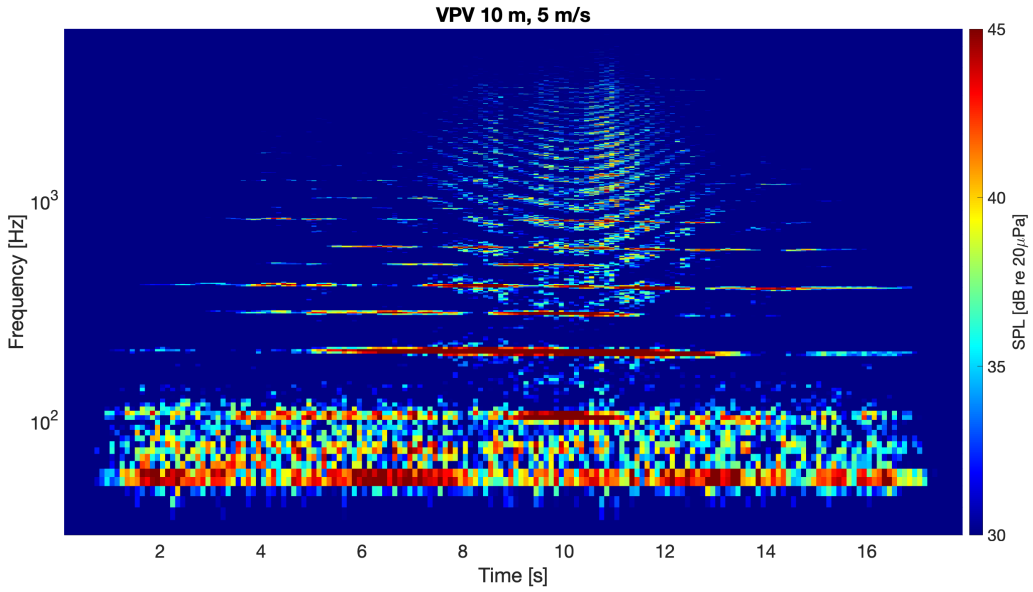


Figure C.35: Full Flyover Spectrogram of VPV sUAS: altitude = 10 m; speed = 5 m/s.

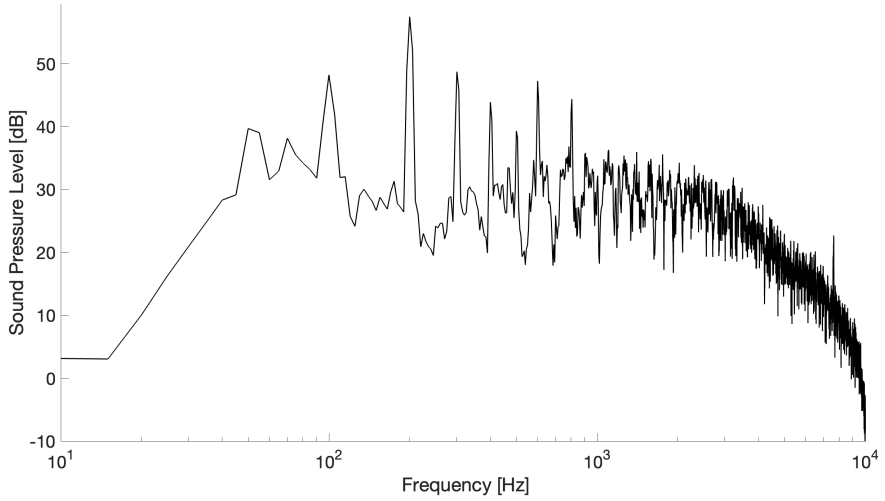


Figure C.36: Noise Spectra VPV sUAS: altitude = 10 m; speed = 5 m/s 0.5s before and after microphone flyover.

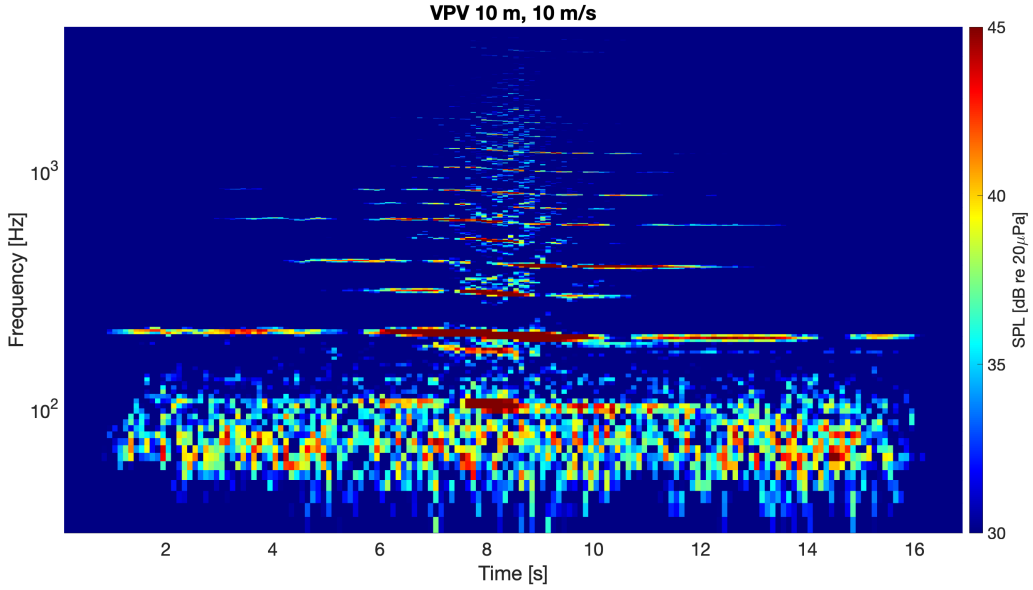


Figure C.37: Full Flyover Spectrogram of VPV sUAS: altitude = 10m; speed = 10 m/s.

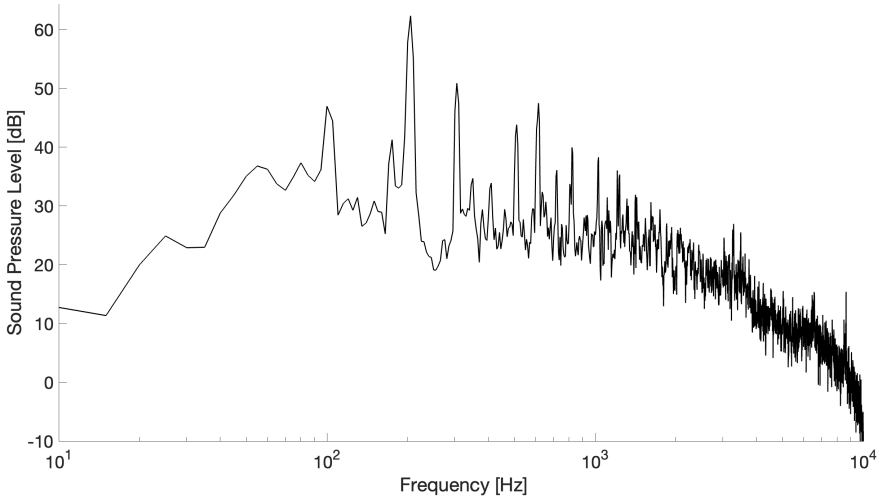


Figure C.38: Noise Spectra VPV sUAS: altitude = 10 m; speed = 10 m/s 0.5s before and after microphone flyover.

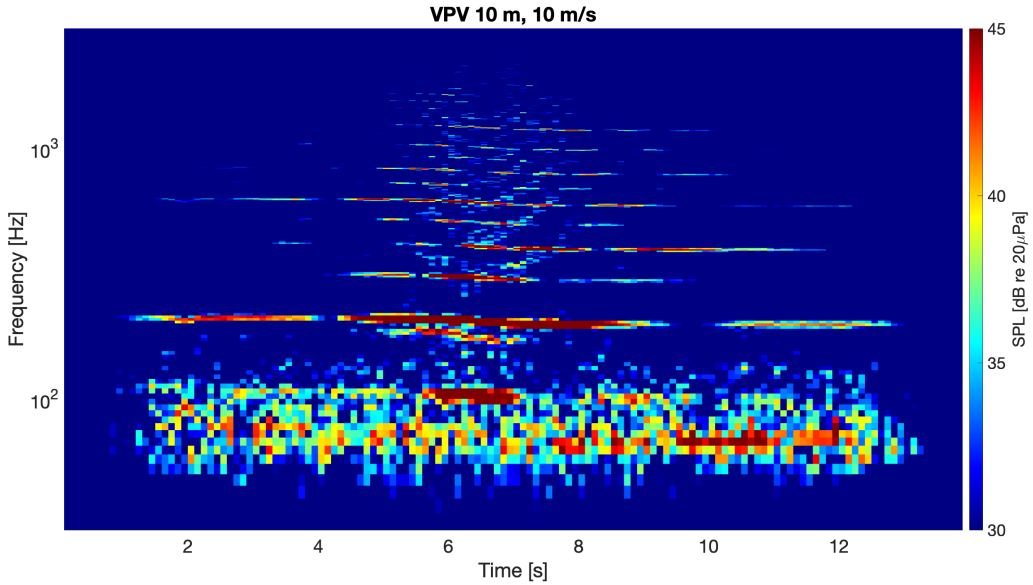


Figure C.39: Full Flyover Spectrogram of VPV sUAS: altitude = 10 m and speed = 10 m/s.

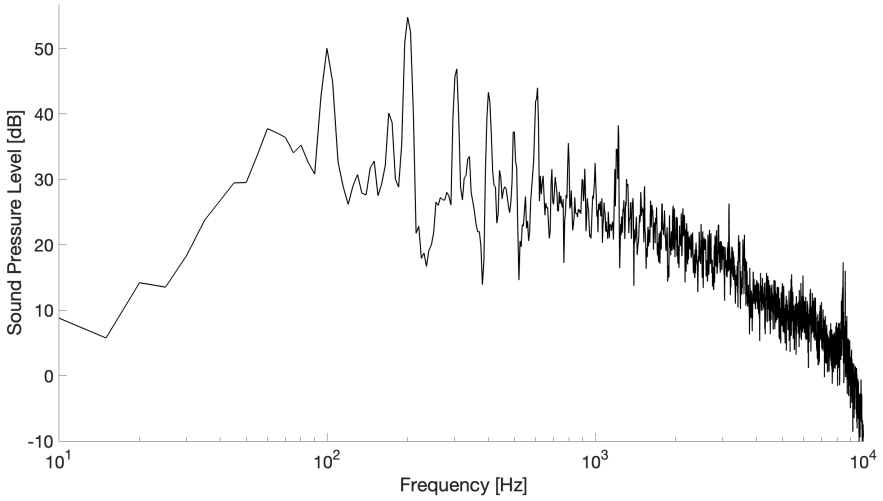


Figure C.40: Noise Spectra VPV sUAS: altitude = 10 m; speed = 10 m/s 0.5s before and after microphone flyover.

## REFERENCES


[1] *68% of the world populations projected to live in urban areas by 2050, says un*, Available at https://www.un.org/development/desa/en/news/population/2018-revision-of-world-urbanization-prospects.html, May 2018.

[2] "Travel demand forecasts", 2012, RRP PRC 45022.

[3] M. Iqbal, *Uber Revenue and Usage Statistics (2020)*, Available at https://www.businessofapps.com/data/uber-statistics/, Oct. 2020.

[4] M. Iqbal, *Lyft Announces Record Fourth Quarter and Fiscal Year Results*, Available at https://www.businessofapps.com/data/lyft-statistics/#4, Oct. 2020.

[5] J. Ho, *Shipping company profits and costs have increased amid pandemic e-commerce boom*, Available at https://www.marketplace.org/2021/02/01/shipping-company-profits-and-costs-have-increased-amid-pandemic-e-commerce-boom/, Oct. 2020.

[6] J. Greene, *Amazon now employs more than 1 million people*, Available at https://www.washingtonpost.com/technology/2020/10/29/amazon-hiring-pandemic-holidays/, Oct. 2020.

[7] *Urban Air Mobility Adds a New Dimension to Travel*, Available at https://www.mitre.org/publications/project-stories/urban-air-mobility-adds-a-new-dimension-to-travel, Jul. 2018.

[8] B. Garret-Glaser, *Uber's Aerial Rideshare Project Entering the Next Phase*, Available at https://www.aviationtoday.com/2020/01/22/ubers-aerial-rideshare-project-entering-next-phase/, Jan. 2020.

[9] K. Korosec, *Uber sells air taxi business elevate to joby aviation, shedding its last moonshot*, Available at https://techcrunch.com/2020/12/08/uber-sells-air-taxi-business-elevate-to-joby-aviation-shedding-its-last-moonshot/, Dec. 2020.

[10] *Jaunt air mobility: Aircraft*, Available at https://www.jauntairmobility.com/.

[11] *Joby aviation home page*, Available at https://www.jobyaviation.com/, 2021.

[12] *Amazon Prime Air*, Available at https://www.amazon.com/Amazon-Prime-Air/b?ie=UTF8&node=8037720011.

[13] *What Is Last Mile Delivery? Costs & How to Optimize*, Available at https://optimoroute.com/last-mile-delivery, May 2020.

[14] *Faa Aerospace Forecast Fiscal Years 2020-2040 Full Forecast Document and Tables*, https://www.faa.gov/data_research/aviation/aerospace_forecasts/media/unmanned_aircraft_systems.pdf, 2019.

[15] *Drone Deliveries Coming Soon, as Wing Unveils Plans for First-of-its-Kind Trial with Fedex and Walgreens*, Available at https://newsroom.fedex.com/newsroom/drone-deliveries-coming-soon-as-wing-unveils-plans-for-first-of-its-kind-trial-with-fedex-and-walgreen/, Sep. 2019.

[16] Evan, *5 Surprising Examples of Drones Used in Domestic Delivery*, Available at https://www.zdwired.com/watch-drones-used-in-domestic-package-delivery/.

[17] P. Vascik and J. Huelsman, "Scaling Constraints for Urban Air Mobility Operations: Air Traffic Control, Ground Infrastructure, and Noise", *Prepared for the Airports Commission. Centre for Psychiatry Barts & the London School of Medicine Queen Mary University of London*, 2015.

[18] Federal Aviation Administration, *Minimum safe altitudes: General*, https://www.law.cornell.edu/cfr/text/14/91.119, 2003.

[19] C. Clark, "Aircraft Noise Effects on Health", *Prepared for the Airports Commission. Centre for Psychiatry Barts & the London School of Medicine Queen Mary University of London*, 2015.

[20] T. English, *Faa's Noise Complaint Initiative (NCI) Overview*, Aviation Noise and Emissions Symposium, 2020.

[21] S. Rizzi and a. et al, "Urban Air Mobility Noise: Current Practice, Gaps, and Recommendations", National Aeronautics and Space Administration, Tech. Rep., 2020.

[22] HyperPhysics, *Frequencies for maximum sensitivity of human hearing*, Available at http://hyperphysics.phy-astr.gsu.edu/hbase/Sound/maxsens.html.

[23] "Handbook of Aircraft Noise Metrics", National Aeronautics and Space Administration, Tech. Rep., 1981.

[24] *Decibels, Phons, and Sones*, Available at https://www.physicsclassroom.com/getattachment/actprep/act9ag.pdf.

[25] S. More, "Aircraft Noise Characteristics and Metrics", Massachusetts Institute of Technology, Tech. Rep., 2011.

[26] C. Roberts, *Tonal Noise Analysis with Optimus Green Sound Level Meters*, Available at https://www.cirrusresearch.co.uk/blog/2012/03/tonal-noise-analysis-with-the-optimus-green-sound-level-meters, Mar. 2012.

[27] S. Vaseghi, "Impulsive Noise. In: Advanced Signal Processing and Digital Noise Reduction", *Vieweg+Teubner Verlag*, 1996.

[28] A. Christian and R. Cabell, "Initial Investigation into the Psychacoustic Properties of Small Unmanned Aerial System Noise", NASA Langley Research Center, Tech. Rep., 2017.

[29] D. Manvell, "Full revision of international standards for equal-loudness level contours (iso 226)", International Standards Organization, Tech. Rep., 2003.

[30] Y. Suzuki, *Precise and full-range determination of two-dimensional equal loudness contours*, Available at http://www.mp3-tech.org/programmer/docs/IS-01Y-E.pdf, Aug. 2003.

[31] G. Busch, *Aircraft Noise*, AE 6344: Aircraft Design II Lecture Slides, 2020.

[32] L. Beebe, *Aircraft Noise Terminology*, Available at https://discover.pbcgov.org/airports/pages/noise-terminology.aspx.

[33] *Noise Levels for U.S. Certificated and Fforeign Aircraft*, Available at https://www.faa.gov/documentLibrary/media/Advisory_Circular/AC_36-1H.pdf, May 2012.

[34] *Aircraft noise levels & stages*, Available at https://www.faa.gov/air_traffic/noise_emissions/noise_levels/, Sep. 2015.

[35] *Fundamentals of Noise and Sound*, Available at https://www.faa.gov/regulations_policies/policy_guidance/noise/basics/, Jul. 2020.

[36] "John Wayne Airport (SNA) - Aircraft Noise Abatement Departure Procedure (NADP) Analysis - Task 1", HMMH, Tech. Rep., 2018.

[37] "Aircaft Noise Terminology and Metric", San Francisco International Airport Noise Abatement Office, Tech. Rep., 2014.

[38] *2014 noise exposure map*, Available at https://www.flysfo.com/sites/default/files/sfo_p150_2014-nem-36x24-plot-signed_ada.pdf, 2014.

[39] A. Gabrielian, T. Puranik, M. Bandarkar, M. Kirby, D. Mavris, and D. Monteiro, "Noise model validation using real world operations data", AIAA Aviation Conference, Tech. Rep., 2021.

[40] *Sound Insulation Program*, Available at https://www.flysfo.com/community/noise/sound-insulation-program.

[41] *2050.1f desk reference*, Available at https://www.faa.gov/about/office_org/headquarters_offices/apl/environ_policy_guidance/policy/faa_nepa_order/desk_ref/, Mar. 2020.

[42] 115th Congress of the Unites States, *Faa Reauthorization Act of 2018*, https://www.congress.gov/bill/115th-congress/house-bill/302/text?q=%7B%22search%22%3A%5B%22PL+115-254%22%5D%7D&r=1, 2018.

[43] L. Carey, "House members send letter to FAA about inadequate aircraft noise mitigation efforts", *Transportation Today*, Sep. 2020, Available at https://transportationtodaynews.com/news/19802-congress-members-send-letter-to-faa-about-inadequate-aircraft-noise-mitigation-efforts/.

[44] N. Miller, "Tc214 Analysis of NES", Federal Aviation Administration, Tech. Rep., 2021.

[45] C. Theodore, "A Summary of the NASA Design Environment for Novel Vertical Lift Vehicles (DELIVER) Project", NASA Langley Research Center, Tech. Rep., 2018.

[46] J. Frost, *How to Interpret R-squared in Regression Analysis*, Available at https://statisticsbyjim.com/regression/interpret-r-squared-regression/, 2021.

[47] J. FIELDS, R. DE JONG, T. GJESTLAND, I. FLINDELL, R. JOB, S. KURRA, P. LERCHER, M. VALLET, T. YANO, R. GUSKI, U. FELSCHER-SUHR, and R. SCHUMER, "Standardized general-purpose noise reaction questions for community noise surveys: Research and a recommendation", *Journal of Sound and Vibration*, 2001.

[48] A. R. George, "Helicopter Noise: State of the Art", *AIAA*, vol. 15, no. 11, pp. 707–715, 1978.

[49] A. A. Ltd., *20 reasons why wav is better than mp3*, Available at https://www.audioanimals.co.uk/news/quick-tips/why-wav-is-better-than-mp3, Apr. 2013.

[50] C. Natoli, "Classical designs: Full factorial designs", Air Force Institute of Technology, Tech. Rep., 2018.

[51] N. Zawodny, D. D. Boyd, and C. Burley, "Acoustic Characterization and Prediction of Representative, Small-Scale Rotary-Wing Unmanned Aircraft System Components", NASA Langley Research Center, Tech. Rep., 2016.

[52] A. Chidbachian, *El pollo loco testing drone delivery services in parts of southern california*, Available at https://www.foxla.com/news/el-pollo-loco-testing-drone-delivery-services-in-parts-of-southern-california, Jun. 2021.

[53] F. P. Office, *Press release – new drone rules take effect today*, Available at https://www.faa.gov/news/press_releases/news_story.cfm?newsId=25980, Apr. 2021.

[54] *Calculating db(A) from Octave Band Sound Levels*, Available at https://www.cirrusresearch.co.uk/blog/2020/03/calculation-of-dba-from-octave-band-sound-pressure-levels/, Mar. 2020.